Hydrophob/hydrophil schaltbare Nanoteilchen für die Biomarkierung

Hydrophobic/Hydrophilic Switchable Nanoparticles for Bioimaging

DISSERTATION

zur Erlangung des akademischen Grades
Doctor rerum naturalium
(Dr. rer. nat.)
vorgelegt der Fakultät Mathematik und Naturwissenschaften
der Technischen Universität Dresden
von

M. Sc. Aliaksei Dubavik
geboren am 23 April 1982 in Krementschug (Ukraine)

Gutachter: Prof. Dr. rer. nat. habil. Alexander Eychmüller
Prof. Dr. rer. nat. habil. Rainer Jordan

Eingereicht am: 29. März 2011

Tag der Verteidigung: 15. Juli 2011

Die Dissertation wurde in der Zeit von Januar/ 2008 bis März / 2011 im Institut für Physikalische Chemie und Elektrochemie (TU Dresden) angefertigt.

Dedication

To outstanding women in my life:
to my mother, to Ludmila Vladimirovna, to my wife Ekaterina.

ACKNOWLEDGEMENTS

This work described in the thesis was carried out at the department of Physical Chemistry, Technische Universität Dresden, from January 2008 to March 2011. The first thankful words go to my supervisors Dr. Vladimir Lesnyak, Dr. Nikolai Gaponik and Prof. Dr. Alexander Eychmüller for their faith in my abilities and constant encouragement throughout this process. I shall always appreciate their guidance, wisdom and wholehearted cooperation. They gave me a truly interesting topic to work in and sparked my interest for the nanochemistry. Besides, I thank them for giving me the opportunity to participate in many national and international conferences.

Thanks also to Prof. Dr. Thomas Wolff (Physical Chemistry, TU Dresden) for giving an idea of this work and for the very helpful discussions. I would like to thank Dr. Wladimir Thiessen for collaboration in the field of synthesis of amphiphilic nanoparticles.

The grateful words from my side go to Christian Waurisch who was always ready to help and cheer up me in difficult minutes, who was the best office neighbour and colleague easy to deal with. Special thanks to Tobias Otto for his talents in repairing TEM and other neccessary devices. Many thanks to Stephen Hickey for valuable discussions and pieces of advice concerning the present work. I am very much obliged to Susi Krüger and Nadja Bigall for their help and support. I am grateful to Lydia Liebscher, Stefanie Tscharntke, Jan Poppe for the provided samples of quantum dots. My thankful words are addressed to Thomas Hendel, Anne-Kristin Herrmann and Christoph Ziegler for the assistance with gold nanoparticles synthesis and discussions. The brilliant work of SHK-students Marco Kunaschk, Evgeni Sperling and André Wolf made a valuable contribution to the present work.

Many thanks are addressed to Ellen Kern (Physical Chemistry, TU Dresden) for the SEM and EDX measurements, Christine Mickel (IFW Dresden) for the TEM measurements. Moreover, I would like to thank Erdinc Serzin (Biotechnologisches Zentrum der TU Dresden) for confocal imaging and diffusion measurements of GUVs and the useful discussion. I also thank Alexander Ohlinger and Dr. Andrey Lutich (LMU) for assisting with the DFM measurements.

The serious and indispensable office responsibilities of Mrs. Ahnefeld and Mrs. Kube made my life easier at the department because much paper work has been done by them.

I want to thank Mrs. Bardoux-Hess and Mr. Püschel for all that huge amount of chemicals supplied, to Mrs. Ahlers and Mrs. Bibrach - for their open-hearted smiles and help in providing all necessary glassware.

I thank my mother for her all my life long support, her inexhaustible optimism, motherly love and wisdom. Last, but certainly not least, I thank my wife Ekaterina who helped me not only with the imaging of synthetical set-ups and dissertation design but with all her love, patience and tenderness which are making me better, with her all my dreams are coming true.

CONTENT

CONTENT

NOTATIONS

AET	Aminoethanethiol
CTAB	Cetyltrimethylammonium bromide
DDA	Dodecylamine
DDT	Dodecanethiol
DHLA	Dihydrolipoic acid
DLS	Dynamic light scattering
DMA	N,N-Dimethylacetamide
DMF	N,N-Dimethylformamide
DOPC	1,2-Dioleoyl-sn-glycero-3-phosphocholine
DOPS	1,2-Dioleyl-sn-glycero-3-{ghospho-L-serine} sodium salt
GUV	Giant unilamellar vesicle
LED	Light-emitting diod
MPA	Mercaptopropionic acid
mPEG	Methoxypolyethylene glycol
NC	Nanocrystal
NP	Nanoparticle
NMR	Nuclear magnetic resonance
OA	Oleic acid
OVDAC	Octadecyl-p-vynilbenzyldimethylammonium chloride
PEG	Polyethylene glycol
PEI	Polyethylene imine
PL	Photoluminescence
PLE	Photoluminescence excitation
PMAA	Poly(methacrylic acid)
PMOEGMA	Poly(methoxyl oligo(ethylene glycol) methacrylate)
PNIPAM	Poly(N-isopropylacrylamide)
PS	Polystyrene
QD	Quantum dot
QE	Quantum efficiency
QY	Quantum yield
TEM	Transmission Electron Microscopy
TGA	Thioglycolic acid
TOAB	Tetraoctylammonium bromide
TOP	Tri-n-octylphosphine
TOPO	Tri-n-octylphosphineoxide
TPP	Triphenylphosphine
XRD	X-ray diffraction
UV	Ultraviolet light

1. INTRODUCTION AND MOTIVATION

Nanochemistry is the utilization of synthetic chemistry to make nanoscale building blocks of different size and shape, composition and surface structure, charge and functionality. These building blocks can be useful in a self-assembly processes, forming architectures for intelligent functions.[1] Nanomaterials are cornerstones of nanoscience and nanotechnology. The nature of all nanomaterials is diverse. One of the most important classes of the nanomaterials is nanoparticles (NPs) which are very attractive for application in different fields of nanotechnology. To assure efficient applicability of the NPs they should be, as a rule, dispersible in desired media (solvent).

Water-soluble functional NPs are indispensable for various biomedical applications, including imaging of cellular and subcellular structures or cell labeling, drug delivery, diagnostics and therapy of tumour diseases. However, the controllable and reproducible synthesis of monodisperse, robust and functional NPs compatible with aqueous media is challenging. Indeed a lot of reliable synthetic methods available for noble metal, semiconductor quantum dot (QD), and magnetic oxide NPs have been developed for nonpolar organic media. To be stable in this synthetic media, the NPs possess hydrophobic surfactant coating. Because water solubilization and functionalization of NPs are the key issues determining their bio-application, the design of surface coating becomes a significant research field.[2, 3] The proper designed coating should help not only to convert hydrophobic NPs into hydrophilic water soluble materials, but also introduce demanded specific chemical functionality onto the particle surface, so that different (bio)molecules can be covalently attached. Moreover, proper designed surface of NPs may allow controllable electrostatic and/or coordination coupling to surfaces of other particles or to biosystems.

In spite of great research interest to the surface design and hydrophilisation of the NPs, efforts to obtain NPs intrinsically soluble and stable in both aqueous and nonpolar organics are limited. Even fewer success is achieved to date in the one-pot synthesis of such intrinsically amphiphilic NPs.

Nanocrystals of metals, semiconductors and oxides are intensively studied by various research groups. They are of a great interest in many fields because of their attractive electronic, optical, magnetic and chemical properties. Some of these properties may be also significantly size-dependent.

1. INTRODUCTION AND MOTIVATION

Optical properties of nanomaterials are essential for detection, lasing, imaging, lighting, and give rise their potential application in optoelectronics, photovoltaics, photocatalysis, etc. Biomedical detection and treatment based on optical properties of nanomaterials is another area of fast growth. E.g., gold nanoparticles are effective for *in vitro* and *in vivo* cancer imaging and treatment,[4] semiconductor quantum dots have been successfully used for bioimaging *in vivo*.[5]

Magnetic properties are used for magnetoseparation, in magnetic storage media, have proven to be especially promising in molecular biology and medicine in magnetothermal therapy and as contrast agents.[6]

There are many points of interaction between nanoscience and biological sciences. Enzymes, motors, membranes, nucleic acids - different biological systems which are able to include in their structure nanosized particles. The colloidal NPs have the size of a typical protein. They could be used for labeling not only the biomolecules, but also much larger bioobjects like cancer cells and tumour cell cultures.

In present work successful attempts to amphiphilize such widely used and important materials as luminescent CdTe QDs, surface plasmon tunable Au NPs and magnetic Fe_3O_4 NPs are demonstrated. In spite of the diversity of the materials, all developed methods are based on so named "one-pot" synthetic approach. Moreover, they deliver nanoparticles being intrinsically amphiphilic, i.e. able for spontaneous phase transfer without any additional adjustment of solvent properties.

2. LITERATURE OVERVIEW

Colloidal inorganic nanoparticles are very small, nanoscale objects dispersed in a solvent. Nanoparticles possess a number of different very attractive properties such as high electron density and strong optical absorption (e.g. metal and semiconductor particles), photoluminescence in the form of fluorescence (semiconductor quantum dots) or phosphorescence (doped oxide materials), or magnetic moment (e.g. iron oxide, cobalt, etc.).

Prerequisite for every possible application is the proper surface functionalization of such nanoparticles, which determines their interaction with the environment. These interactions ultimately affect the colloidal stability of the particles, and may yield a controlled assembly or the delivery of nanoparticles to a target, e.g. by appropriate functional molecules on the particle surface.

There are different strategies of surface modification, functionalization and ligand exchange which are necessary for phase transfer of inorganic colloidal nanoparticles. These strategies are often of general nature and may be applied in similar way to various nanoparticle types.

2.1. General strategies of nanoparticles solubilization

Colloidal semiconductor, metal, metal oxide nanocrystals are composed of a core, constituted of between a few hundred and a few thousand atoms, surrounded by an organic outer layer of surfactant molecules (ligands).

One of the most important parameters controllable in the colloidal synthetic approach is particles' surface coverage protecting them from surrounding environment and preventing their aggregation. The surface agents determine the solubility of colloidal particles and their compatibility with dispersive medium, what is important for their processing, assembly etc. In this respect, an ideal stabilizer would provide solubility and compatibility of nanoparticles with various media from polar to nonpolar. Usually, NPs capped by some certain stabilizer are compatible with compounds of similar nature (via polar-polar or nonpolar-nonpolar interactions), that limits range of their applicability. In order to make nanoparticles compatible with different medium media various stabilizer exchange techniques are employed for their phase transfer. These methods have been reported for transfer of semiconductor CdTe nanocrystals synthesized in aqueous solution into organics [7, 8] and in the opposite direction, [9] CdSe [10] and PbSe [11] from organics into water, for transport of Au, Ag, Pt, Pd nanocrystals from organic to aqueous media,[12, 13] as well as of iron oxide NPs by ligand exchange [14] and by polymer stabilizer adjustment [15].

Commonly used solubilization strategies include:

1. Direct solubilization in a synthesis
2. Ligand exchange
3. Ligand shell modification:
   a) chemical modification
   b) physical modification

Depending on the reaction media as synthesized nanoparticles may bare on the surface hydrophobic or hydrophilic ligand molecules, the most typical representatives of which are displayed in Figures 1 and 2, respectively.

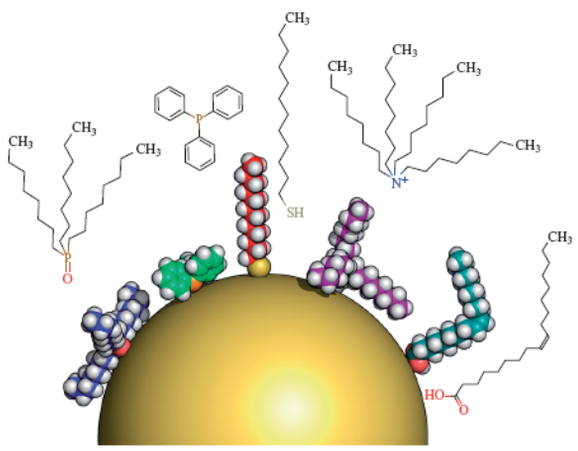

Figure 1. *A nanoparticle of 5 nm core diameter with different hydrophobic ligand molecules both drawn to scale. Left to right: trioctylphosphine oxide (TOPO), triphenylphosphine (TPP), dodecanethiol (DDT), tetraoctylammonium bromide (TOAB) and oleic acid (OA). [16]*

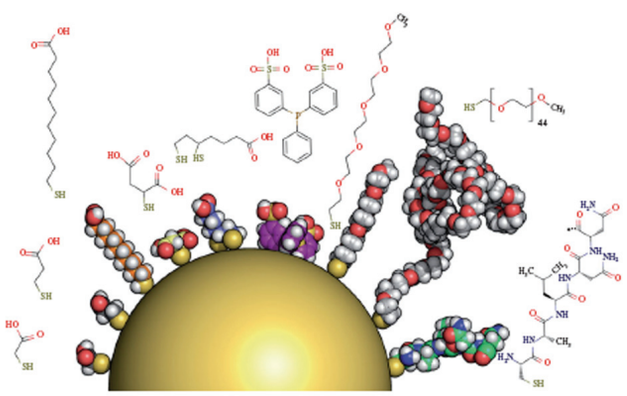

Figure 2. *A nanoparticle of 5 nm core diameter with different hydrophilic ligand molecules drawn to scale. Left to right: mercaptoacetic acid (MAA), mercaptopropionic acid (MPA), mercaptoundecanoic acid (MUA), mercaptosuccinic acid (MSA), dihydrolipoic acid (DHLA), bis-sulphonated triphenylphosphine, mPEG5-SH, mPEG45-SH (2000 g mol^{-1}) and a short pentapeptide of the sequence CALNN. [16]*

2. LITERATURE OVERVIEW

Surface modification becomes necessary if the desired particle type cannot be directly synthesized with the corresponding ligand on the surface. However, proper surface modification is often challenging task and should be very carefully approached: even slight changes of surface of quantum dots may seriously deteriorates their physical properties. In general, for phase transfer in both directions, there are two main strategies: ligand exchange and ligand modification (Figure 3).[16] Since the binding of a ligand depends strongly on the chemical composition of the nanocrystal surface, and for successful exchange the hydrophilic ligand has to bind more strongly than the hydrophobic one, there exists no general protocol for hydrophobic-hydrophilic phase transfer that may work for any type of nanocrystals.

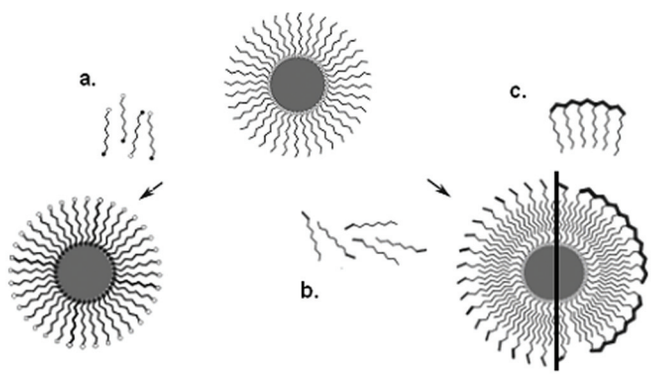

Figure 3. *Different strategies for phase transfer of nanoparticles.*

Ligand exchange: *a. the incoming ligand has one head group binding to the nanoparticles surface (filled circles), the other end (empty circles) is e.g. hydrophilic.*

Ligand modification *by additional solubilizing layer: b. Additional layer of ligand molecules adsorbing e.g. by hydrophobic interaction. c. Amphiphilic polymer with hydrophobic side chains and a hydrophilic backbone (strong black). Adapted with modification from [16].*

The first strategy of the surface modification (route a in Fig. 3) is based on the exchange of the original organic layer with hydrophilic ligands,[17, 18] bifunctional capping molecules [18] or an inorganic coating such as silica and metal chalcogenides.[2, 19-21]

The second approach consists of incorporating hydrophobic nanoparticles into amphiphilic micelles, leading to a connected closely bilayer (Fig. 3b, c). [3, 22, 23] Surfactants, such as phospholipids and R-cyclodextrin, are one example of such encapsulants, and they can successfully transfer nanocrystals into pure water. However, often nanoparticulate materials are not generally stable in biological conditions because of a relatively weak anchoring of the hydrophobic tails to the particle. Additionally, the hydrophilic end groups of even biocompatible surfactants may not protect nanocrystals from nonspecific biomolecular interactions.[23-25]

Using amphiphilic polymers to encapsulate nanocrystals through hydrophobic interactions is one of the useful extensions of the second strategy. Indeed, with the aid of this approach the problems of additional functionalization for selective solubilization can be overcome, since amphiphilic polymers offer more options for tailoring both the hydrophobic and hydrophilic interactions between particles and their coatings.[3, 5, 26] The external functionality of the nanocrystal-polymer assembly can be widely varied through the introduction of different amphiphilic moieties. Though promising for coating nanocrystals, amphiphilic polymers containing hydrophobic tails most appropriate to particle stabilization are not available commercially. A few examples of their use to date have relied on coupling schemes that use reactive end groups (-SH, -NH_2) found only on a limited and expensive set of polymers [26, 27]. As a result, the range of amphiphilic polymers for creating stable and non-aggregating nanocrystals in biological conditions is relatively limited.

To fully explore the structure and optimize amphiphilic polymers for nanocrystal stabilization, simple methods to design amphiphilic polymers through coupling of single component hydrophobic and hydrophilic constituents are required. The incorporation of poly(ethylene glycol) (PEG) into the surface coatings is of particular interest for biocompatibility.[5, 25, 28] Nanocrystals possessing PEG-functionalized exteriors exhibit generally much less toxicity and longer circulation time than water-soluble nanocrystals covered by other hydrophilic ligands.[29-31] A few schemes for producing such materials require the use of derived PEG polymers such as mPEG-NH_2 (primary amino group terminated poly(ethylene glycol) methyl ether) or PEG-SH.[25, 28, 32-34]

Following chapters demonstrate applications of the solubilization strategies for each type of nanoparticles: semiconductor, metal and magnetic materials.

2.2. Quantum dots

Nanoscale materials, having optical properties which in particular differ greatly from the corresponding molecular and bulk materials, are also known as quantum dots (QDs). Their small size results in an observable quantum-confinement effect, defined by Bohr radius of the material and leading to the quantization of the energy levels to discrete values and consequently to the dependence of a band gap on the size of nanoparticle.

QDs are mainly composed of binary II-VI (e.g., CdSe), III-V (InP) and IV-VI (PbS) materials.[35-38] They are robust fluorescence emitters with size-dependent emission wavelengths. Their extreme brightness and resistance to photobleaching enables application of very low laser intensities over extended time periods, making them especially useful for live-cell imaging.

The intense brightness is also particularly helpful for single-particle detection and an increasing number of biomedical assays. The tunable emission wavelength and distinct emission spectra of QDs facilitate data acquisition and analysis of multiple tagged molecules of interest.

Fluorescence probes are widely used in cell biology. Organic fluorophores, the most commonly used probes, suffer from fast photobleaching and broad, overlapping emission lines, and therefore are limited in applications involving long-term imaging and multicolor detection. Thus, QDs are considered as promising alternative to organic dyes for fluorescence-based bioapplications (Fig. 4).[39, 40]

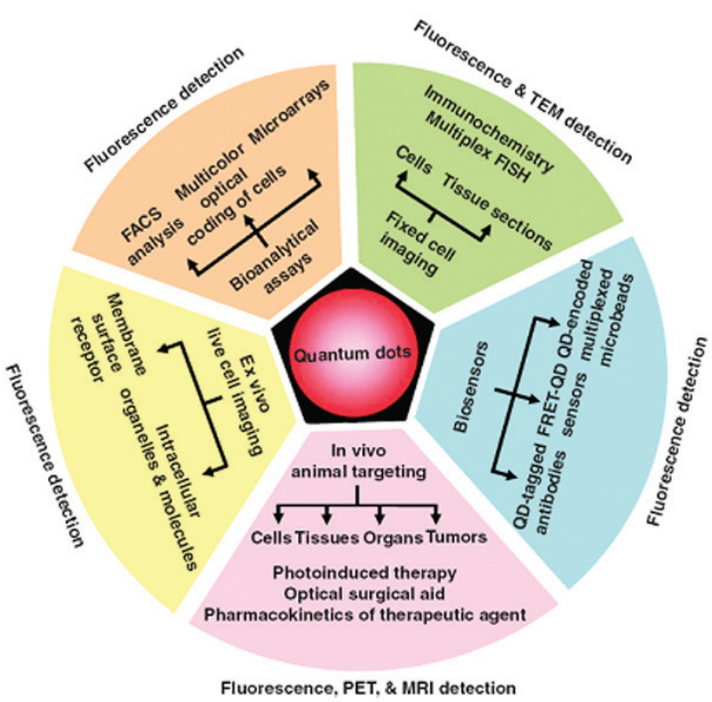

Figure 4. *Applications of quantum dots as multimodal contrast agents in bioimaging. [40]*

The progress in a synthesis and optimization of QDs for biological environments has opened the doors to an expanding a variety of biological applications, such as serving as specific markers for cellular structures and molecules, tracing cell lineage, monitoring physiological events in live cells, measuring cell motility, and tracking cells *in vivo*.

Some apparent advantages of using QDs over fluorescent dyes/probes are outlined below.[41]

1. Spectral properties: a) broad optical absorbance and narrow photoluminescence of the QDs are very favorable for biological detection (Fig. 5); b) the emission spectra of QDs can be tuned across a wide range by changing the size and composition of the QD core (Fig. 6).

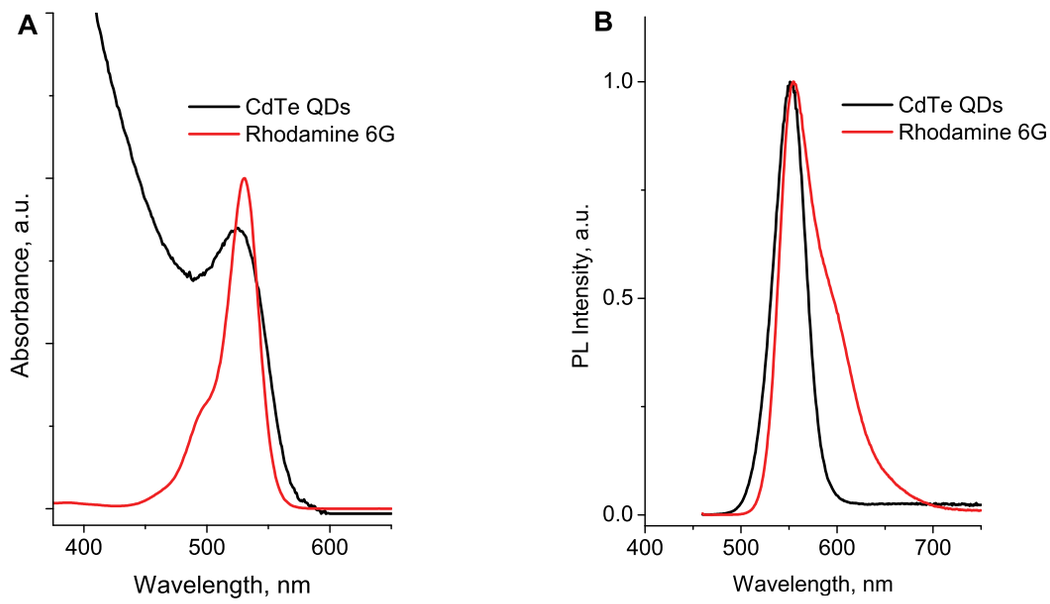

Figure 5. *Comparison of the absorption (A) and emission (B) profiles of CdTe QDs (black) and rhodamine 6G dye (red). The QD emission spectrum is nearly symmetric and much narrower in peak width. Its absorption profile is broad and continuous. The QDs can be excited at any wavelength shorter than 530 nm. In contrast, the organic dye rhodamine 6G has a broad and asymmetric emission peak and can be excited only in a relatively narrow wavelength range.*

2. Resistance to photobleaching (photobleaching is a process in which molecular structure of a dye is irreversibly altered as a result of absorption of excitation light that renders it non-fluorescent). The photostable nature of the QD usually results from the specially designed protecting shell surrounding the core.[42, 43] QDs have more degrees of freedom than organic fluorophores and they don't lose their emission properties even if the bonding has been slightly changed.

Figure 6. *Example of colloidal CdTe NPs possessing size-tunable emission.*

3. Resistance to metabolic degradation: the inorganic nature of QDs and their passivating coatings determine their resistance to metabolic degradation.

4. High extinction coefficients: QDs have very large molar extinction coefficients and high quantum yields resulting in bright fluorescence. Their molar extinction coefficients are in the order of 0.5-5×10^6 M^{-1} cm^{-1}, which makes them bright probes in aqueous solutions and also under photon-limited conditions *in vivo* environment (where light intensities are severely attenuated by scattering and absorption). Moreover, QDs have long fluorescence lifetimes in the range of 20-50 ns, which allow them to be distinguished from background and other fluorophores by increased sensitivity of detection.

5. Conjugation ability: bioconjugation of QDs is achievable using several approaches, e.g., they can be conjugated to the linker (avidin, protein A or protein G, or a secondary antibody etc.) by covalent binding and passive adsorption, multivalent chelation, or by electrostatic interactions. Since most proteins contain primary amine and carboxylic acid functional groups, carbodiimide-mediated amide formation cross-linking reactions are perhaps the most common as it obviates the need for any surface modification before conjugation. In the electrostatic self-assembly approach, the linker is bound to a positively charged peptide enabling its conjugation to dihydroxylipoic (DHLA) acid-capped zinc sulfide-coated QDs (fig. 7).[44]

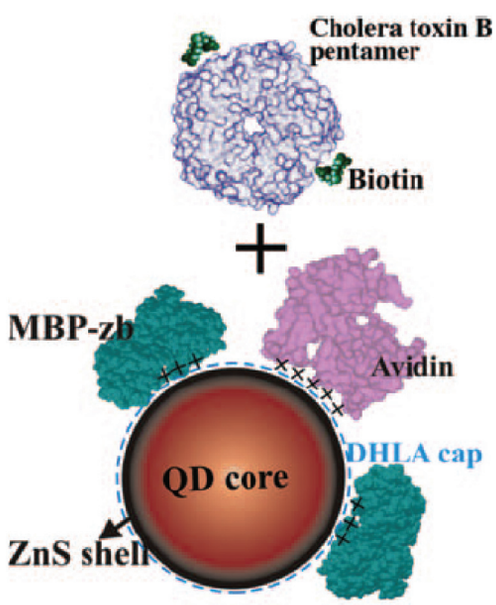

Figure 7. *The mixed surface approach for conjugating biomolecules to DHLA-capped QDs using avidin as the linker molecule. [44]*

2.2.1. QDs synthesis

Historically the synthesis in aqueous media was the first successful preparation method of colloidal semiconductor nanoparticles.[35, 37, 45-47] Water is a natural medium for all forms of life. This is one of the reasons why any solution-based techniques and processes in aqueous media are considered to be environmentally friendly and safe in comparison with the others which demand organic solvents or melts.

QDs, particularly of type II-VI semiconductors, have been prepared in aqueous media with the aid of water-soluble phosphates and polyphospates, citrate, thiol ligands.[48-52] These methods offer a number of advantages such as relatively low cost, potential for up-scaling, and environmental friendliness.[7, 53] As a rule the size distribution of the colloidal QDs prepared in water is relatively broad, and size-selective precipitation approaches are used to optimize it.

The most successful aqueous synthesis approach is based on the use of various thiol containing organic compounds (acids, alcohols, amines) as stabilizers.[52] The typical synthetic setup is schematically presented in Fig. 8.[54]

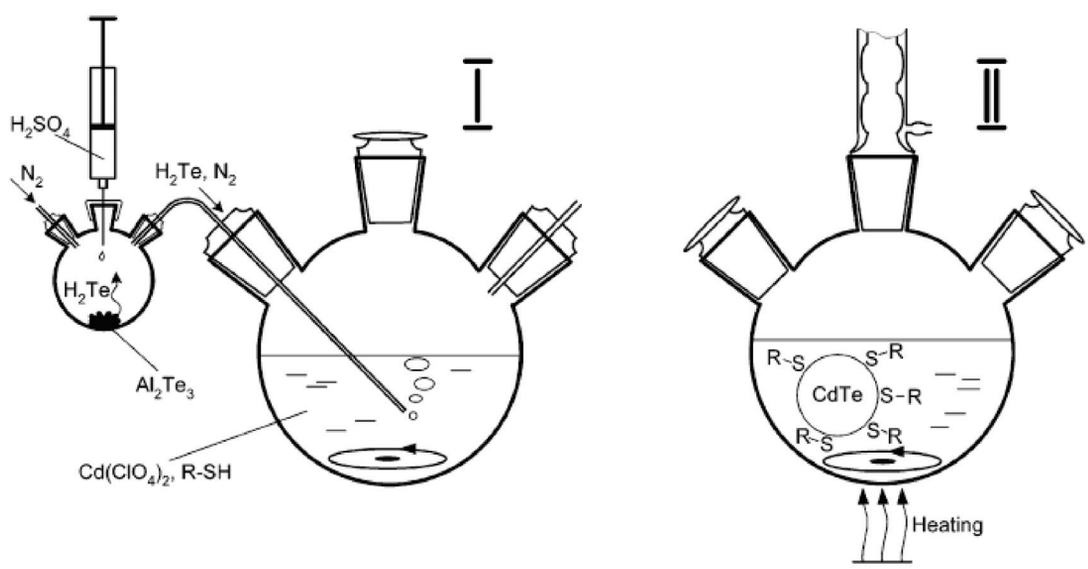

Figure 8. *Experimental setup for a synthesis of thiol-capped CdTe NCs in water. [54]*

The solubility of thiol-capped QDs is not limited to aqueous solutions. The QDs could be successfully transferred into nonpolar organic solvents with the aid of surface exchange by using 1-dodecanethiol [7], octadecyl-*p*-vynilbenzyldimethylammonium chloride (OVDAC).[55] QDs transferred in organic media were used for fabrication of composites with functional polymers [7, 55] and applied for fabrication of hybrid LED.[56]

However, relatively lower stability, the difficulty of efficient control of crystallinity and shape, limited freedom for core-shell design and low synthesis temperature are the main limitations of the aqueous synthesis.[57] These are the reasons why the heat-elevated methods in organic media became more popular and demanded.

The introduction of a hot-injection approach using high temperature boiling organic solvents in 1993 constituted an important step towards the fabrication of monodisperse CdS, CdSe and CdTe NPs.[58]

The advantages of the organically prepared QDs are monodispersity, shape control, narrow size distribution which are necessary to obtain a pure emission colour, strongly size-dependent physical properties as photoluminescence and absorption peaks. To expand the list we could add the synthesis of core/shell structures which are intensively studied due to their superior photoluminescence quantum yields and higher stability compared to core NCs.[43, 59, 60]

However, these nanoparticles are generally capped with hydrophobic ligands. Special challenges are faced to design and fabricate QDs with high fluorescence in aqueous environments and to conjugate QDs with biomolecules that recognize specific biological structure. Hydrophobic quantum dots could be converted into water soluble nanocrystals by various surface treatment approaches including encapsulation with amphiphilic phospholipids, siloxanes and copolymers. As these approaches appear to be very relevant to a topic of the present work, some of them will be discussed in more detail below.

2.2.2. Surface modification and bioconjugation of QDs

All basic surface modification strategies presented in fig. 1 are applicable to QDs. For example, according to the first strategy, trioctylphosphine/trioctylphosphine oxide-coated (TOP/TOPO) CdSe/ZnS QDs could be transferred to an aqueous solution by replacing the phosphine/phosphine oxide hydrophobic ligands with hydrophilic thiol-based molecules, like mercaptocarboxylic acids (mercaptoacetic, mercaptopropionic, mercaprosuccinic, mercaptoundecanoic, DHLA).[61-63] Colloidal CdTe QDs prepared in trioctylphosphine/dodecylamine (TOP/DDA) were transferred into water by the use of aminoethanthiol hydrochloride (AET) or mercaptopropionic acid (MPA) to prepare positively or negatively charged water-soluble NCs. Monoexponential exciton decay and slight defects in emission after the ligand exchange were observed. The method is also attractive for its simplicity.[9] Spherical PbSe semiconductor NCs (near-infrared absorption 1100-2500 nm) were made water-soluble through exchange of surface hydrophobic ligands (TOP) for hydrophilic ones (1-mercaptoundecanoic acid). Figure 9 shows the transfer of the black PbSe NCs from the organic phase to the water phase after the ligand exchange.[11]

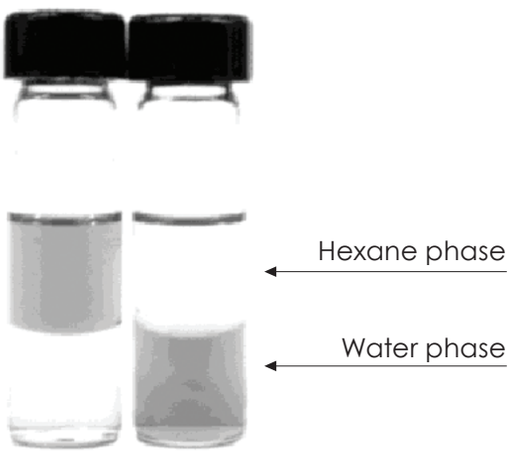

Figure 9. *Phase transfer of PbSe from hexane into water after the ligand exchange.[11]*

Another successful example is a use of specific peptide coating (Fig. 10). Specific peptide-coated CdSe/ZnS QDs show that it is possible to target hybrid organic-inorganic nanometer sized colloidal materials in a living mammal. It is proved that the aggregation problem could be overcome by either decreasing the population of peptides on the QDs surface or by co-coupling peptides and PEG, a polymer known to minimize molecular interactions (nonspecific binding) and improve colloidal stability.[64]

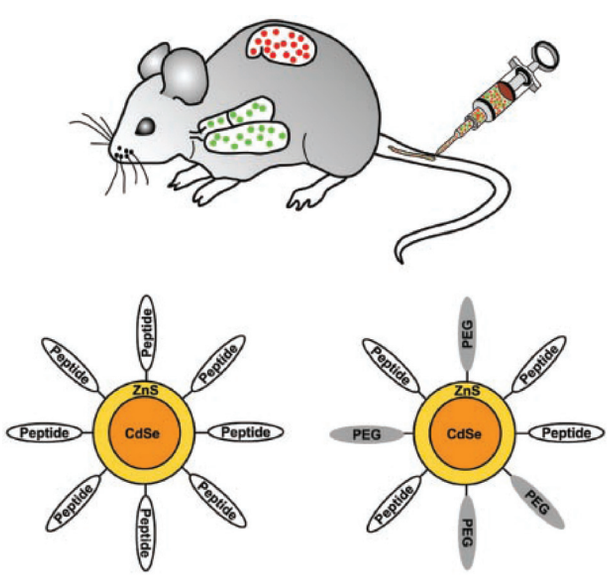

Figure 10. *Schematic representation of QD targeting. Intravenous delivery of QDs into specific tissues of a mouse (upper) Design of peptide-coated particles (lower) QDs were coated with either peptides only or with peptides and PEG which helps to maintain solubility of QDs in aqueous environment and minimize nonspecific binding. Adapted from [64]*

The encapsulation approach, reported for core/shell CdSe/ZnS QDs wrapped in polyethylene glycol phospholipid micelles, is attractive for several reasons: (i) the encapsulation step does not alter the surface, (ii) the optical properties of the QDs are retained, and (iii) the micelles display a high density of PEG on their surface which prevents nonspecific adsorption.[65] Using amphiphilic polymers to encapsulate QDs through hydrophobic interactions is superior to the ligand exchange method because it preserves the quantum yield of QDs synthesized in organic phase and constructs more stable nanostructures.[3, 27, 66] Quite a few amphiphilic polymers such as alkylated alginate,[67] poly(maleic anhydride-alt-1-tetradecene),[3] poly(maleic anhydride-alt-1-octadecene),[66, 68] and alkylated poly(acrylic acid) [69] have been used to encapsulate QDs. Organic QDs could be transferred into aqueous phase by amphiphilic biocompatible cationic polysaccharide chitosan grafted with alkyl chains (chitosan-QD).[70]

Nie et al. reported the development of bioconjugated QD probes suitable for *in vivo* targeting and imaging of human prostate cancer cells growing in mice. This new class of QD conjugates contains an amphiphilic tri-block copolymer for *in vivo* protection, targeting-ligands for tumor antigen recognition and multiple PEG molecules for improved biocompatibility and circulation. The application of this ABC tri-block copolymer has solved the problems of particle aggregation and fluorescence loss previously encountered for QDs stored in physiological buffer or injected into live animals.[5]

2.3. Metal Nanoparticles

Metal nanoparticles such as Au and Ag are excellent nanomaterials providing a powerful platform in biomedical applications of biomolecular recognition and sensing, drug delivery, and imaging.[71, 72]

Optical sensing, for example, exploits the change in surface plasmon resonance (SPR) peak position and its intensity to detect binding events on Ag or Au surfaces. As the surface of Ag and Au nanoparticles can be readily conjugated with biologically relevant ligands, a number of detection strategies has been developed to probe biomolecules with high sensitivity and at a low cost.[73, 74] The SPR absorption, arising from the collective oscillation of conducting electrons in the metal NP core upon interacting with the incident light, is dependent on the NP size and shape, the dielectric property of the media, and the distance between particles. This provides a unique and convenient platform for monitoring the molecular recognition event occurring close to the surface of the nanoparticles. Colorimetric bioassays have thus been achieved based on the SPR shift when molecular interactions take place at the surface of the nanoparticles, and have been employed

to study fundamental biorecognition processes including cell-cell communication, enzymatic activity, protein-protein interaction, and DNA hybridization. When the ligand-receptor interaction causes additional aggregation of nanoparticles, very large SPR shifts occur producing intense color changes visible to the naked eyes.[75] These optical properties, induced by single particles or interactions between particles, allow the highly sensitive detection of molecular binding events. Moreover, the SPR absorptions are not a subject to quenching/photobleaching that are frequently associated with organic fluorophores, or blinking that occurs in quantum dots.

In addition to the scattering and absorption of light, plasmonic nanoparticles are useful to enhance local electromagnetic fields. SPR can generate intense local electric fields within a few nanometers of a particle surface. This near-field effect can improve Raman scattering cross sections of molecules adsorbed onto the surface. This kind of enhancement has led to the development of a new field of scientific exploration known as surface-enhanced Raman spectroscopy (SERS), with the SERS effect being first demonstrated by Fleischman and Van Duyne.[76, 77]

Au NPs are among the most used and studied nanomaterials owing to their ease of preparation, stability, well-established surface functionalization chemistry, and their unique optoelectronic properties. An early example of bioapplication of gold NPs was demonstrated by Mirkin and coworkers using oligonucleotide-capped Au NPs.[78] Hybridization of the complementary oligonucleotide strands induced the aggregation of Au NPs leading to a distinct solution color change easily visualized by naked eyes.

Bioconjugated Au NPs are used as colorimetric biosensors detecting proteins, viruses, and bacteria at an extremely sensitive level.[72] An additional advantage of nanoparticles is that the multiple ligands presented on the nanoparticle surface could drastically enhance affinities of specific monovalent interactions via the multivalent binding between NPs and the biological target. The authors attributed the enhanced activity to the multivalency effect where multiple ligands presented on the nanoparticle surface greatly enhanced the overall binding affinity to the protein.

2.3.1. Synthesis and phase transfer

The first reported synthesis of plasmonic metal nanoparticles occurred more than 150 years ago when Faraday prepared Au colloids by reducing an aqueous solution of Au chloride with phosphorus.[79] Nowadays, the synthesis of Au nanoparticles with diameters from a few to hundred nanometers is well established in aqueous solution and in organic solvents. Typically $HAuCl_4$ or $AuCl_3$ are directly reduced by reducing agents in the presence of sulfur-terminated polymers and directly formed metal nanoparticles, in which the

polymer chains act as a stabilizer for the nanoparticles.[80-82] One of the most popular approaches is introduced by Brust et al.[83] $AuCl_4^-$ was transferred from water to organic phase (toluene) using tertiary ammonium salt (tetraoctylammonium bromide) as the phase transfer agent. The gold precursor was reduced with aqueous sodium borohydride in the presence of dodecanethiol leading to a simple way for the direct synthesis of metallic clusters.[83] Tenhu's group fabricated composite gold nanoparticles which were grafted with mixed poly(N-isopropylacrylamide) (PNIPAM) and polystyrene (PS) or poly(methacrylic acid) (PMAA) chains. They also grafted PNIPAM on gold nanoparticles by three different ways for comparison, and found the one-step way was most interesting due to the feasibility and facile control over the average sizes of nanoparticles.[81] The poly(methoxyl oligo(ethylene glycol) methacrylate) (PMOEGMA) modified gold nanoparticles were prepared by similar methods as a salt-responsive polymer/gold nanocomposites.[82] The obtained polymer/gold nanocomposites have a relatively good dispersity and have a long-term stability based on the strong steric protection of polymer chains.

2.3.2. Surface modification and bioconjugation

Colloidal gold offers some unique features over other labeling agents, e.g., QDs and organic dyes. For instance, Au NPs do not undergo any photodecomposition (and largely retain their optical properties; however, they may vary depending upon the medium surrounding), which is a common problem encountered while using fluorescent dyes. Secondly, they are not apparently toxic, in sharp contrast to potential toxicity of Cd, Hg, Pb containing semiconductor QDs (e.g. CdTe, HgTe, PbS). Third, they are reasonably stable and can be stored in dry state. Finally, their ability to shift the SPR, in a controlled fashion, to the spectral region best suited for optical bioimaging and bio-sensing would open the way to numerous additional bioapplications.[41]

The most hydrophobic and hydrophilic ligands presented in Figures 1 and 2 are applicable for stabilization of Au NPs. Since thiol moieties exhibit high affinity to gold surfaces forming Au-sulfur bonds, they are used most frequently for Au particles synthesis.[84] According to the strategies presented in chapter 1, after synthesis of the Au particles their stabilizer molecules can be replaced in a ligand exchange or ligand modification procedures.

Biological molecules can be attached to the Au NPs in several ways. If the biological molecules have a functional group which can bind to the gold surface (like thiols or specific peptide sequences), they can replace some of the original stabilizer molecules when they are added directly to the particle solution. In this ligand exchange approach molecules like oligonucleotides, peptides or PEG can be readily linked to Au particles. In this case subsequent

sorting techniques even allow particles with an exactly defined number of attached molecules per particle to be obtained.[85]

It should be noted, the ligand modification approaches in the case of noble metal nanoparticles not only limited to those based on physical absorption and electrostatic interactions as is mainly the case for QDs. In contrast to QDs noble metal NPs are explicitly chemically stable, which opens up an opportunity of chemical design of their surface ligand, e.g. by covalent bonding.[86]

As a fascinating branch, various polymers are artificially decorated onto gold NPs in physical or chemical manner and show much potential in advanced material science. The polymer chains grafted/coated on the surface of gold NPs can not only enhance the stability of gold cores, but also functionalize the gold core due to the special properties of outside polymer layers.[82]

The main preparative methods of gold-polymer composites are based on two interactions between polymer chains and the gold cores: covalent linkage ("graft-to" and "graft-from" strategies) and physical adsorption (hydrophobic interior, nonspecific/coordination adsorption, electrostatic interaction) (Figure 11).[85] "Graft-to" strategy is a method when sulfur-terminated polymers can directly bind to the surface of previously prepared gold nanoparticles through sulfur-gold interaction. If the polymer chains are grafted to pre-formed gold nanoparticles, the obtained polymer/gold nanocomposites may have cores of improved crystallinity.[87, 88] Generally, the polymer graft density in the "graft-to" method is quite low due to the steric hindrance from the large polymer chains, which limits their application. According to "graft-from" strategy, an initiator is previously immobilized on the surface of uniform gold nanoparticles. Then, the initiator-modified nanoparticles can initiate the polymerization of various monomers through living/controlled polymerization providing advantageously controlled polymer molecular weight with its relatively narrow distribution according to the polymerization mechanism, enabling the adjustment of the polymer shell thickness and regularity.

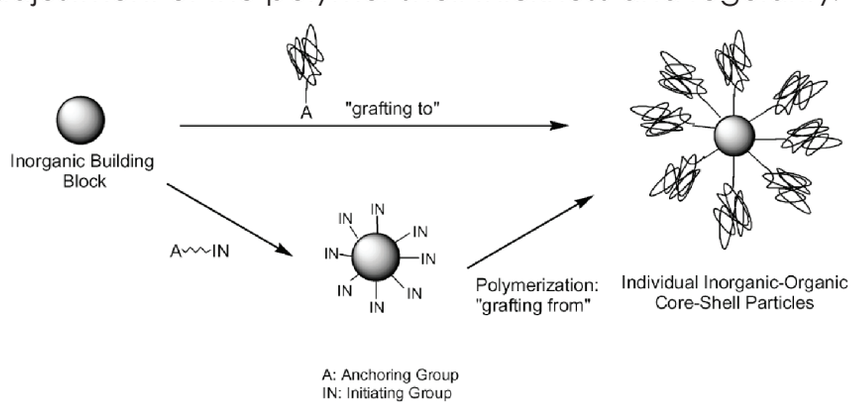

Figure 11. *Grafting-to and grafting-from approaches of inorganic core with a the polymer shell. [89]*

The so called "intelligent" or "smart" polymers [90, 91] are also known as stimuli responsive or environmentally sensitive polymers which will undergo physical or chemical changes as responses to external stimuli in the environmental conditions.[82] For polymers, the temperature and pH stimuli have been widely studied due to the reversibly responsive features. The stimuli response of the polymer chains could be ascribed to the polymer solubility in different environments, which is a similar phenomenon to amphiphilicity described by Edwards (Fig. 12).[82] In spite of the great interest to smart polymer - NP composites, reports on reversible phase transfer methods are still limited.[92, 93] One of the interesting approaches describes Au NCs stabilized by polybutadiene-poly(ethylene glycol) (PB-PEG). These NPs possess exceptional thermal and solvent stability and can stay in solution (water as well as various organic solvents, including hexane) without precipitation, agglomeration, or decomposition for more than 2 years.[94, 95] Foos et al. investigated gold nanoclusters stabilized by the thiols after the ligand exchange reaction: the hexanethiol stabilized Au clusters were synthesized followed by the replacement with thiolated methoxy-ethylene glycols CH_3-(O-CH_2-CH_2)$_n$-SH (n = 2-4).[96, 97] Although the synthesis of PEG stabilized gold NPs has been already quite well investigated, amphiphilic behavior of these colloids was not addressed thus far.

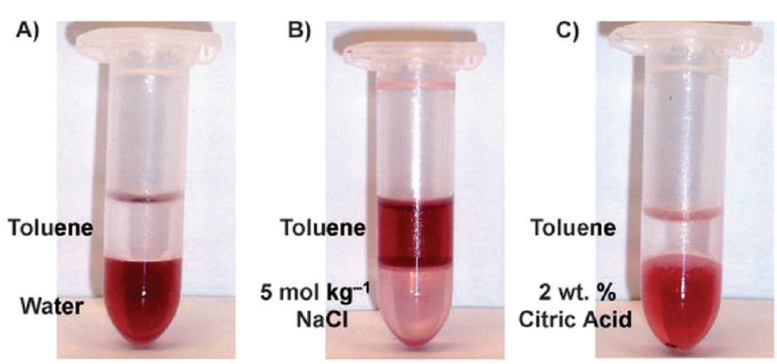

Figure 12. *Image of phase transfer of Au NPs (a) from water to organic phase by addition of NaCl (b) to water or citric acid (c).[82]*

2.4. Magnetic Nanoparticles

The synthesis of superparamagnetic nanoparticles has been intensively developed not only for its fundamental scientific interest but also for many technological applications: magnetic storage media, biosensing and medical applications, targeted drug delivery, contrast agents in magnetic resonance imaging.

Magnetic nanoparticles (MNPs) are commonly protected with a polymer coating to improve their dispersity and stability. Most investigated polymers for this purpose include poly(vinyl alcohol) (PVA), poly(D,L-lactide-co-glycolide) (PLGA), dextran, PEG, and chitosan.[98] One of the most promising coating materials is PEG because of its ability to provide a steric barrier to protein adsorption, which results in reduced uptake by macrophages of the reticuloendothelial system (RES).[98]

In 1975 Blakemore discovered magnetotactic bacteria, which now represent the most intensively studied biomagnetic system. Magnetotactic bacteria form a heterogeneous group of Gram-negative prokaryotes with morphological and habitat diversity which have an ability to synthesize fine (50-100 nm) intracellular membrane-bound ferromagnetic crystalline particles (Fig. 11) consisting of magnetite (Fe_3O_4) or greigite (Fe_3S_4) covered with an intracellular phospholipid membrane vacuole, forming structures called "magnetosomes". Chains of magnetosomes act as simple compass needles which passively torque the bacterial cells into alignment with the earth's magnetic field.[99]

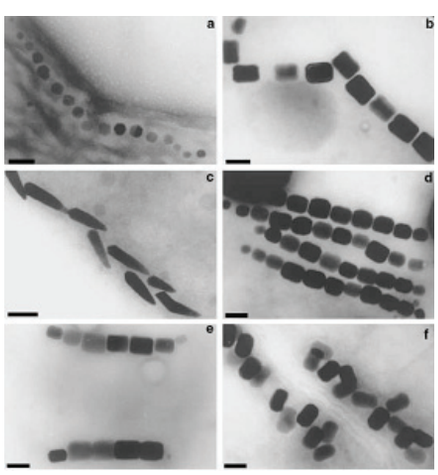

Figure 13. *Electron micrographs of crystal morphologies and intracellular organization of magnetosomes found in various magnetotactic bacteria. Shapes of magnetic crystals include cubo-octahedral (a), elongated hexagonal prismatic (b, d, e, f), and bullet-shaped morphologies (c). The particles are arranged in one (a, b, c), two (e), or multiple chains (d) or irregularly (f). The scale-bar is 100 nm. [99]*

Superparamagnetic iron oxide nanoparticles are engineered y-Fe_2O_3 or Fe_3O_4 particles that exhibit magnetic interaction when placed within a magnetic field. In addition, when encountered by an alternating magnetic field, the particles heat up, allowing for both imaging and therapy applications. Specifically, their utilization as an MRI contrast agent has been extensively studied.

2.4.1. Synthesis and phase transfer

The solution based synthetic methods for producing superparamagnetic iron oxide NPs can roughly be classified into two categories - hydrolytic and non-hydrolytic routes. Hydrolytic routes include among others: precipitation of iron oxides from aqueous Fe^{2+}/Fe^{3+} solutions by the addition of a base, use of microemulsions as templating nanoreactors, hydrothermal synthesis of ferrites under high pressure and temperature, sol-gel processes, electrochemical and sonochemical methods.[100-102]

Non-hydrolytic method for obtaining of magnetic NPs includes thermal decomposition of organometallic compounds in high-boiling organic solvents in the presence of surfactants (fatty acids, oleic acid or hexadecylamine), analogous to high-quality semiconductor nanocrystals.[103, 104] Another non-hydrolytic method is based on a phase transfer and separation mechanism occurring at the liquid-solid and the solid-solution interface, respectively, and it affords high pressure. From all methods so far described, this allows the best size and shape control for preparation of magnetic nanoparticles which are stabilized by surface-capping agents.[105]

Nonhydrolytically synthesized magnetic NPs are typically of high quality, but they are coated with hydrophobic ligands. Therefore in the case of biological applications it is necessary to exchange these ligands to achieve high colloidal stability in aqueous biofluids and to avoid aggregation which can occur under harsh physiological conditions.

The solvent- and ligand-exchange processes are usually time-consuming, exchange efficiencies can vary vastly, and complete removal of the hydrophobic surfactants is difficult. The remaining solvents or surfactants may result in opsonization (the binding of an opsonin, i.e., antibody, to a receptor on the pathogen's cell membrane) *in vivo* and other potential side effects, and thus the related biocompatibility issue needs to be addressed. It is the main reason to synthesize oxide NPs using hydrophilic or amphiphilic stabilizers.[66]

2.4.2. Surface modification and bioconjugation

Irrespective of how the stabilized magnetic nanoparticles have been prepared, usually they have to be protected from oxidation in air, or erosion by acids or bases.[106, 107] There are two strategies developed: coating with organic shells including surfactants and polymers, or coating with inorganic shells including silica, noble metals or oxides. The chemically simplest protection would be surface passivation by mild oxidation. Generally, the coatings of magnetic NPs may be performed *in situ* (during the "one-pot" synthesis) or by post-synthetic treatment following the approaches displayed in chapter 1.

To avoid aggregation of the nanoparticles and enhance the colloidal stability of ferrofluids, careful control of the surface charge and/or the use of specific surfactants are necessary. It may be achieved by the introduction of surface groups which become charged at a certain pH: for example, nowadays commercial ferrofluids are available which are stable either at pH <5 or pH >8 (alkaline ferrofluid).[108-110]

A polymer coating is among widely used methods to protect functional nanoparticles and enhance their colloidal stability by introducing a defined surface charge. This can be achieved by using simply the adsorption of polymers containing functional groups, such as carboxylic acids, phosphates and sulfates, to the surface of magnetite nanoparticles. Suitable polymers are poly(pyrrole), poly(aniline), and polyesters, which all may interact with the surface of the magnetic nanoparticle due to their free electron pairs [111-114]. Instead of adsorption, or grafting-onto, the polymer coating alternatively can be grown by a grafting-from polymerization from the nanoparticle surface, analogous to the process shown for noble metal particles.[115] Surface-grafting of the initiator is the crucial step to obtain well-defined core-shell architecture. In general, an important drawback of polymer coatings is that, if they are too thin, they provide an insufficient barrier towards oxygen or small ions, and therefore cannot protect the magnetic nanoparticles from degradation. Also, a polymer coating usually is not very stable at elevated temperatures.

An alternative protection of magnetic nanoparticles from oxidation is a noble-metal (e.g. Au) or silica coating. [116] A silica shell not only protects the magnetic core, but since it can easily be chemically modified, also may serve as a spacer to separate the core and additional functionalities, as for example organic dye molecules, to avoid unwanted interactions like luminescence quenching. As an example, magnetic nanoparticles were first coated with a thin silica shell, onto which the dye molecules were grafted.[117]

The easiest way to achieve water compatibility is the coating of magnetic NPs with hydrophilic ligands, containing charges or being hydrophilic polymer brushes, like PEG or dextran, alginate and chitosan.[118-122] Whereas the charges stabilize the colloidal particles against aggregation by Coulomb repulsion, a polymer coating of the NPs introduces a shorter-range steric repulsion.

As in the case of above described QDs and metal NPs the coating of magnetic nanoparticles with amphiphilic ligands attracts more and more attention. Among successful examples are the use of amphiphilic ligands, such as tetradecylphosphonate and PEG-2-tetradecylether inducing the formation of micelles around the magnetic NPs,[123] amphiphilic PEG-phospholipids or

contributing to the water solubility,[124] amphiphilic polystyrene-poly(acrylic acid) (PS-PAA) block copolymer,[125] and polylactide-PEG block copolymers.[123, 126, 127] Taking into account a variety of promising applications of magnetic nanoparticles each demanding particular material and surface design this list will be widely extended in the future. Some successful attempts to this extension are also performed in present work.

2.5. Cytotoxicity of Nanoparticles

2.5.1. Cytotoxicity of QDs

The question of nanotoxicity is still opened and needs much time for collecting all effects to get full impression. This topic is new and not so well and deeply explored. Toxicity of NCs causes problems while using them in bioapplications and also attracted by insufficient knowledge about them. That is why I see fit to shed a little light in my work to describe the problem of toxicity of the NPs. Main toxicity factors will be mentioned below.

Despite the potential health risks, promising applications of quantum dots include their use in the medical field as new drug-delivery and biomedical-imaging agents. For biological applications, QDs typically have a core/shell conjugate structure. The core of the QD is composed of II-VI materials (e.g., CdSe, CdTe, CdS, HgTe) and III-V materials (e.g., GaAs, GaN, InP, and InAs).[32] Many of these core constituents are known to be toxic at low concentrations; examples include cadmium, selenium, mercury, lead and arsenic. Therefore, if these QDs are exposed to conditions promoting degradation, such as an oxidative environment, toxicity related to the release of free ions is expected. Thus one of the crucial factors in QD toxicity is their stability. The cytotoxicity of QDs is reduced when their cores are protected from degradation. To prevent core degradation, an additional shell layer is complemented, making the QD more biocompatible. Additional functionalities or bioconjugates can be added to the surface in order to improve bioavailability or introduce bioactivity.[128] At the same time it is important to note, that surface charge also plays a role in toxicity with cationic surfaces being more toxic than anionic, and neutral surfaces being most biocompatible.[31, 129-131]

One of the options for biocompatible QDs is to use amphiphilic polymers to encapsulate the inorganic/organic system. Most commercial manufacturers of QDs prepare their biocompatible systems in this way. While larger polymeric coatings increase the hydrodynamic size, they yield very bright and stable materials. Kirchner et al. found PEG to lower cellular uptake of silica-coated QDs resulting in lower cytotoxicity.[31] Polyehtylene imine (PEI) coated QDs were tested in HeLa cells and it was found out that they are

endocytosed or macropinocytosed after one to two hours of incubation. However, since PEI-coated dots are toxic to cells, PEG was added to reduce this toxicity. The two different forms (PEI grafted with two PEG and PEI grafted with four PEG chains) of coated QDs exhibited different distribution patterns inside the cells and different cytotoxicity. The PEI-g-PEG4 QDs accumulated in the perinuclear region yielding better cell viability while the PEI-g-PEG2 QDs were distributed in the cytoplasm and had significant cytotoxic effects. The authors believe the cytotoxicity is due to the PEI polymer and not the presence of cadmium ions.[131]

While much of the properties of nanoparticles are due to their core structure, the surface coating determines much of their bioactivity. NonPEG-substituted QDs are exhibiting the highest cell toxicity. PEG substitution of QDs resulted in increased cell viability.[29]

Aggregation of QDs in solution takes place when the stabilizing ligands are removed from the nanocrystal surface via protonation or photooxidation. Cannot be excluded the possibility that similar processes may occur during *in vitro* or *in vivo* imaging, depending on the subcellular localization of the QDs and the local pH and redox environment they encounter. Protein or polymer QD coatings could be degraded *in vivo*, yielding exposed inorganic cores. Such unprotected QDs could represent a hazard for long-term use of QDs.[132]

2.5.2. Cytotoxicity of Au NPs

Gold nanoparticles have been used in medical applications during clinical testing of heavy metals to treat rheumatoid arthritis as early as the 1920s.[133] It was found (and confirmed recently [134]) that the gold nanoparticles accumulated inside the cells. The observed cellular changes were both dose- and time-dependent. It was also observed that the gold nanoparticles are not digested in the lysosomes, and even though the vacuoles accumulate near the nucleus, no nuclear penetration was seen. The gold nanoparticles used for bioapplications are typically represented by nanospheres, nanorods or nanoshells.[135]

More recently, it has been found that the chemicals involved in the synthesis of gold nanorods play a role in their potential cytotoxicity. Niidome et al. investigated the effect of PEG-modified gold nanorods on HeLa cells after 24 hours of incubation.[136] The strong cytotoxicity was associated with a low concentration of CTAB-stabilized gold nanorods. They proposed that free CTAB in solution was the source of the cytotoxic effect. This was corroborated when removal of excess CTAB from the PEG-modified gold-nanorod solution yielded 90% cell viability at the highest concentration tested (0.5 mM).

Since gold nanoparticles are reported to induce little toxicity, the polymer modified gold nanoparticles may display significant advances in the medical and clinical applications. For instance, PEG shells can greatly diversify the nanoparticle's properties and potential applications based on the multifunctionality of this polymer, such as organic solubility, water solubility and biocompatibility.

2.5.3. Cytotoxicity of magnetic NPs

In terms of cytotoxicity, while bare iron oxide nanoparticles exert some toxic effects, coated NPs have been found to be relatively nontoxic. Gupta et al. showed that PEG-coated nanoparticles were biocompatible as exposed cells remained more than 99% viability relative to control.[137] Using different PEG-based coatings, PMAO-PEG-coated iron oxide NPs were relatively nontoxic.[124] The effects of three surface coatings on iron oxide cytotoxicity were tested and one found MPEG-Asp3-NH_2-coated iron oxide nanoparticles almost non cytotoxic at the concentrations tested.[138] In comparison, MPEG-PAA- and PAA-coated iron oxide nanoparticles significantly reduced cell viability with only 16% of the cell remaining at an iron concentration of 400 μg ml^{-1}. The mechanism for iron oxide NPs cytotoxicity, when it does occur, has been linked to both cellular uptake and radical oxygen species production. Hu et al. found P(PEGMA)-immobilized nanoparticles relatively nontoxic, as exposed cells had greater than 93% viability.[139] Magnetic NPs coated with PEG exhibit long blood-circulation time [140]. Furthermore, the presence of PEG may increase the nanoparticle's colloidal stability through steric hindrance and provide non-fouling properties, making an iron oxide system capable of stable binding, protecting and delivering DNA for gene expression while maintaining superparamagnetic properties and high biocompatibility. [141]

Therefore, main factors determining cytotoxicity of NPs are shell protection, core and ligand nature, NP's charge, size and shape. Nevertheless many of the types of toxicity and their effects could be decreased by using cheap, simple, biocompatible, amphiphilic polyethyleneglycol and its derivatives. PEG is nontoxic, nonimmunogenic and resistant to protein fouling. PEG has been widely accepted as a nanoparticle coating for biomedical applications.[142, 143] Using of PEGs is proven to be perspective especially in bioapplications because it forms a sick shell around the NPs, makes it soluble in different solvents especially biofluids. Design of PEGs functionalities makes them suitable and promising for immobilization of peptides, proteins, antibodies. The reduced toxicity due to the PEG shell is also very important for using NCs of different nature in imaging and labeling.

3.1. Synthesis of stabilizers

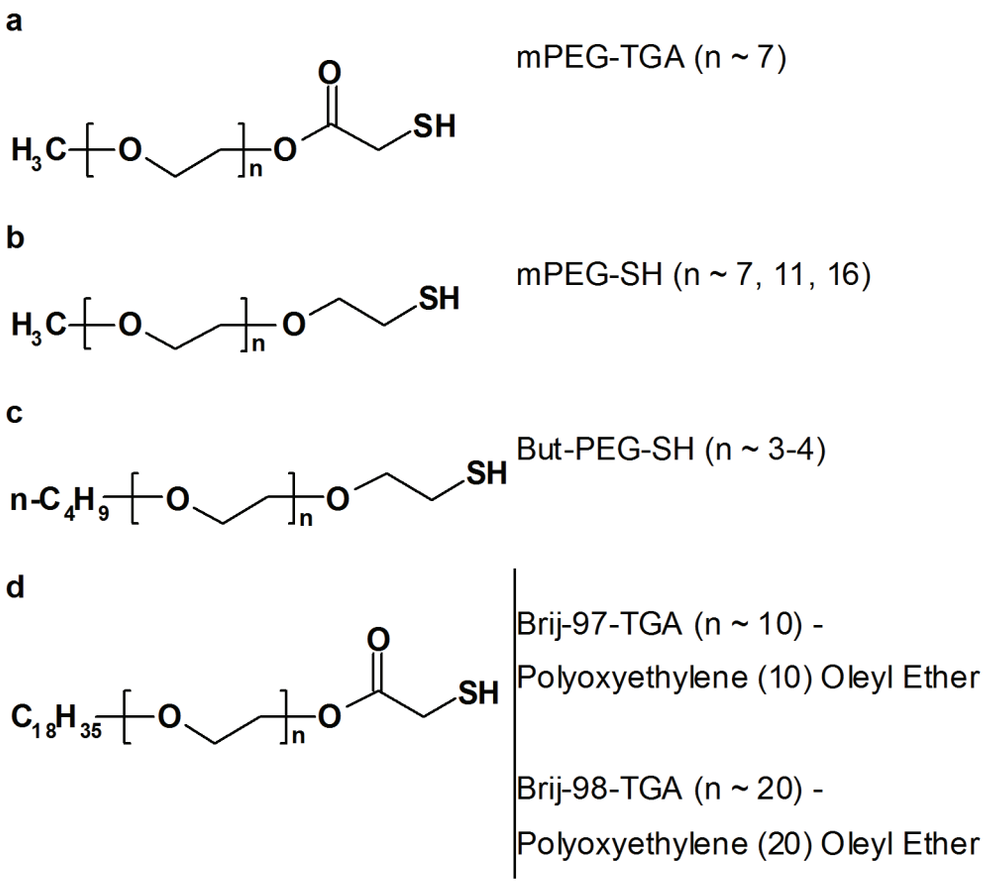

Scheme 1. *Chemical structure of the stabilizers used in present work*

3.1.1. mPEG-TGA

This compound was synthesized via the esterification of methoxypolyethylene glycol 350 by thioglycolic acid according to Essahli et al., Du and Brash without the usage of catalysts (see scheme 2).[144, 145]

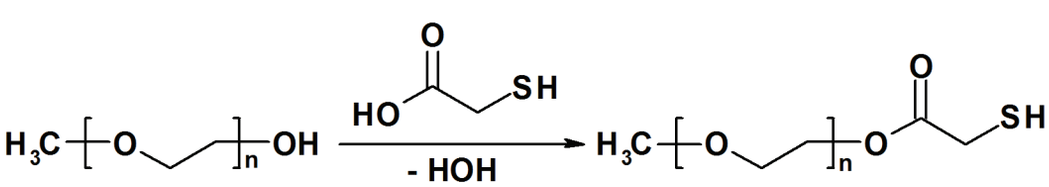

Scheme 2. *Synthesis of a stabilizer mPEG-TGA*

In a typical synthesis, 17.5 g (0.05 mol) of mPEG-350 were loaded into a 50 ml three-necked flask, equipped with a thermometer, thermocouple and Dean-Stark apparatus, and evacuated to drive off water from the chemicals before the addition of 13.8 g (0.15) mol of TGA. The mixture obtained was diluted with toluene up to 30-35 ml, the distillation trap was also filled with toluene. The mixture was heated at 125-130 °C for 48 hours till the end of water elimination. The solvent was evaporated and the excess of TGA was removed by vacuum distillation. ^{1}H NMR spectrum of the product is shown in figure 14. ^{1}H NMR (500 MHz, $CDCl_3$): δ (ppm) 2.0 (t, 0.44, *SH*), 3.25 (d, 0.93, CH_2S), 3.3 (s, 1.97, OCH_3), 3.6 (m, 16.77, CH_2CH_2), 3.7 (t, 1.37, OCH_2), 4.25 (t, 1.0, CH_2-O-C(O)).

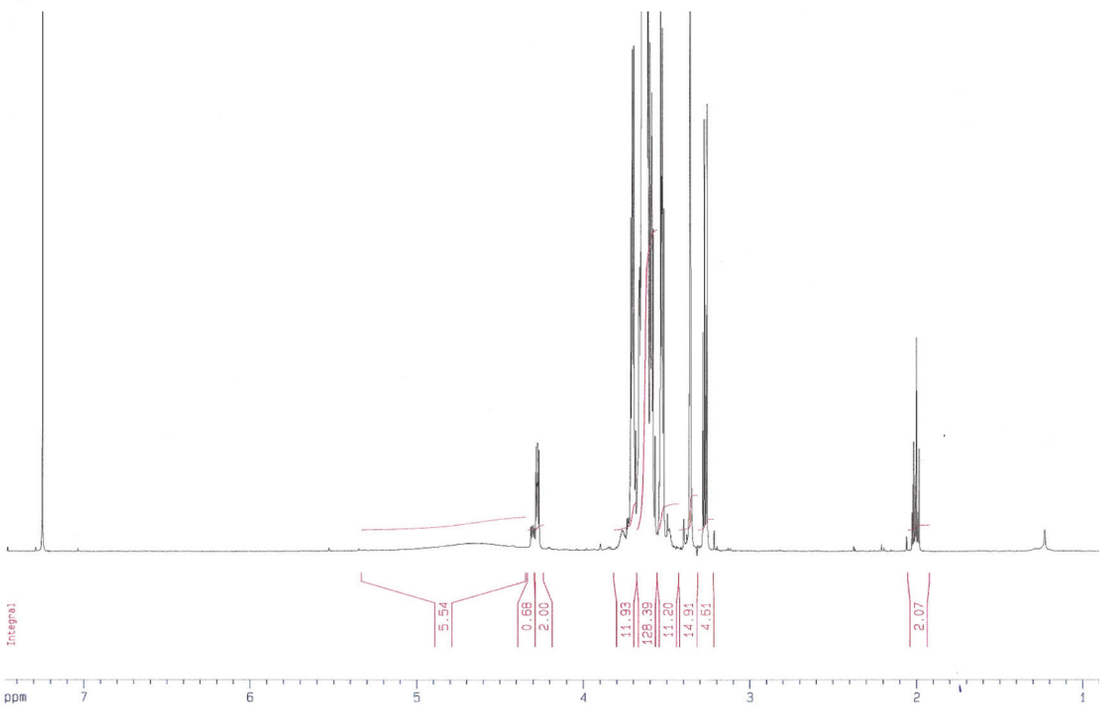

Figure 14. *^{1}H NMR (500 MHz) spectrum of mPEG-TGA in $CDCl_3$.*

3.1.2. mPEG-SH

This compound was synthesized according to Shimmin et al.[94] from methoxypolyethylene glycols possessing different molar weights of 350, 550 and 750 (see scheme 3).

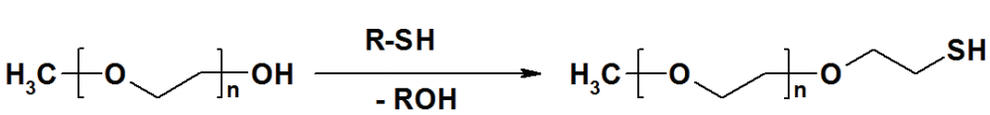

Scheme 3. *Synthesis of a stabilizer mPEG-SH*

Firstly, the adduct of diisopropyl azodicarboxylate with triphenylphosphine was obtained in THF at -30°C by slow dropping of 9.7 g (0.024 mol) of diisopropyl azodicarboxylate to 12.58 g (0.024 mol) of triphenylphosphine dissolved in tetrahydrofuran (THF), accompanied by precipitate formation. Subsequently, solution of 10.12 g (0.016 mol) of mPEG-350 and 3.8 g (0.024 mol) of thiolacetic acid in 50 mL of THF was added dropwise. The reaction proceeded at room temperature overnight. The solvent and excess of thiolacetic acid were evaporated. The mixture obtained was dissolved in water and filtered. The aqueous phase was washed with diethyl ether and evaporated. The dried product was treated three times with pentane to extract triphenylphosphine oxide. Thus synthesized ω-acetylthiomethoxypolyethylene glycol 350 was treated with 0.1 M HCl in methanol under argon atmosphere. The resulting thiol was separated from the methanol solution by drying in vacuum. ^{1}H NMR spectrum of the product is shown in figure 15. ^{1}H NMR (500 MHz, $CDCl_3$): δ (ppm) 1.58 (t, 0.94, *SH*), 2.68 (q, 1.96, CH_2SH), 3.36 (s, 3.0, CH_3O), 3.5-3.7 (m, 30.6, OCH_2CH_2O).

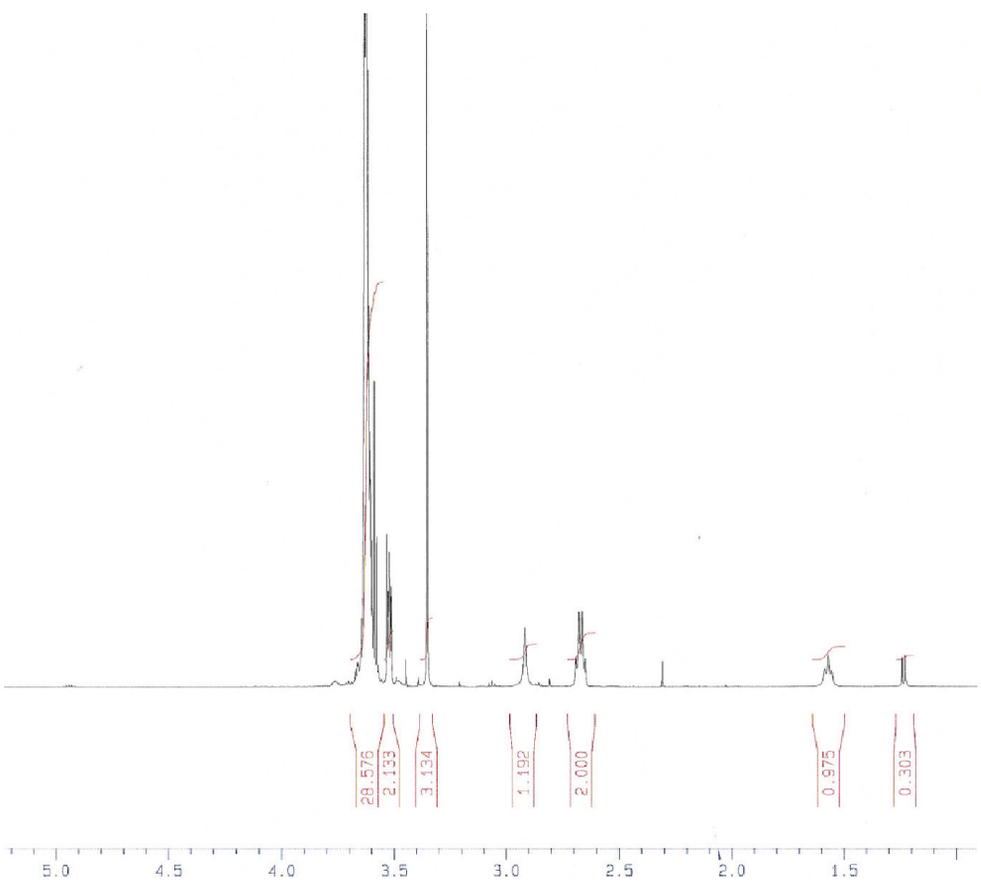

Figure 15. *^{1}H NMR (500 MHz) spectrum of mPEG-SH in $CDCl_3$.*

3.1.3. mPEG-COOH

A synthesis of mPEG-COOH was realized using a strong oxidizing agent - Jone's reagent (prepared by adding 70 g of chromium trioxide to 500 mL of distilled water in an ice bath) that converts terminal hydroxyl group of mPEG into carboxyl group according to scheme 4. [146]

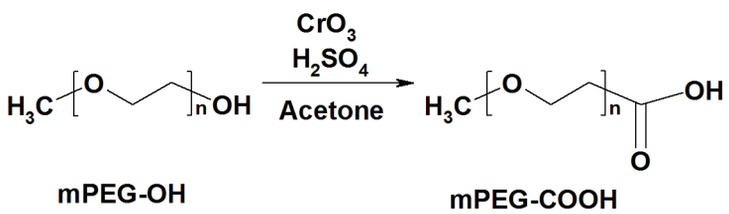

Scheme 4. *Synthesis of a stabilizer mPEG-COOH*

61 mL of concentrated sulfuric acid was added slowly into solution obtained. To obtain mPEG-COOH, 40 g of monomethoxy PEG were dissolved in 400 mL of acetone followed by the addition of 17 mL of Jone's reagent. The mixture was stirred for 24 h and quenched by addition of 5 mL of isopropanol. In order to remove chromium salts, the reaction mixture was filtered under vacuum yielding a clear acetone solution. This solution was concentrated to a viscous liquid using a rotary-evaporator and then dried in air. ^{1}H NMR spectrum of the product is shown in figure 16. ^{1}H NMR (500 MHz, $CDCl_3$): δ (ppm) 3.3 (s, 3.33, OCH_3), 3.6 (m, 20, CH_2CH_2), 4.2 (d, 1.93, $OCH_2C(O)$), 9.0 (br, 0.45, $COOH$).

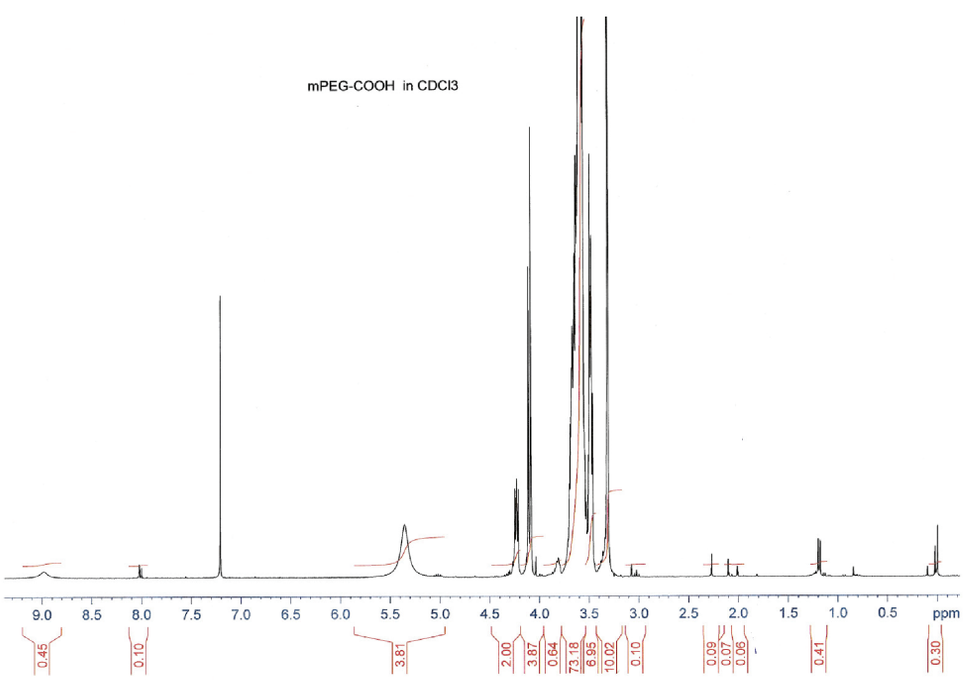

Figure 16. *^{1}H NMR spectrum of mPEG-COOH in $CDCl_3$.*

3.1.4. But-PEG-SH

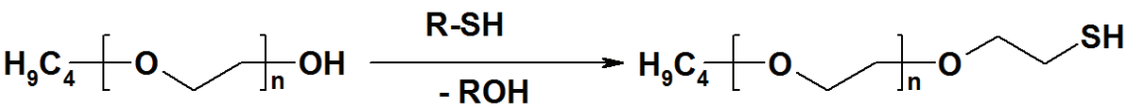

Scheme 5. *Synthesis of a stabilizer mPEG-SH.*

This stabilizer was obtained according to the synthetic procedure for mPEG-SH with slight modification: after the addition of water to the dried residue the suspension formed was filtered, yellow viscous intermediate was extracted by ether from the aqueous phase. The product after boiling in a solution of centimolar hydrochloric acid in methanol was distilled at 80-90 °C under reduced pressure (~0.2 mbar). ^{1}H NMR spectrum of the product is shown in figure 17. ^{1}H NMR (500 MHz, $CDCl_3$): δ (ppm) 0.9 (t, 0.9, CH_3), 1.25 (d, 1.2, *SH*), 1.35 (m, 0.98, -CH_2-), 1.55 (m, 1.3, -CH_2-), 2.7 (m, 0.89, CH_2SH), 3.4 (t, 1.0, CH_2O), 3.6 (m, 2.4, OCH_2CH_2O).

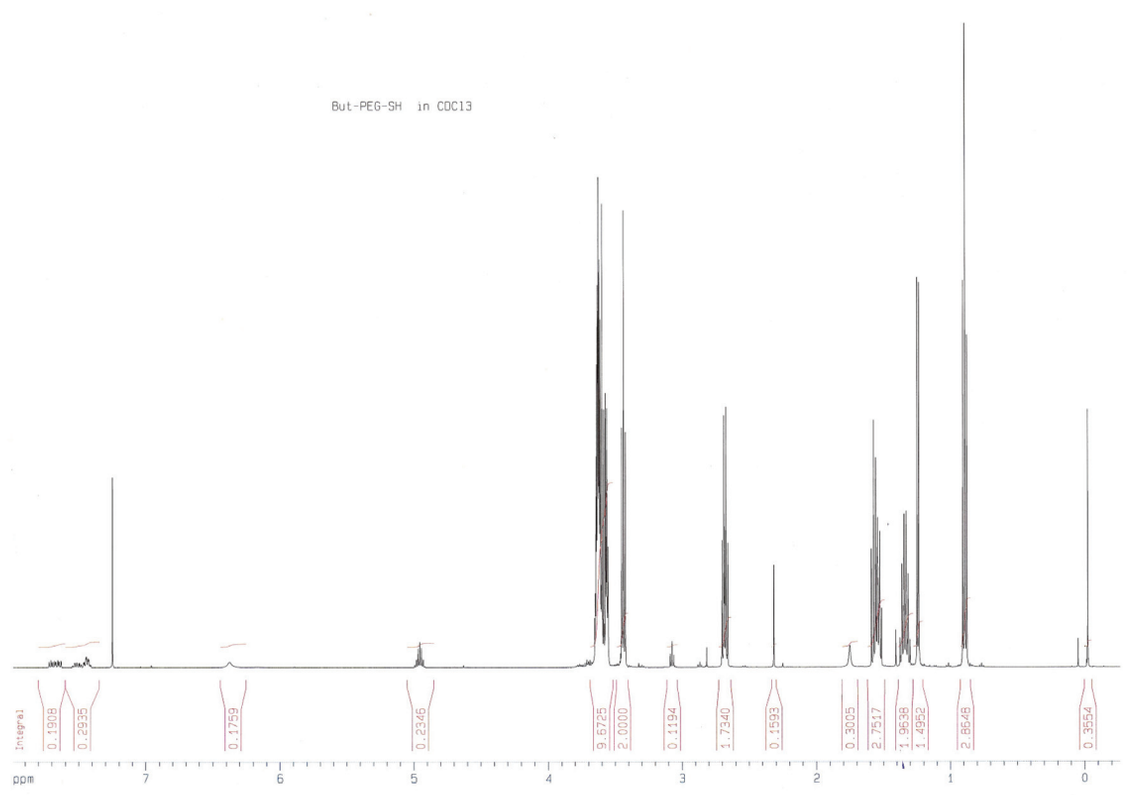

Figure 17. *^{1}H NMR (500 MHz) spectrum of But-PEG-SH in $CDCl_3$.*

3.2. Synthesis of amphiphilic CdTe nanocrystals

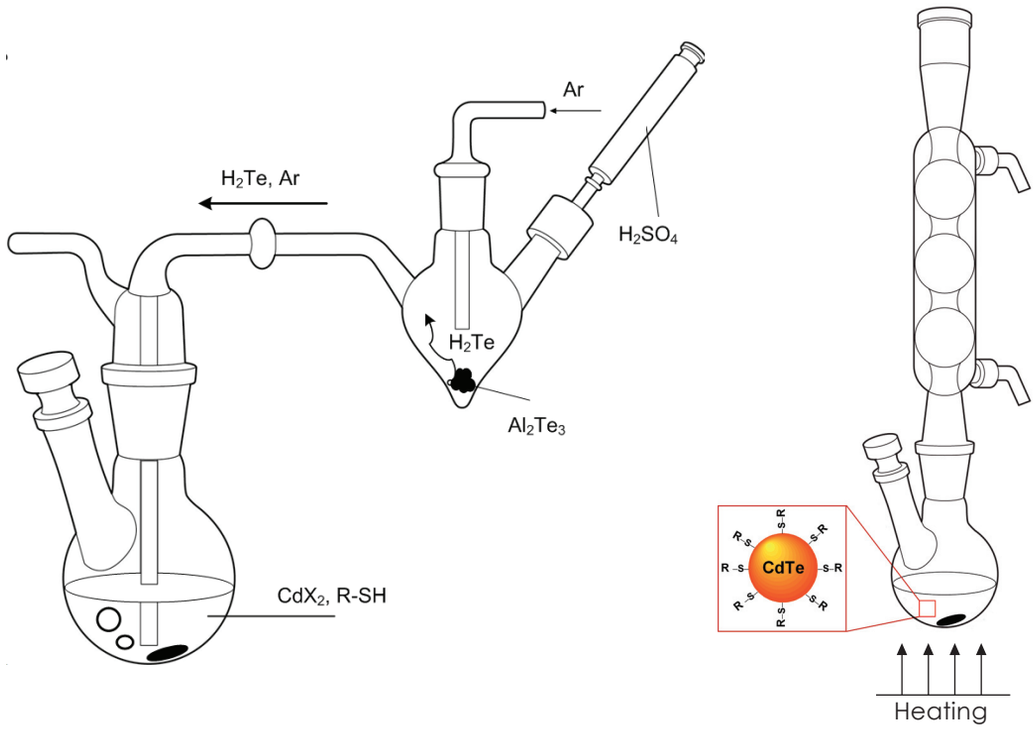

Figure 18. *Experimental setup for a synthesis of amphiphilic CdTe NCs both in water and in organic solvents (toluene, dimethylformamide, dimethylacetamide).*

3.2.1. Synthesis of CdTe/mPEG-TGA nanocrystals

CdTe NC colloids were synthesized using experimental set-up presented in figure 18, according to Gaponik et al.[51, 54] Typically, for toluene-based synthesis, 0.158 g (0.685 mmol) of $Cd(CH_3COO)_2$ were dissolved in 30 ml of toluene and 0.756 g (1.78 mmol) of mPEG-TGA were added under stirring. The resulted transparent solution was carefully deaerated by bubbling Ar for 20-30 min. Then H_2Te gas, generated by the reaction of 0.05g (0.114 mmol) of Al_2Te_3 with an excess of 0.5M H_2SO_4, was passed through the solution with slow Ar flow. The molar ratio of Cd^{2+}/Te^{2-}/mPEG-TGA was 1/0.5/1.3. Further nucleation and growth of NCs proceeded by refluxing at 110°C under open-air conditions. Colloid obtained was purified by reprecipitation procedure using diethylether as a non-solvent. Reprecipitation procedure includes addition of excess volume of diethylether (3:1) to the as prepared NPs solution and centrifugation for 3 min at 13400 rpm. The formed precipitate is redissolved in a desired solvent.

3.2.2. Synthesis of CdTe/mPEG-SH nanocrystals

Owing to intrinsic amphiphilicity of mPEG-SH stabilizer, synthesis of CdTe NCs is achievable in different media: water, dimethylformamide (DMF), dimethylacetamide (DMA), toluene, employing the same procedure and amounts of precursors. In the case of aqueous approach $Cd(ClO_4)_2 \times 6H_2O$ was used as a Cd source. Additionally, before H_2Te gas injection, pH of the precursor solution was adjusted to 12 by 1M NaOH. In organic media $Cd(CH_3COO)_2$ was used instead of $Cd(ClO_4)_2 \times 6H_2O$ without pH adjustment. The organics-based NC colloids were purified by reprecipitation procedure employing hexane as a non-solvent. The aqueous colloids were purified using dialysis against Milli-Q water.

In a typical synthesis in DMA (or DMF), 0.16 g (0.7 mmol) of $Cd(CH_3COO)_2$ and 0.33 g (0.9 mmol) of mPEG-SH (Mw ~ 366) were dissolved in 30 mL of DMA (DMF) followed by deaeration by argon bubbling for 30 min. Under vigorous stirring, H_2Te gas, generated by the reaction of 0.1 g (0.228 mmol) of Al_2Te_3 lumps with an excess of 0.5 M H_2SO_4 solution, was injected into the reaction mixture with a slow Ar flow. The molar ratio of Cd^{2+}/Te^{2-}/mPEG-SH = 1/1/1.3. Formation and growth of the nanoparticles proceeded upon reflux. The reaction was terminated after the PL maximum reached 640 nm (4 h - in DMA, 36 h - in DMF). Purification of NCs was achieved via precipitation by a non-solvent (n-hexane). The initial as-prepared solution of QDs was firstly mixed with the equal volume of diethylether. n-Hexane was added in three-fold excess. The mixture obtained was centrifuged and the precipitate was dried before the dissolution in other necessary solvents.

3.2.3. Phase transfer of CdTe/mPEG-SH nanocrystals

Purified CdTe/mPEG-TGA or CdTe/mPEG-SH colloid which was dissolved in toluene was added to water forming 2-phase system (upper layer of CdTe NPs in toluene and bottom layer of pure water. After ca. 1 hour the nanoparticles permeated spontaneously from organic phase into water. In the same manner performed transfer of CdTe/mPEG-SH nanocrystals from initial aqueous solution into chloroform takes 10-12 hours. In both cases the transfer can be strongly accelerated by vigorous shaking. Similarly, tri-phase spontaneous transport of toluene-based CdTe/mPEG-SH nanoparticles from toluene through water into chloroform was carried out.

3.2.4. GUV preparation

As a reference sample for the GUV (giant unilamellar vesicles) experiment, hydrophilic CdTe nanoparticles stabilized by thioglycolic acid (TGA) were

prepared according to the procedure reported in ref.[51] Before GUV experiment CdTe/TGA nanoparticles were purified by reprecipitation procedure described in ref.[54].

GUV preparation with platinum wire is described in detail in ref.[147] Briefly, platinum wires and vials were cleaned by sonication in ethanol for 20 minutes. 4 µL of 1,2-dioleoyl-sn-glycero-3-phosphocholine (DOPC) solution in chloroform (25 mg/ml) and 0.5 µL of dye 3,3'-dioctadecyloxacarbocyanine perchlorate (DiO) dye solution in chloroform (1.3 mM) were mixed and diluted with 96 µL of chloroform. 5 µL of this mixture were spread onto platinum wires. After deposition the wires were dipped into 350 mL of 300mM sucrose solution. For electroformation, the platinum wires were exposed to 10 Hz AC for 1 hour and following 2 Hz AC for 30 min with a 2 V voltage.

For microscopy LabTek chambers were filled with buffer solution (BSA) (10 mg/mL) for 1 hour for coating. Then 50 µL of GUV solution and 350 µL of 1X buffer solution (PBS) were injected into the wells. Afterwards, 5 µL of amphiphilic CdTe/mPEG-SH QDs colloid (concentration $8.4x10^{-5}$ M) and 10 µL of hydrophilic CdTe/TGA QDs colloid (concentration $4x10^{-5}$ M) were added to different wells. The sizes of CdTe/mPEG-SH and CdTe/TGA QDs were estimated using sizing curve reported in ref.[51] and were 2.9 and 3 nm, respectively.

3.3. Synthesis of Au/mPEG-SH nanoparticles

3.3.1. Two-phase (Brust's) method with mPEG-SH instead of dodecanethiol.

0.118 g (0.3 mmol) of $HAuCl_4x3H_2O$ was dissolved in 30 mL of water. 0.328 g (0.6 mmol) of tetraoctylammonium bromide (TOAB) as phase transfer agent in 80 mL of toluene was added. After the intensive stirring the toluene phase turned yellow due to transfer and water phase became colourless. 0.11 g (0.3 mmol) mPEG-SH (Table 1b) in 10 mL of toluene was added to the solution and after 10 min of mixing reduced by 0.114 (3 mmol) $NaBH_4$ dissolved in cooled 30 mL of water. Formed brown solution was left stirring overnight. After the synthesis Au NCs were accumulated in the aqueous phase.

3.3.2. Direct synthesis of Au/mPEG-SH NCs.

For a preparation of Au/mPEG-SH NCs at a molar ratio of gold/stabilizer = 1/1, 10 mL of water solution containing 0.1098 g (0.3 mmol) of mPEG350-SH (or mPEG500-SH, mPEG750-SH) were vigorously mixed with $HAuCl_4x3H_2O$ (0.118 g, 0.3 mmol) dissolved in 30 mL of H_2O, for 10-15 min at room temperature (Figure 19). Thereafter 30 mL of the freshly prepared $NaBH_4$

(0.113 g, 3 mmol) aqueous solution were added to the mixture obtained. The reaction mixture turned dark brown and has been stirred overnight. The thus prepared gold colloid was filtered in order to separate large aggregates of NCs. Au nanoparticles were isolated from supernatant by evaporation of water on rotor evaporator. The nanocrystals synthesized are soluble both in polar and non-polar solvents.

3.3.3. Au/citrate NCs (3±1 nm)

Au/citrate NCs (3±1 nm) were synthesized according to Braun [148] at room temperature: 1 mL of 1% $HAuCl_4$ solution was added to 90 mL H_2O. 1 mL of 1% trisodium citrate was injected to the precursors after 1 min of stirring. Another 1 min was followed by reducing with 0.075% $NaBH_4$ in 1 mL of 1% trisodium citrate.

3.3.4. Au/citrate NCs (30±10 nm)

Au/citrate NCs (30±10 nm) were synthesized according to Ziegler's method [149]: 2.5 mL of 0.2% $HAuCl_4$ solution in H_2O was heated to boiling point and then 1 mL of the 1% trisodium-citrate with 0.05% ascorbic acid solution was added under intensive stirring. After 5 min boiling it was cooled down.

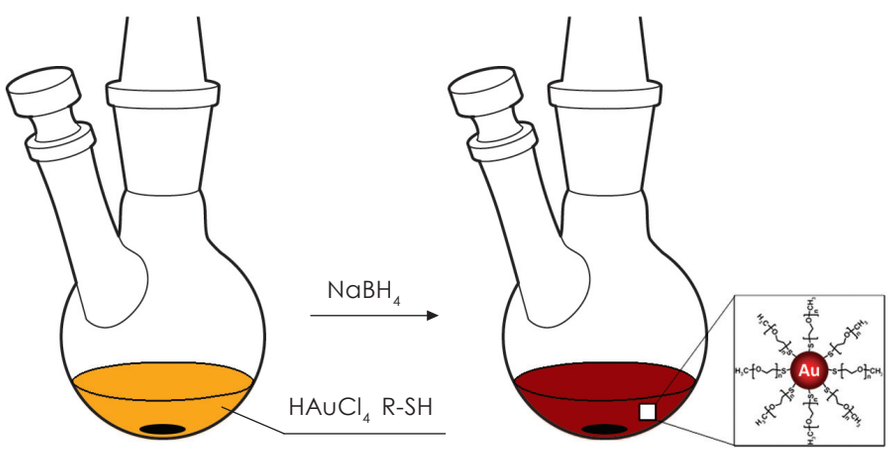

Figure 19. *Experimental setup for a "one-pot" one-phase synthesis of amphiphilic Au NCs in water.*

3.3.5. Phase transfer of Au/mPEG-SH nanoparticles

Phase transfer was demonstrated using three solvents of different polarity: toluene, water and chloroform. Au NCs being dispersed in toluene were precipitated by addition of hexane in order to remove unreacted species. After subsequent dissolving of gold NPs in toluene, colloid obtained was carefully placed on top of water layer poured over chloroform layer in 10 mL vial. The NPs have migrated spontaneously from toluene phase via water into chloroform without any treatment.

3.3.6. Preparations of polymer films with Au/mPEG-SH nanoparticles

With polystyrene (PS): 0.1 g of commercial PS (Aldrich) was dissolved in 0.5 mL of toluene and mixed with Au/mPEG-SH NPs. The mixture was dropped on the quartz glass and dried in the oven until toluene evaporation forming thin film.

With polyvynilalcohol (PVA): 10% aqueous solution of PVA was mixed with Au/mPEG-SH NPs and dried in the oven.

3.4. Synthesis of iron oxide nanocrystals

The general strategy of the Fe_3O_4 NCs synthesis was pyrolysis of $Fe(acac)_3$ (Scheme 6) at 280 °C.

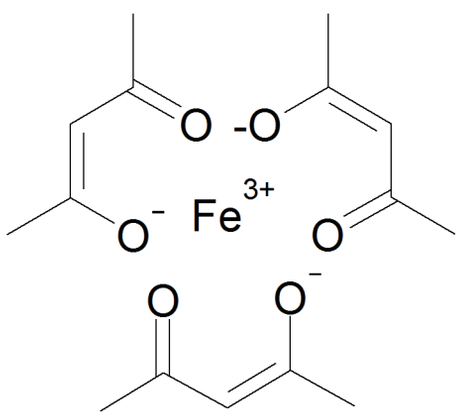

Scheme 6. *Formula of Iron (III) acetylacetonate.*

$Fe(acac)_3$ was firstly dissolved in the high boiling solvent. The resultant solution was evacuated for 1 h at 70 °C and purged with argon at room temperature to remove oxygene and subsequently heated to 280 °C. The reaction system was protected by argon flowing throughout the whole process (Fig. 20). Black product was redissolved in toluene and precipitated by hexane.[150]

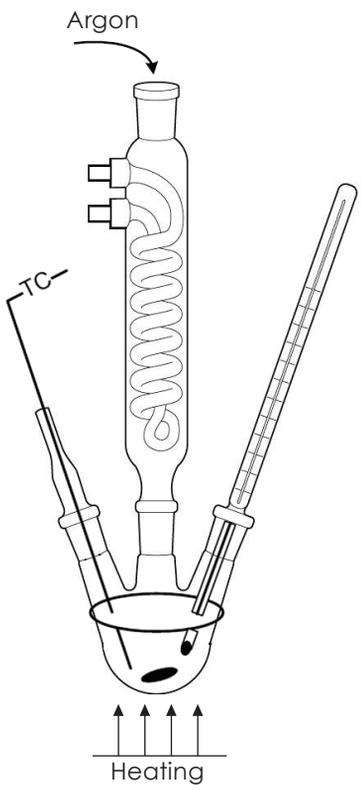

Figure 20. *Experimental setup for a synthesis of amphiphilic Fe_3O_4 NCs.*

Synthesis 1:

Mixture of 7.2 g (8mmol) of Fe (III) oleate and 1.14 g (4mmol) of oleic acid was dissolved in 40 g of 1-octadecene at room temperature. The reaction flask with all components was evacuated at elevated temperature (50-60 °C) for removing the volatile solvents and filled by inert Ar atmosphere. It was heated to 320 °C for 4-5 hours.

Synthesis 2:

Iron acetylacetonate 0.10g (0.28mmol) was added to the solution of Ph_2O 18 mL, mPEG350-COOH 0.53g (1.4mmol), oleylamine 0.29g (1mmol). After the dearation reaction T = 255-260 °C during 24 h.

Synthesis 3:

a. iron acetylacetonate 0.04g (0.1mmol), mPEG350-COOH 0.3g (0.8mmol), dodecylamine 0.056g (0.3mmol), mPEG-OH (MW 350) 4mL, T = 280 °C, 5 hours.

b. iron acetylacetonate 0.04g (0.1mmol), mPEG750-COOH 0.62g (0.8mmol), dodecylamine 0.06g (0.3mmol), mPEG-OH (MW 350) 7mL, T = 290 °C, 5 hours.

Synthesis 4:

iron acetylacetonate 0.04g (0.1mmol), mPEG-OH (MW 350) 7mL, T = 280-285 °C, 5 hours.

Synthesis 5:

iron acetylacetonate 0.04g (0.1mmol), mPEG750-COOH 0.62g (0.8mmol), mPEG-OH (MW 350) 8mL, T = 280-285 °C, 5 hours.

3.4.1. Phase transfer of Fe_3O_4 nanocrystals

Phase transfer was demonstrated using three solvents of different polarity: toluene, water and chloroform. Fe_3O_4 NPs being dispersed in toluene were precipitated by addition of hexane in order to remove unreacted species. After subsequent dissolving of iron oxide NPs in toluene, colloid obtained was carefully placed on top of water layer which respectively was poured on to chloroform layer in a 3 mL vial. The NPs have migrated spontaneously from toluene phase via water into chloroform without any treatment.

3.5. Characterization of nanocrystals

UV-Vis absorption spectra were collected with a Cary 50 spectrophotometer (Varian Inc., Palo Alto, USA). Fluorescence spectra were measured at room temperature using a FluoroMax-4 spectrofluorimeter (HORIBA Jobin Yvon Inc., Edison, NJ, USA). All spectra were taken at room temperature. The photoluminescence quantum efficiency (PL QEs) of the CdTe nanocrystal solutions were estimated according to the procedure described in ref.[151] by comparison with Rhodamine 6G and Rh101 in ethanol assuming their PL QEs to be 95 and 96%, respectively. PL life times were measured by FluoroCube Time Correlated Single Photon Counting (TCSPC) HORIBA Jobin Yvon.

Powder X-ray diffraction (XRD) measurements were carried out with a D5000 diffractometer (Siemens, Cu Kα radiation). Samples for XRD were made by placing finely dispersed powders of nanocrystals on a standard Si wafer.

FT-IR spectra were recorded on a Thermo Nicolet Avatar 360 spectrometer.

TEM images were obtained on a Tecnai T20 microscope (FEI) and on a EM208 microscope (Philips), operating at 200 kV and 100 kV, respectively. Samples for transmission electron microscopy (TEM) were prepared by dropping diluted nanoparticle solutions in toluene on to copper grids coated with a thin Formvar-carbon film with subsequent evaporation of the solvent.

3. EXPERIMENTAL PART

Nuclear magnetic resonance (NMR) spectra were recorded on a Bruker DRX 500 P, 500 MHz for ^{1}H-NMR.

Dynamic light scattering (DLS) and zeta-potential measurements were performed at room temperature using a Beckman Coulter Delsa Nano C Particle Analyzer instrument having a He-Ne laser at a wavelength of 632 nm. All colloids were filtered through Millipore membranes (0.2 μm pore size) before the measurements.

Confocal microscopy images were acquired using Zeiss LSM 510 Meta microscope equipped with a 40X NA 1.2 UV-VIS-IR C-Apocromat water-immersion objective (Zeiss) and a 488 Argon-Ion laser with 10% power as an excitation source. NFT 545 filter was used to separate the signals from green emitting dye DiO and orange fluorescing QDs. For additional filtering band pass 505-550 was employed for green emission and long pass 585 - for orange emission. Imaging was performed immediately after QDs addition and in 1, 2, 3, 4, 5 hours after addition as well as after overnight incubation. Nearly 400 GUVs were observed after 5 hours and overnight incubation.

Dark field microscopy imaging was carried out in a Carl Zeiss Axio Scope upright microscope using an oil condenser (Carl Zeiss Achroplan) and equipped with a digital camera (Panasonic Lumix DMC FZ50).

4. RESULTS AND DISCUSSION

As it was shown in the literature overview, there is a demand for new straightforward approaches for stabilization and solubilization of various nanoparticulate materials in their colloidal form, that pave way for fabrication of materials possessing compatibility with wide range of dispersing media. Therefore in this thesis a new general method to form stable nanocrystals in water and organics using amphiphilic polymers generated through simple and low cost methods is presented and discussed. Amphiphilic coating agents are formed using a thiolated polyethylene glycol methyl ether (mPEG-SH) as a starting material. These materials are available with a wide variety of chain lengths. PEG size influences physiological stability and biocompatibility of entire nanoparticle.

The amphiphilic PEG-based polymers are generally commercially available for relatively low prices that make them more attractive in comparison to other molecules such as peptides and phospholipids in large-scale preparation.

The incorporation of poly(ethylene glycol) has been well-known as the best method to obtain water-soluble and biocompatible materials because of its high solubility in aqueous media, non-toxicity, easy clearance from the reticuloendothelial system and low immunogenicity.[152] PEG not only enhances the aqueous solubility of the QDs but also reduces nonspecific adhesion to biological cells. Pegylation has been proven to be fully compatible with QD surface chemistries and is bound to play a prevalent role when optimizing *in vivo* pharmacokinetics of QD bio-probes.

The method of obtaining of amphiphilic NPs is quite general, and below we demonstrate the technique using our model systems comprising semiconductor CdTe nanocrystals as well as nanoscale noble metal (Au) and magnetic (Fe_3O_4) nanoparticles. This approach is based on anchoring PEG segment to the surface of nanoparticle to form an amphiphilic palisade. Anchoring is realized via interaction of -SH (for CdTe and Au) or -COOH (in the case of magnetite) functional groups with particle's surface. The resulting amphiphilicity of the nanocrystals is an inherent property of their surface and it is preserved also after careful washing out of solution of any excess of the ligand. The nanocrystals reversibly transfer between different phases spontaneously, i.e. without any adjustment of ionic strength, pH or composition of the phases. Such reversible and spontaneous phase transfer of nanocrystals between solvents of different chemical nature has a great potential for many applications as it constitutes a large degree of control of nanocrystals compatibility with technological processes or with bio-environments such as water, various buffers and cell media as well as their assembly and self-assembly capabilities.

4. RESULTS AND DISCUSSION

4.1. Synthesis and Characterization of Amphiphilic CdTe nanocrystals

The synthesis of CdTe nanocrystals capped with thiolated methoxypolyethylene glycols (Table 1 in Experimental Part) can be performed both in aqueous and organics media (toluene, dimethylacetamide (DMA), dimethylformamide (DMF)). The nanocrystals obtained are found to be compatible with a variety of solvents.

Up to date, there is no report on a direct synthesis of QDs with mPEG-SH used as a stabilizer. This method would be very useful to avoid the ligand exchange step and obtain amphiphilic QDs in one-pot way.

4.1.1. CdTe/mPEG-TGA

The well-developed aqueous synthesis of thiol-capped CdTe NCs was chosen as a starting system for the purpose of the present work.[51] Since TGA is known as one of the best ligands for these particles, the first amphiphilic ligand developed here was the ester of TGA and methoxypolyethylene glycol (mPEG) (Table 1a, Experimental Part). This mPEG-TGA ester is readily soluble both in water and in nonpolar organics (toluene, chloroform). The addition of this ligand to an aqueous colloidal solution of CdTe NCs stabilized with short chain thiols (TGA, mercaptopropionic acid) resulted in the spontaneous phase transfer of these nanoparticles into the organic phase (toluene) thus confirming the ability of this stabilizer to serve as a phase transfer mediator.

In a second step the synthesis of the nanoparticles was performed in water in the presence of this mPEG-TGA ligand only. The properties of the evolving well emitting CdTe nanocrystals were comparable to those prepared with pure TGA. However, no amphiphility was observed.

To understand, which possible chemical transformations might happen with a mPEG-TGA during a synthesis a detailed FTIR investigation of these molecules before and after boiling at reaction conditions was performed. The results (Figure 21) showed that the ester bond of mPEG-TGA is not stable and breaks during boiling in water at a relatively high pH used. Indeed, the spectrum of hydrolysis products does not show the band corresponding to C=O bond vibration at 1700-1735 cm^{-1}, which is characteristic for carboxyl and ester groups, confirming decomposition of ester group due to hydrolysis. Most probably the growing nanocrystals were stabilized by TGA being formed as a product of the hydrolysis of the ester. The stabilization by TGA can explain a formation of strongly emitting and stable, but not amphiphilic colloidal particles.

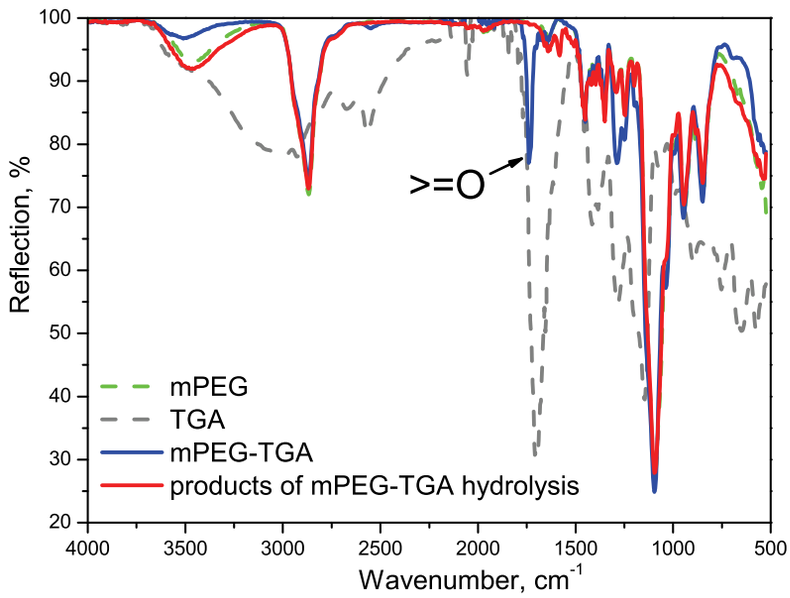

Figure 21. *IR-spectra of mPEG 350 and TGA (as the references), mPEG-TGA ester, the product of mPEG-TGA hydrolysis after boiling at 100 °C for 24h in water solution at pH 12.*

In order to avoid this hydrolysis, in a third step the synthesis with mPEG-TGA as the stabilizer molecule was performed in water-free toluene.

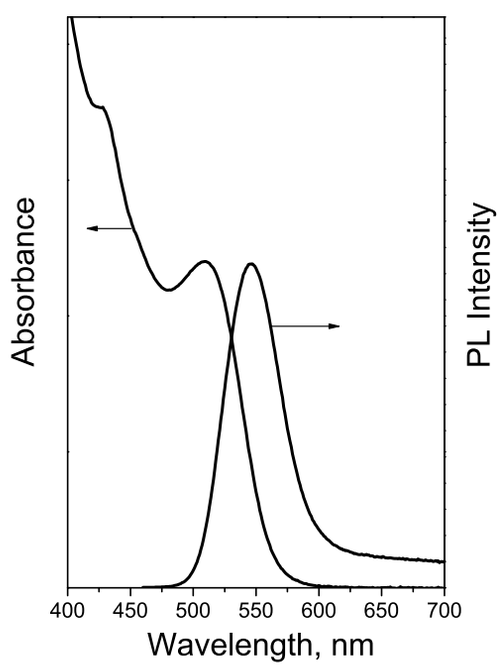

Figure 22. *Absorbance and PL (λ_{ex} = 450 nm) spectra of CdTe/mPEG-TGA NCs synthesized in toluene.*

The resulting nanocrystals are small (below ca. 2 nm according to sizing curve shown in ref. 2) and possess moderate band-gap emission in the green spectral region (PL QY is ca.13%) together with a pronounced trap-related emission appearing as a shoulder to the low energy side of the band-gap emission (see Figure 22). The appearance of additional absorption maximum at ca. 428 nm can be attributed to the formation of small molecular-like species (so named nanoclusters) which were not further explored in the framework of the present study.

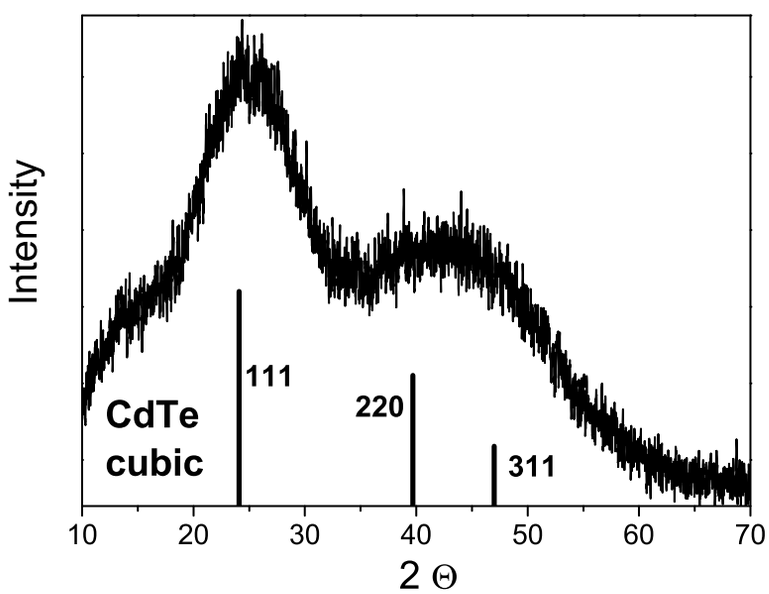

Figure 23. *XRD pattern of CdTe/mPEG-TGA nanocrystals synthesized in toluene. The line spectra show the bulk cubic CdTe reflexes.*

The powder XRD (Figure 23) revealed the main features of very small crystallites exhibiting the cubic phase of CdTe. The reflexes are shifted to the larger angles, indicating formation of CdS crystal phase, which is characteristic for thiol-capped CdTe nanocrystals.[50, 51, 54] This synthesis was relatively slow and larger sized particles were not achieved even under prolonged reflux. After separating from the remaining excess of ligand and reaction by-products (multiple precipitations with diethyl ether, centrifugation and dissolving in pure toluene) the nanoparticles were found to be spontaneously soluble also in water. However, the reversible transfer from water into nonpolar organics is possible only by addition of the excess of mPEG-TGA.

4.1.2. CdTe/mPEG-SH

As the use of the ester in the aqueous synthesis has to be avoided, another closely related ligand was synthesized by the direct thiolation of the mPEG. Obtained mPEG-SH (Table 1b, Experimental Part) molecules show solubility in water and in nonpolar solvents and may be used as a post-preparative phase transfer mediator similar to mPEG-TGA. The nanoparticle synthesis in the presence of mPEG-SH was successfully performed both in water and in toluene. In both cases we still were not able to grow the nanocrystals larger than 2 nm. However, the optical quality of mPEG-SH stabilized CdTe NCs (pronounced absorption maxima, almost no trap emission) is doubtless superior than that of the mPEG-TGA stabilized nanoparticles synthesized in toluene (see Figure 24). As awaited, mPEG-SH imparts inherent amphiphilicity to the nanoparticles. Moreover, the nanocrystals prepared with this ligand in water are compatible with most of the common polar and nonpolar solvents. It was literally impossible to find any "bad solvent" to perform common size-selective precipitation procedure for their cleaning. These NC colloids were purified solely by dialysis.

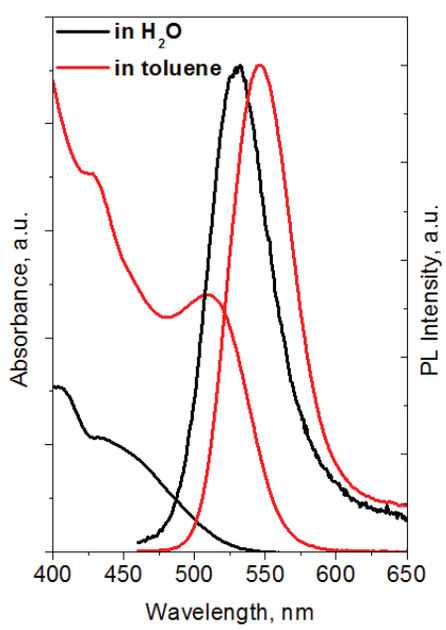

Figure 24. *Absorbance and PL (λ_{ex} = 450 nm) spectra of CdTe/mPEG-SH NCs synthesized during 27 hours in toluene (red) and 29 hours in aqueous (black) solutions.*

TEM images of green-emitting CdTe/mPEG-SH NCs synthesized in toluene show that their averaged size is about 2 nm in diameter (see Figure 25). It is clearly seen, that the particles are almost spherical in shape. However, the formation of some aggregates and merged bigger nanocrystals could not be excluded.

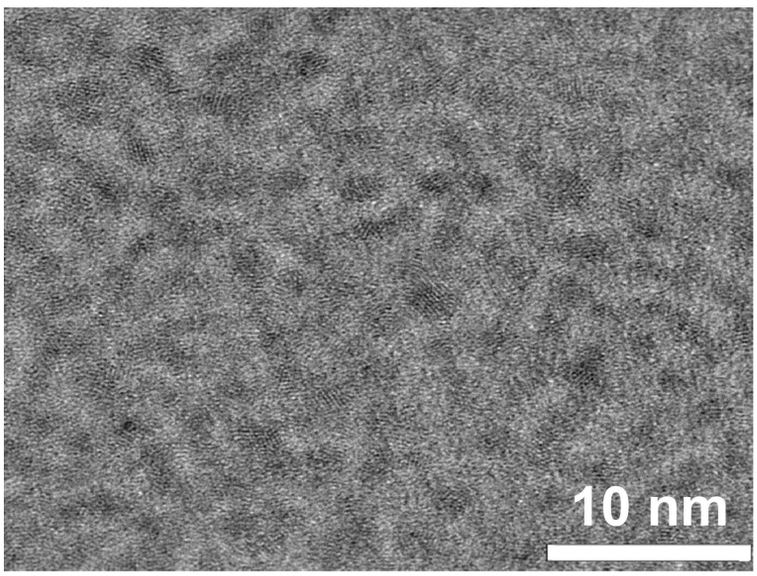

Figure 25. *TEM image of green-emitting CdTe/mPEG-SH NCs.*

In order to achieve size control and to grow bigger nanoparticles following investigations have been performed. As the syntheses performed in toluene and water proceeded at 110°C and 100°C respectively, these relatively low temperatures may limit the growth of NCs by size of ~2 nm. Employing as solvents DMF and DMA possessing higher boiling temperature (T_{bp} of DMF = 153.1°C, T_{bp} of DMA = 166.1°C) [153] allows obtaining CdTe NCs with average diameter of up to ~4 nm emitting in a wide spectral region from 540 to 640 nm (Fig. 26). Absorbance and PL spectra of CdTe/mPEG-SH colloids grown in DMA are shown in Fig. 27.

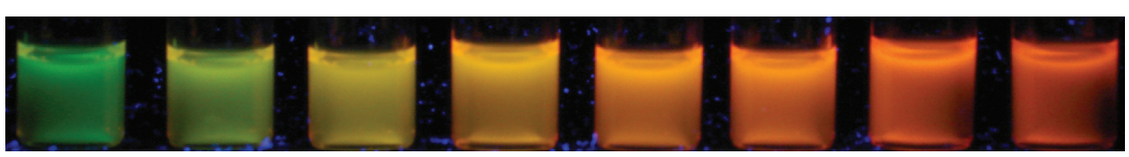

Figure 26. *Set of amphiphilic colloidal CdTe solutions having different emission, synthesized in DMF after 16 min, 30 min, 45 min, 1 h, 1.5 h, 2 h, 3 h, 4 h, respectively, under UV light (λ_{ex} = 365 nm).*

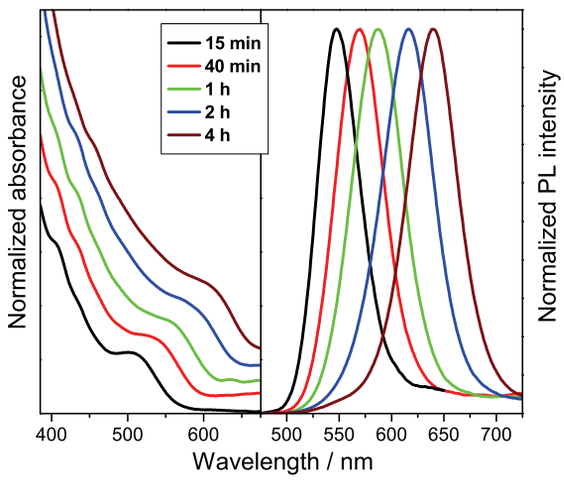

Figure 27. *Absorbance and PL (λ_{ex} = 450 nm) spectra of CdTe/mPEG-SH NCs synthesized in DMA as a function of the reflux time.*

Interesting that in DMA the growth of nanoparticles is app. 10 times faster than that in DMF (PL maximum of 640 nm was reached in 4 h for reaction in DMA and in 41 h for DMF) (see Fig. 28), at the same time the difference between their boiling temperatures is only 13oC (see above). This observation suggests that besides the temperature of the reaction mixture important role plays solvation ability of the medium towards precursors and nuclei. DMA and DMF are known as coordinating solvents which act as n-donors and thereby are good for solving cations.[153] Thus DMA possessing higher boiling point, donor number (Lewis basicity) and dielectric constant (in terms of polarity) in comparison with DMF, facilitates growth rate of CdTe nanocrystals to a greater degree. The difference in growth rates could be explained by different diffusion of the monomers to the CdTe nuclei and different stability of CdTe-thiol complexes.

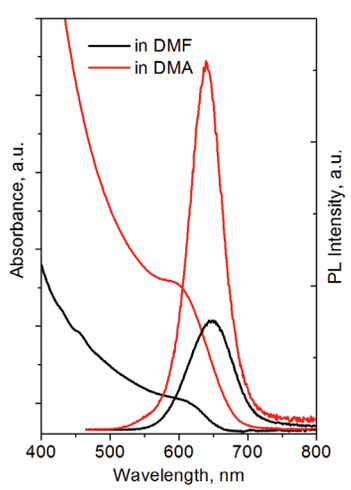

Figure 28. *Absorbance and PL (λ_{ex} = 450 nm) spectra of CdTe/mPEG-SH NCs synthesized in DMF (41 hours, max emission 648 nm) and in DMA (4 hours, max emission 640 nm).*

Figure 29 shows PL decay curves for amphiphilic CdTe in three solvents used for the phase transfer - toluene, chloroform and water (see below). All decay curves exhibit multiexponential recombination kinetics, which has been observed for different kinds of II-VI nanocrystals [154, 155]. For example, a distribution of decay times causing nonexponential decays in CdTe NCs has been generally discussed in terms of a variation in the nonradiative decay rates caused by trap states [156]. As it seen from the figure, the average PL decay times increase steadily in a series chloroform-water-toluene: the average time constants are 12.04, 18.4 and 19.2 ns, respectively.

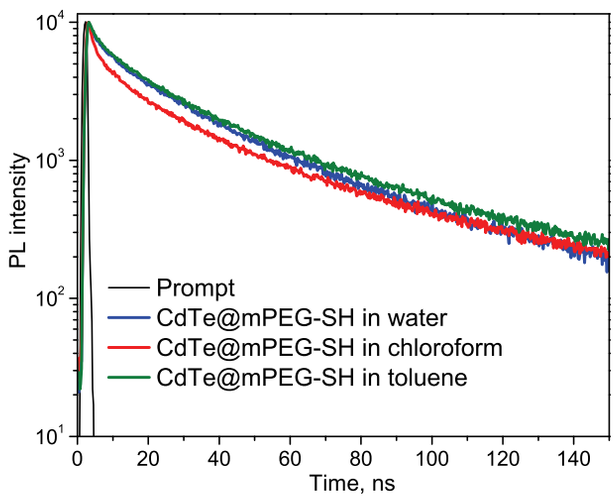

Figure 29. *PL life-time spectra of CdTe/mPEG-SH NCs in water, toluene and chloroform.*

Synthesis in both DMA and DMF results in a relatively broad size distribution of CdTe/mPEG-SH QDs in comparison with those synthesized in aqueous media. TEM image of CdTe/mPEG-SH NCs synthesized in DMA reveals their good crystallinity and average size of 4 nm (Fig. 30).

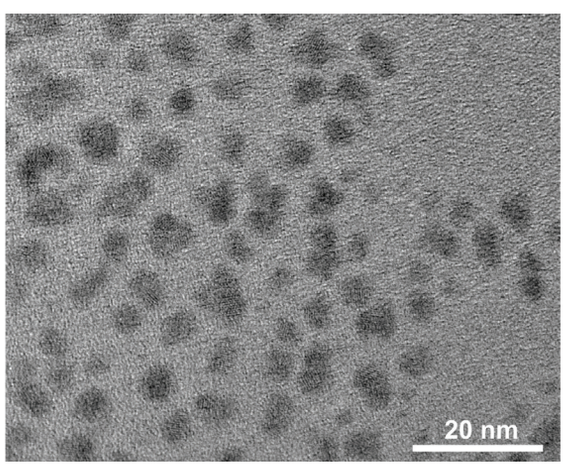

Figure 30. *TEM image of CdTe/mPEG-SH NCs synthesized in DMA.*

The irregular shape and broad size distribution of the nanoparticles observed may result from their partial aggregation and merging. The presence of different size fractions is proven also by relatively broad (FWHM in the range of 55-80 nm) PL emission spectra as well as by PL excitation (PLE) spectroscopy (see Fig. 31). In contrast to absorption and PL measurements, the PLE method enables distinguishing of several species sensitive for some certain PL excitation wavelength.

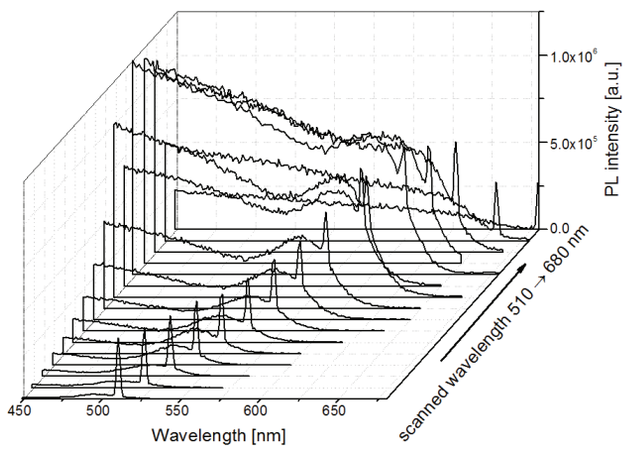

Figure 31. *PL excitation spectra of CdTe/mPEG-SH QDs, scanned PL wavelengths from 510 to 680 nm.*

The XRD pattern of CdTe NCs synthesized in DMA reveals their crystalline structure assigned to face-centered cubic (fcc) CdTe lattice (fig. 32). In contrast to the pattern of smaller NCs formed in toluene (see fig. 23), this spectrum exhibits distinct (220) and (311) reflexes. The shoulder located at about 22° in the XRD pattern indicates the first stages of the formation of the CdTe hexagonal phase.[157]

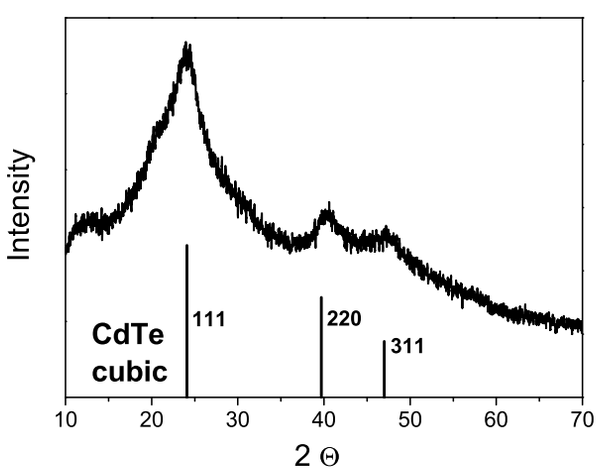

Figure 32. *XRD pattern of CdTe/mPEG-SH nanocrystals (orange emitting) synthesized in DMA. The line spectra show the bulk cubic CdTe reflexes.*

4.1.3. CdTe/But-PEG-SH

In order to show tuneability of hydrophobic-hydrophilic properties of CdTe NCs, the synthesis employing But-PEG-SH stabilizer has been performed in the same way as for CdTe/mPEG-SH colloid. Butyl group in this case enhances hydrophobic properties of the stabilizer and consequently of resulting nanoparticles, especially impacting their solubility in water. Indeed, although resulting nanoparticles are amphiphilic, they form rather emulsion as a true colloidal solution in aqueous media.

Absorption and photoluminescence spectra of as prepared CdTe/But-PEG-SH NC colloid in DMA are shown in Fig. 33. This synthetic approach provides NCs emitting with PL maximum of up to 650 nm. Samples show a well resolved absorption maximum of the first electronic transition indicating a sufficiently narrow size distribution of the CdTe QDs which shifts to the longer wavelengths with increasing size of the NCs as a consequence of the quantum confinement.

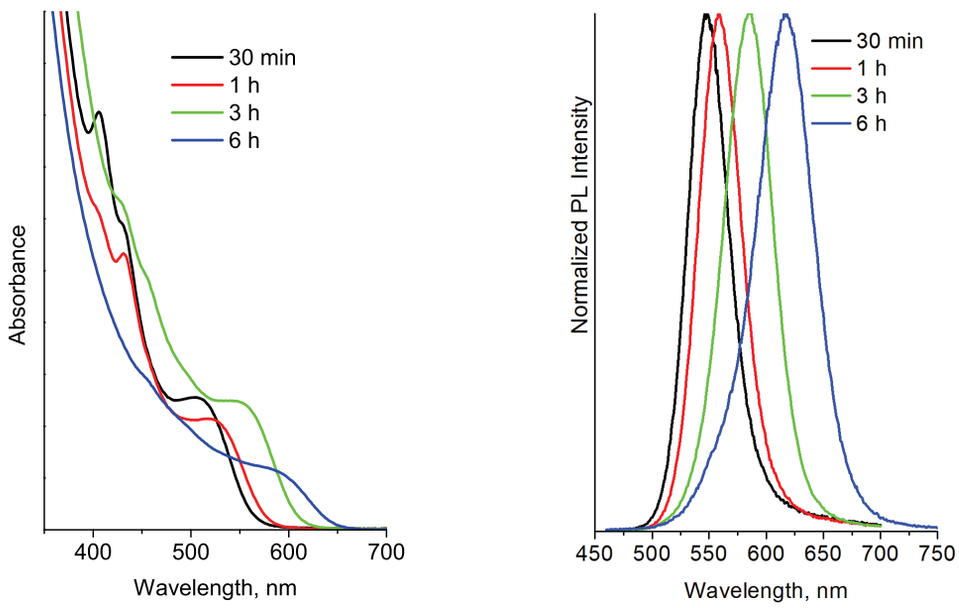

Figure 33. *Absorption and PL spectra of amphiphilic CdTe/But-PEG-SH in DMA. Inset values show heating time.*

PL lifetime measurements of But-PEG-SH capped CdTe NCs were carried out in H_2O and in toluene. In the case of aqueous colloid, one observes a significantly faster PL decay (Fig. 34). Averaged PL lifetimes are of 13.3 and 26.3 ns in water and in toluene respectively. We may assume that luminescence lifetime of CdTe/But-PEG-SH decreases due to the interaction of particles being in close proximity to each other in formed emulsion drops (micelles) leading to nonradiative energy loss.

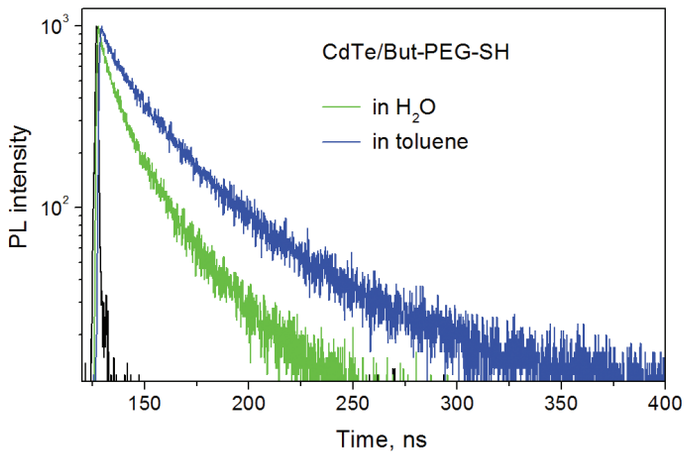

Figure 34. *PL life-time spectra of amphiphilic CdTe/But-PEG-SH NCs in H_2O and in toluene.*

As is seen from TEM overview (Fig. 35) the nanoparticles obtained possess average size of about 5-6 nm. HRTEM reveals their crystalline structure and formation of small aggregates similar to the above described cases.

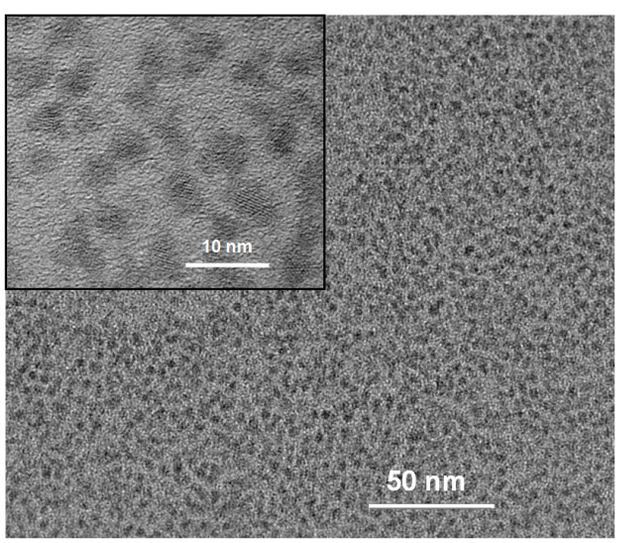

Figure 35. *TEM overview and HRTEM (inset) images of But-PEG-SH-capped CdTe NCs.*

4.1.4. Stability of CdTe/mPEG-SH compared to CdTe/TGA

In order to assess applicability of the amphiphilic CdTe nanocrystals for the bio-imaging and other related applications comparative photostability test was performed using colloidal solutions of CdTe/TGA and CdTe/mPEG-SH NCs. The solutions possessing equal concentrations were exposed to the UV-lamp at 365 nm monitoring their absorption and photoluminescence properties.

Figure 36 demonstrates changes of optical properties of these two types of CdTe NCs. As is seen from the spectra, absorption and luminescence of CdTe/mPEG-SH NC colloid experience blue shift, accompanied by strong luminescence quenching. These changes suggest partial degradation of the particles' surface via photo-oxidation processes that also leads to the creation of surface trap states diminishing PL efficiency. Nevertheless, even by the partial corrosion of the inorganic core, entire particle preserves its colloidal stability, that follows from the absence of the scattering part in absorbance spectra after 28 hrs of UV-light irradiation. Additional absorption features at short wavelengths characteristic for initial CdTe/mPEG-SH NC colloid (e.g. at ca. 428 nm) disappear likely due to dissolution of the small clusters, which usually possess lower stability than larger particles [54].

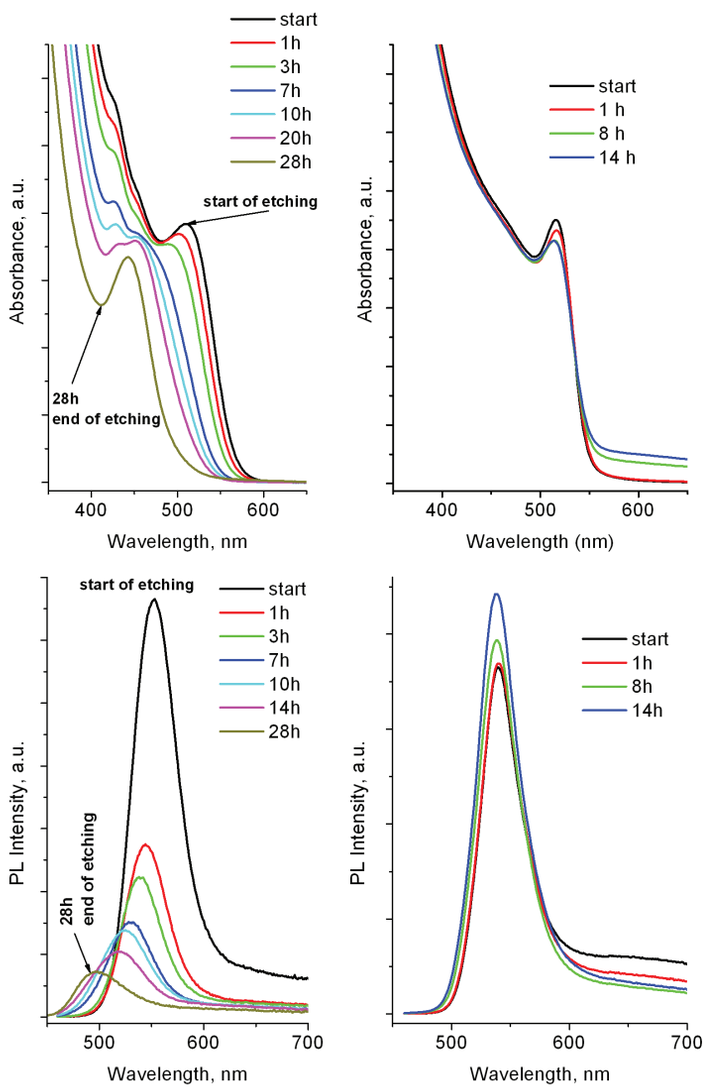

Figure 36. *Absorption (top) and PL (bottom) spectra of CdTe/mPEG-SH (left) and CdTe/TGA (right) NC colloids under the UV-lamp (365 nm) during the stability test. Illumination times are in top right hand corner.*

Quite opposite behaviour exhibit CdTe/TGA NCs treated in the same conditions: the position of absorbance and luminescence maxima are virtually unaltered indicating stability of the CdTe core. At the same time NCs upon irradiation show remarkable tendency to aggregation indicated by scattering part in their absorbance spectra after 8 h of exposure. PL intensity of CdTe/TGA NC colloid enhances owing to photochemical etching of surface trap states in accordance to previous observations.[54, 158, 159]

These results imply, that mPEG-S- ligand binds to the surface of NCs weaker than HOOC-CH_2-S-, providing labile and reversible attachment which makes core accessible for corroding species. At the same time, this ligand's shell itself is much more robust against photo-oxidation than that formed by TGA and maintains overall colloidal stability of nanoparticles.[54]

4.2. Amphiphilic properties of CdTe NC colloids

4.2.1. CdTe/mPEG-TGA

By mixing the as-prepared toluene colloidal solution of CdTe/mPEG-TGA NCs with water fast spontaneous transfer of nanoparticles has been observed (fig. 37). In order to prove complete migration of the particles the toluene and water layers were separated. No emission was detectable for the toluene part, all QDs were found in the aqueous solution. However, reversible transfer from aqueous into organic phase can not be achieved spontaneously and may be performed only by addition of excessive amount of mPEG-TGA.

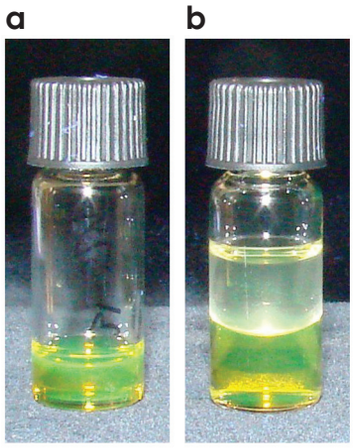

Figure 37. *Photograph of colloidal CdTe/mPEG-TGA NC colloids under day-light with UV-light: A. As-prepared QDs in toluene. B. Phase transfer of CdTe from toluene (upper layer) into water (bottom layer).*

4.2.2. CdTe/mPEG-SH

As was mentioned above, CdTe/mPEG-SH nanoparticles synthesized in water possess high compatibility with various solvents. It is literally impossible to precipitate them, which makes their size selective precipitation and cleaning (by precipitation-redissolution) challenging. Advantageously, the same nanoparticles synthesized in toluene may be precipitated by hexane or diethyl ether in order to perform size-selection and to remove unreacted species. These size-selected particles can be easily redissolved both in pure water and in toluene. As is shown in Figure 38, these NCs being redissolved in toluene migrated spontaneously into the water phase during ca. one hour (or during only several minutes upon shaking bi-phase mixture). Moreover, in contrast to CdTe/mPEG-TGA sample discussed above, CdTe/mPEG-SH NCs being completely transferred into pure water were able (equally spontaneously and completely) to transfer into the next nonpolar phase - chloroform which is known to be better solvent for many organic substances than toluene. It should be noted that the toluene-water transfer is much faster than water-chloroform one, that may result from stronger affinity of nanoparticles to hydrophilic than to hydrophobic media. The process of water-chloroform transfer is accompanied by formation of clearly seen intermediate emulsion layer between two phases (see Figure 38). This effect could be ratioanalized as follows: in toluene, the NCs surrounded by mPEG are dissolved mainly via nonpolar (van der Waals) interactions between solvent and hydrocarbon moieties of mPEG and some dipole-induced dipole interactions involving the aromatic ring of toluene.In water, much stronger hydrogen bond interactions between water and PEG ether oxygen exist. During transfer to chloroform, these hydrogen bonds have to be broken and replaced by dipole-dipole interactions between chloroform and PEG oxygen atoms (whereby water molecules set free, producing entropy). This transfer process can be expected to require more time (because of activation energy) than that from toluene to water.

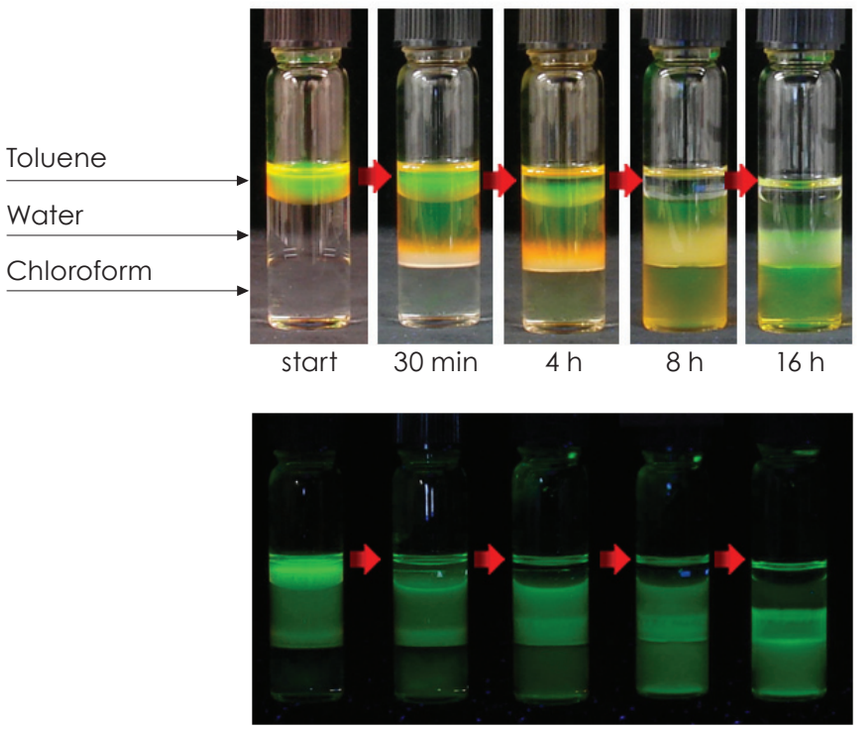

Figure 38. *Photographs of vials demonstrating spontaneous tri-phase transfer of CdTe/mPEG-SH NCs from toluene through water into chloroform with time under UV and day light excitation (top) and under UV light (365 nm) only (bottom).*

The same amphiphilic behaviour was proven also for CdTe NCs of larger size synthesized in DMA and DMF. For example, as prepared CdTe/mPEG-SH QDs were precipitated from DMA by addition of hexane/diethyl ether mixture. After subsequent dissolving of nanoparticles in toluene, colloid obtained was carefully placed on top of water layer poured over chloroform layer. The amphiphilic QDs have spontaneously transferred from toluene phase via water into chloroform without any treatment (Fig. 39). This experiment additionally confirms stability and retained amphiphilicity of ligand shell during NCs synthesis under relatively high temperature.

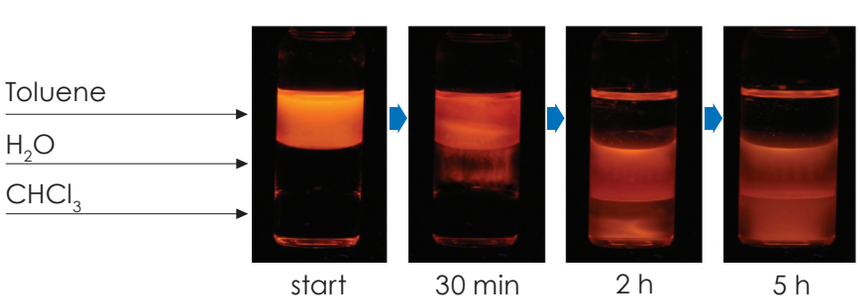

Figure 39. *Photographs of vials demonstrating the spontaneous triphase transfer of CdTe/mPEG-SH NCs from toluene through water into chloroform with time under UV light (365 nm).*

4.2.3. Comparative study of phase transfer of CdTe NCs stabilized by mPEG-SH of different molecular weights

The colloids of CdTe NCs capped by mPEG-SH with molecular masses 350, 500 and 750 were compared by means of the transfer rate in tri-phase system toluene-water-chloroform.

As is seen from Figure 40, after 2.5 hours the toluene layer in the vial with CdTe/mPEG350-SH becomes less concentrated faster than in vials with two other colloids. The colloid stabilized with the shorter polymer chain needs less time to be transferred from toluene to water but then its migration speed is decreased. Colloids stabilized by longer chain polymers, possessing higher affinity to organic phase than to the aqueous, show opposite behaviour. As a result, the accumulation of the latter particles in chloroform phase is observed at relatively shorter time interval.

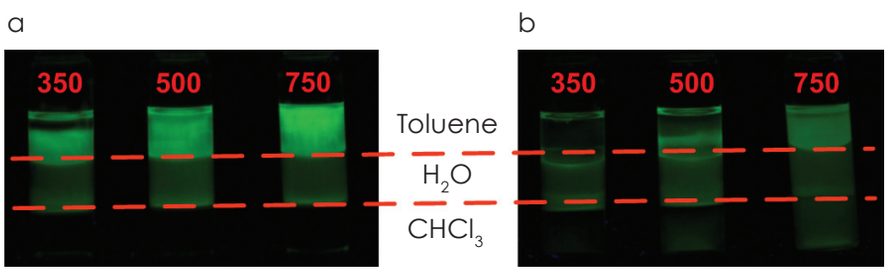

Figure 40. *Photographs of tri-phase transfer of CdTe/mPEG-SH 350, 500 and 750 NCs in time - 2.5 h (a) and 7.5 h (b) (under UV-light).*

4.2.4. CdTe stabilized by But-PEG-SH

All previous attempts to obtain particles capable of transferring from organic phase to water phase were successful. More limitations appear for the attempts to transfer nanoparticles in opposite direction. For example, although water-chloroform transfer was successful, our attempt to transfer nanoparticles from water back into toluene or hexane failed. Using of the next stabilizer made it finally possible.

As is seen from fig. 41, the aqueous solution of CdTe/But-PEG-SH NCs is turbid suggesting a formation of emulsion. Nevertheless, being emulsified colloid obtained retains its emission properties.

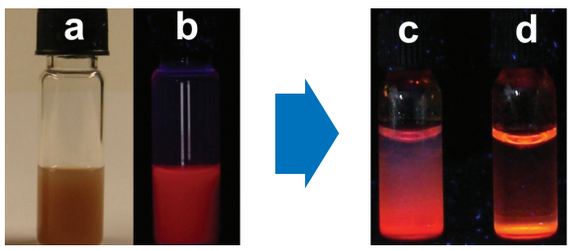

Figure 41. *Photos of amphiphilic aqueous CdTe/But-PEG-SH NC colloids under day light (a) and under UV-light (b, c, d) immediately after dissolving in water (a, b) and after 1(c) and 2 hours (d).*

The emulsion of CdTe/But-PEG-SH NPs is stable without agitating for 1-2 hours. Figure 41 c, d demonstrates sedimentation of the particles in water. The resulting precipitate is redispersible in different polar (except of water) and soluble in non-polar solvents.

Amphiphilicity of the synthesized colloid was checked using two-phase system consisting of water, where the CdTe was redispersed, and toluene (Fig. 42) or hexane (Fig. 43) as the second solvent. The emission of the transferred CdTe NCs was monitored by periodical camera shots after 20 minutes, 1 and 4 hours. The transfer from water to organic phase was spontaneous and fast for toluene (1 hour) and slower in the case of hexane. In addition, the final solution of CdTe/But-PEG-SH in hexane formed less homogeneous layer as compared to the case of toluene. It could be explained by relatively lower solubility of the crystals in hexane due to its lower polarity as well as due to water traces present in (adsorbed by) the stabilizer shell, which affect efficient interaction between PEG chains and hexane.

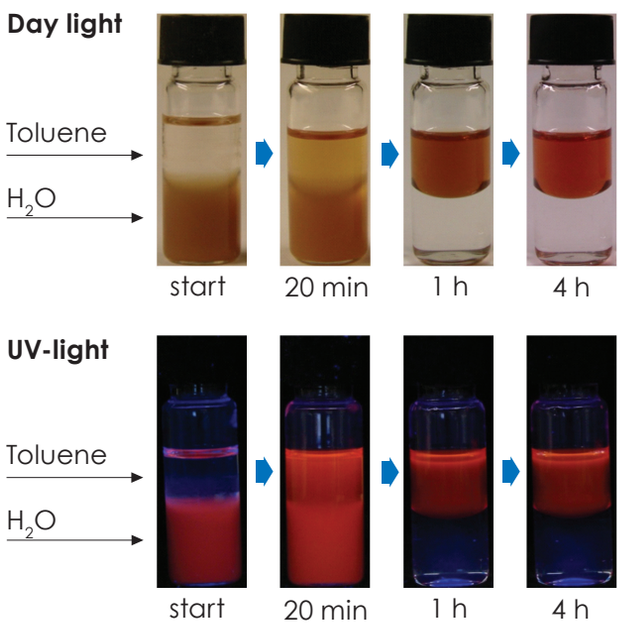

Figure 42. *Images of the phase transfer for CdTe/But-PEG-SH from water to toluene.*

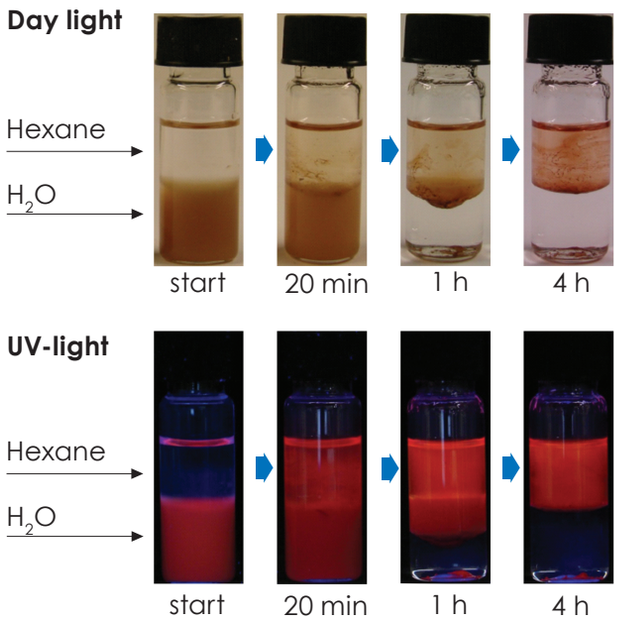

Figure 43. *Images of the phase transfer for CdTe/But-PEG-SH from water to n-hexane.*

4.2.5. Interaction of giant unilamellar vesicles with amphiphilic CdTe nanocrystals

In this part the preliminary results obtained on interaction of the amphiphilic CdTe nanocrystals with the unilamellar vesicles are presented. These vesicles provide a suitable system for mimicking the confinements in cells or in the extracellular space. By this, one of the most useful model systems to study membrane dynamics is giant unilamellar vesicles (GUVs). The first protocol for the preparation of GUVs was issued by Dowben et al. in 1968 [160] and subsequently improved by Angelova et al., who developed the electroformation technique.[161, 162] Afterwards, they have been synthesized by various ways and used for several applications such as investigations of membrane lipid dynamics, lipid-protein interactions and membrane mechanics.[163]

For GUV experiment orange emitting mPEG-SH stabilized CdTe NCs with PL maximum at 610 nm were chosen in order to distinguish their luminescence from green emitting dye 3,3'-dioctadecyloxacarbocyanine perchlorate (DiO). DiO was used as a non-penetrating agent able to stick to the surface of the formed vesicles as it is usually applied as a lipophilic fluorescent stain for labeling membranes. As a control sample aqueous CdTe NCs stabilized with TGA possessing similar size were used. Optical characteristics of both NC samples are shown in Fig. 44. CdTe/TGA NCs bear on the surface deprotonated carboxyl groups and hence possess negative charge. In addition, quite stable bonding of the TGA stabilizer to the nanocrystal surface imparts high colloidal stability against deterioration. Zeta potential

measurements of CdTe/TGA NCs reveal the value of -65 mV. On the contrary, amphiphilic CdTe nanoparticles have low positive zeta potential of 4 mV, which favours their versatile solubility and should prevent their aggregation via electrostatic interaction in biological media. Short chain length of mPEG-SH (H_3C-(O-CH_2-CH_2)$_7$-SH) molecule assures quite small size of resulted nanoparticles which is also beneficial for biological applications. The diameter of amphiphilic QDs was calculated to be of 8.7 nm including the fully extended mPEG-S- chains. Such small size is advantageous for using CdTe NCs because it favors their penetration through the membrane.

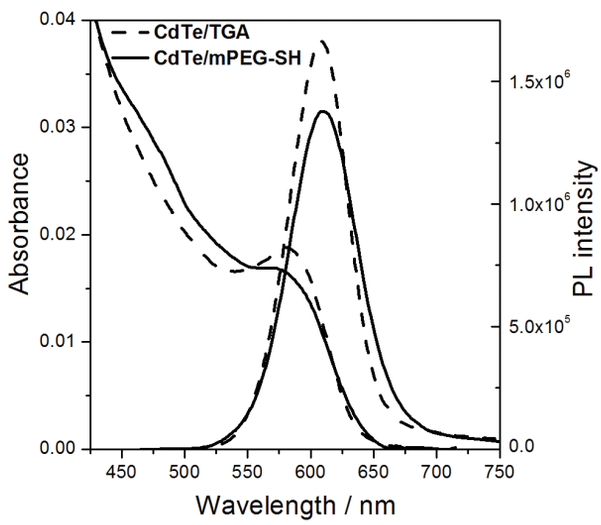

Figure 44. *Absorbance and PL (λ_{ex} = 450 nm) spectra of amphiphilic CdTe/mPEG-SH NCs and hydrophilic CdTe/TGA NCs colloids used for GUV experiment.*

In order to evaluate the ability of QDs to permeate through lipid bi-layer, GUVs prepared via electroformation were incubated in diluted QD colloids. The images obtained during 5 hours of confocal microscope observation are shown in Fig. 45, where black circles are "empty" vesicles and circles colored red are vesicles containing QDs. As is seen from figure, already in 1 h some vesicles started QDs uptake. After 5 hours incubation approx. 40% of the GUVs took up amphiphilic nanoparticles. After overnight incubation ca 60% of the vesicles contained QDs. It should be noted that even after overnight exposure QDs have still retained their emission. Control experiment performed with CdTe/TGA nanoparticles did not reveal their uptake by vesicles. Moreover, we observed some deformation of GUVs after addition of the hydrophilic QDs. This data clearly show that amphiphilic CdTe/mPEG-SH NCs are able to penetrate through the membrane. In order to understand the penetration thoroughly, it is planned to perform test on living cells investigating diffusion characteristics of the amphiphilic QDs by fluorescence correlation spectroscopy.

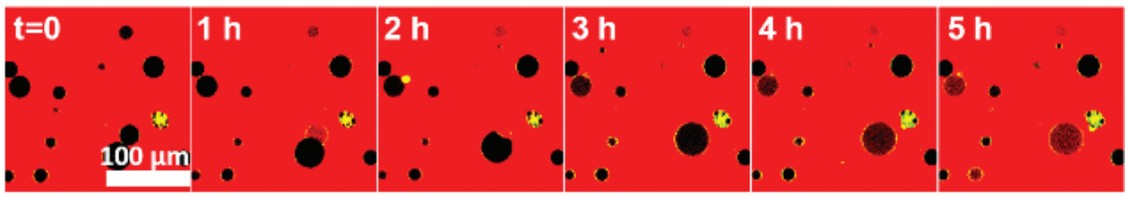

Figure 45. *Confocal microscopy images taken during 5 hours observation of GUVs immersed in CdTe/mPEG-SH NCs colloid (false coloring: green is DiO, red is QDs).*

Conclusions to the chapters 4.1.-4.2.

It has been demonstrated that with the proper design and the fine tuning of its structure ligand such as thiolated polyethylene glycol enables the synthesis of semiconductor CdTe nanocrystals in water as well as in a variety of organic solvents. Employment of high-boiling coordinating solvents dimethylacetamide and dimethylformamide allows obtaining QDs emitting in wide visible region of 540-640 nm with enhanced quantum yield of up to 30%.

mPEG-SH stabilizer developed facilitates the reversible transfer between liquid phases of different polarity while maintaining the emission properties of the CdTe nanocrystals. No further adjustments of the solvent content such as the addition of other surface active species are needed.

It has been shown that QDs synthesized are able to permeate through lipid bi-layers of GUVs and might be good candidates for tracking whole cells and intracellular processes escaping endocytic uptake mechanism.

4.3. Synthesis and characterization of Au/mPEG-SH Nanoparticles

For a synthesis of amphiphilic gold nanocrystals well-known two-phase Brust approach has been used in its modified [83] form. By using the classical protocol including mixed toluene/water solvent and tetraoctylammonium bromide (TOAB) as a phase-transfer agent, it was observed that at the end of reaction gold NPs capped with mPEG-SH were collected in the aqueous phase. It should be noted, that original Brust's dodecanethiol stabilized nanocrystals are soluble in toluene. Therefore our method was simplified by excluding of toluene phase and the TOAB. Thus facile one phase aqueous synthesis providing stable gold NPs colloids employing gold precursor, stabilizer and reducing agent has been developed. In contrast to another well known "citrate" aqueous synthesis, the present protocol provides a great advantage typical for Brust's approach, such as the resulting amphiphilic nanoparticles may be easily concentrated. Literally no solubility limit was observed for these nanoparticles both in pristine aqueous media and after

transfer into unpolar organics. Moreover, the procedure of nanoparticle cleaning from unreacted species (e.g salts) may be simply performed by nanoparticles transfer between media of different polarity.

In order to achieve proper amphiphilicity of nanoparticles (i.e. favorable balance between hydrophilic and hydrophobic properties) we applied three mPEG-SH stabilizers with different chain lengths: (H_3C-(O-CH_2-CH_2)$_n$-SH), n~7 for mPEG350-SH, n~11 for mPEG500-SH, n~16 for mPEG750-SH. Syntheses were monitored by UV-Vis spectroscopy. Absorption spectra of gold NPs capped with different thiolated mPEGs are presented in Figure 1. As is seen from figure, the longer mPEG chain the less pronounced gold plasmon band suggesting decrease of nanoparticles' sizes with increasing polymer chain length[164]. TEM observation confirmed this assumption: average diameters of Au/mPEG350-SH, Au/mPEG500-SH and Au/mPEG750-SH NPs obtained at a molar ratio of Au/stabilizer = 1/1 were found to be 3.9, 2.6 and 2.4 nm, respectively. The similar tendency was observed by Shimmin et al. and explained by acceleration of the particle nucleation rate at very early stages of reduction by possible coordination of ethylene glycol units with gold atoms.[94] Larger polar polymers consisting of larger number of monomer units enhance this effect. Therefore, the larger particles are formed in the presence of the shorter polymer mPEG350-SH. These NPs possess quite pronounced surface plasmon band at around 520 nm which retains its position in different solvents (see Figure 46).

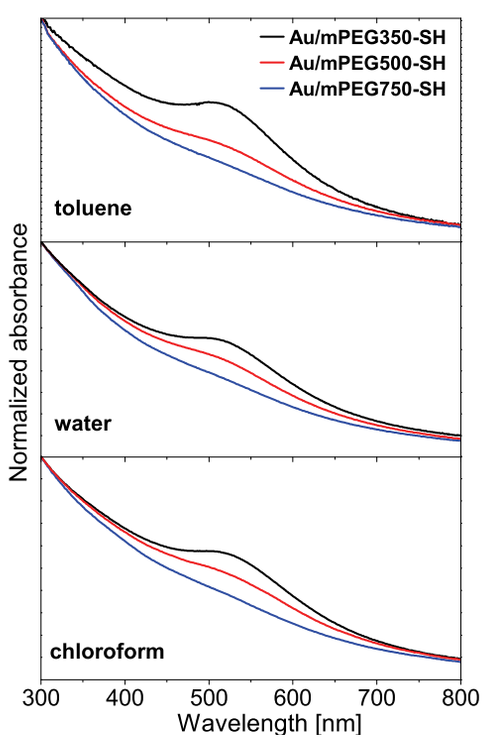

Figure 46. *Absorption spectra of amphiphilic Au NPs stabilized by mPEG-SH of different molar weights in water and after their redissolving in toluene and chloroform.*

This independency of the plasmon position from surrounding media is in contrast with predictions of Mie theory and experimental results previously reported.[165] We may suggest that local proximal surrounding (i.e. hydrated polyethylene glycol shell) of gold particles remains essentially the same in different solvents. This hypothesis is confirmed by DLS measurements: mean average diameter of Au/mPEG350-SH nanocrystals was determined in toluene as high as 70 nm, in water - 40 nm, in chloroform - 20 nm. At the same time, estimated from TEM images sizes of particles including the fully extended mPEG-S- chains are 9.7, 11.2 and 14.6 nm for Au/mPEG350-SH, Au/mPEG500-SH and Au/mPEG750-SH, respectively.

Gold NPs obtained in presence of mPEG-SH form very stable colloids. It was difficult to precipitate the as prepared nanoparticles from aqueous solution due to their inherent amphiphilicity. Therefore in order to purify colloid, firstly water was evaporated, thereafter waxy viscous product of deep brown color was dissolved in toluene with subsequent precipitation of NPs by addition of hexane. The resulting precipitate of nanoparticles was easily soluble in polar and non-polar media: acetone, water, alcohols, toluene, mesitylene, chloroform etc. Owing to high colloidal stability significant concentrations of colloids are achievable. This versatile solubility of Au NPs facilitates their processing. For example, these nanoparticles easily form composites with both water soluble polymers like polyvinyl alcohol (PVA) and those organics soluble such as polystyrene (PSt). Composite with PVA was formed by mixing and subsequent drying of aqueous solutions of both polymer and NPs, whereas composite with PSt was formed by mixing of NPs with polystyrene toluene solution and subsequent evaporation of the solvent. Figure 47 shows absorption spectra of Au/mPEG350-SH NPs in different solvent and polymer surroundings. The shift of plasmon band from 520 in liquid media to 534 nm in solid PVA and PSt is presumably caused by the change of the refractive index of the medium and the increase of its dielectric constant due to high concentration of NPs in polymer matrix and their resulting dipole-dipole interaction.[166]

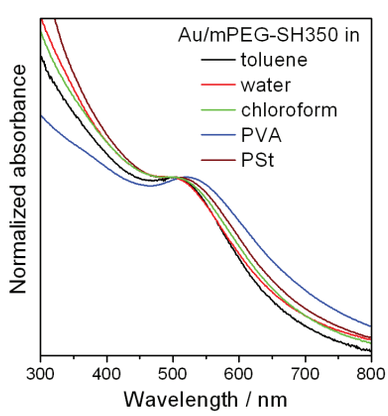

Figure 47. *Absorption spectra of Au/mPEG350-SH NPs dispersed in different media.*

Variation of initial ratio of gold/stabilizer allows for control of particle sizes. This synthesis obeys general rule: the higher content of stabilizer the smaller NPs formed. TEM observation provides following mean diameters of Au/mPEG350-SH nanocrystals: 3.9, 3.1 and 2.5 nm for gold/stabilizer ratios 1/1, 1/2 and 1/3, respectively (Figure 48). As is seen from TEM images, small NPs tend to aggregation on grid surface after solvent evaporation due to quite strong interaction between stabilizer molecules. Further growth of gold nanocrystals via Ostwald ripening was realized by heating at 150-160 °C in mesitylene, similarly to approach reported by Shimizu et al.[167] As an example, TEM images of Au/mPEG350-SH particles heated for 1h and 2h are shown in Figure 48b (insets). NPs grow from 3.1 nm up to 6.6 nm after 1h and up to 7.1 nm after 2h of heating.

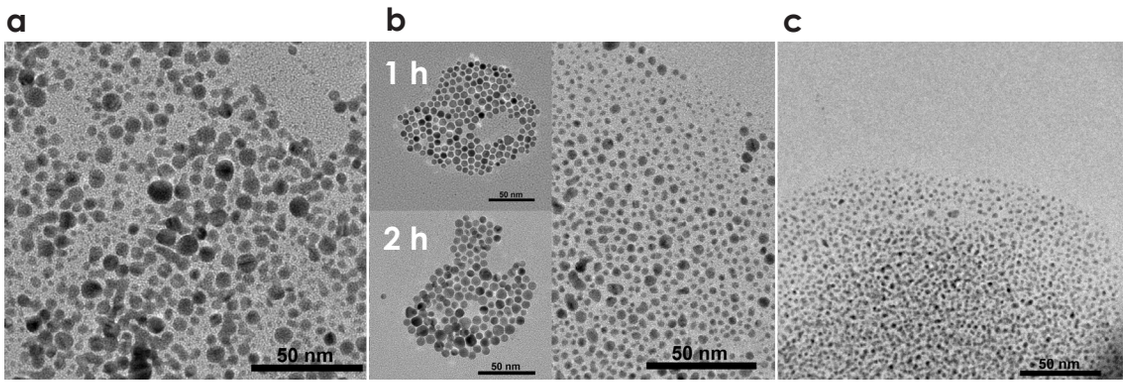

Figure 48. *TEM images of Au NPs synthesized in the presence of the mPEG350-SH at different Au/mPEG350-SH molar ratios: 1/1 (a), 1/2 (b), 1/3 (c). The insets in b show Au NPs after heat treatment for 1h and 2h.*

Additionally to direct synthesis in presence of mPEG-SH, preparation of highly concentrated and stable gold colloids with improved monodispersity is also possible by a ligand exchange applied to "citrate" Au NPs. After the addition of mPEG-SH to the "citrate" gold colloid and overnight boiling the resulting solution may be concentrated simply by rotor evaporation and cleaned similar to above described approaches. These NPs were readily redispersed in water, alcohols, chloroform and toluene. As seen from Fig. 49 the Au NPs in the as prepared citrate solution and mPEG-SH capped Au NPs have the maximum peak of the surface plasmon resonance at 520 nm. The peak for the Au/mPEG-SH NPs is more pronounced due to the improved crystallinity after additional overnight boiling in presence of amphiphilic ligand. These Au NPs after the ligand exchange were used for immobilization on artificial membranes as described below.

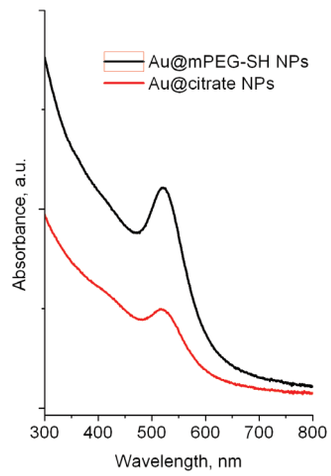

Figure 49. *Absorbance spectra of citrate gold NPs and after ligand exchange with mPEG-SH.*

4.4. Amphiphilic behaviour of Au/mPEG-SH Nanoparticles

4.4.1. Phase transfer of amphiphilic Au NPs

The amphiphilic behaviour of Au/mPEG-SH nanoparticles has been investigated in three phase system analogous to that utilized for CdTe NPs. Thus, the purified gold NPs were dissolved in toluene and placed as the third component above already prepared two-phase solution consisting of chloroform and water (Figure 50). After the addition of toluene solution the Au/mPEG350-SH particles start to transfer from organic layer to water layer within 1 h. After 24 h they completely accumulated inaqueous phase. The process of further full migration to chloroform phase needed approximately one week. The Au NPs stabilized by longer chain stabilizers (mPEG500-SH and mPEG750-SH) also showed similar amphiphilic behaviour. However, in accordance to results obtained for CdTe NPs the transfer rate from toluene to aqueous phase was slower, and that from aqueous phase to chloroform was faster. This fact suggests that increasing of molar mass of mPEG-SH enhances hydrophobic properties of nanoparticles.

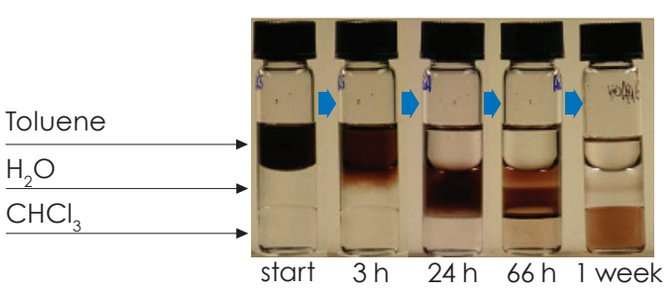

Figure 50. *Photographs demonstrating spontaneous tri-phase transfer of Au/mPEG350-SH NPs from toluene into water and subsequently into chloroform in the course of time.*

Amphiphilic properties of Au capped by mPEG-SH with different polymer chain length are very close to that for CdTe NCs mentioned in corresponding chapter above: Au NPs are soluble in polar and non-polar solvents, able to phase transfer retaining their optical properties.

4.4.2. Interaction of amphiphilic Au NPs with giant unilamellar vesicles

Here we present results of investigations of interaction between Au/mPEG-SH NPs and artificial lipid membranes. The interaction of Au NPs and surface of lipid membrane was explored by dark-field microscopy method (DFM).

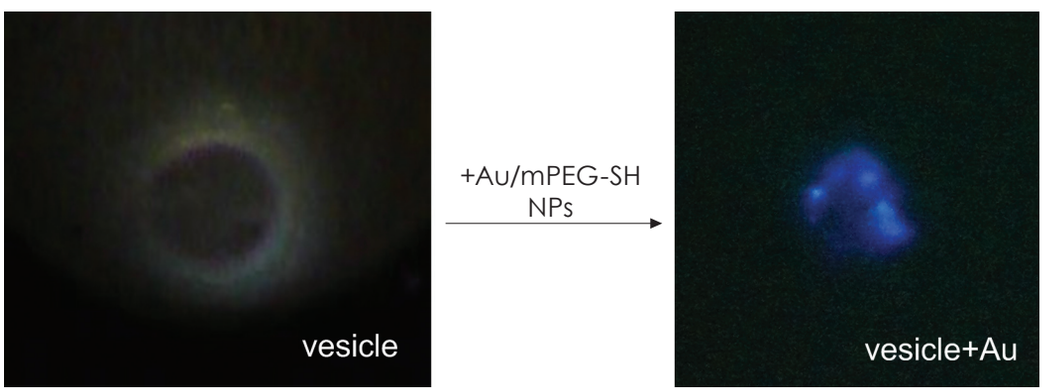

Figure 51. *Dark-field microscopy image of a DOPC giant unilamellar vesicle freshly prepared before incubation (left) and after incubation with Au/mPEG-SH350 NPs (right).*

Uncharged DOPC (dioleoylphosphatidylcholine) lipid was used for vesicles preparation. DFM image of a vesicle prior to incubation is shown in Fig. 51 (left). After addition of small Au/mPEG-SH nanoparticles (average size of ca. 5 nm) small blue spots appear around a vesicle (Fig. 51 (right)). These spots may be detected only from Au NPs forming aggregates on the surface of vesicles. Indeed, the size of the single gold nanoparticles was too small to be seen by dark-field microscope and only aggregates might become detectable at this measurement conditions.

To observe single particle interacting with the surface of vesicles utilization of bigger (>30 nm) nanoparticles is necessary. Au NPs were synthesized according to Ziegler seeded growth method in presence of sodium citrate and ascorbic acid allowing to reach an average nanoparticle size of about 30 nm.[149] The mPEG350-SH was used as an agent for ligand exchange. After the ligand exchange Au NPs were readily redispersible in water and non-polar solvents such as toluene and chloroform. These bigger Au/mPEG-SH NPs were used in vesicles to observe their interaction with membrane surface and/or possible penetration into the vesicle bubble.

Original not treated with mPEG-SH nanoparticles were used as reference. No specific binding or interactions with vesicles have been observed for these reference NPs.

The Au/mPEG-SH nanoparticles were injected to the solution with the suspended vesicles and analyzed by DFM. Some of the vesicles burst after injection of NPs presumably due to osmotic pressure. The binding of Au/mPEG-SH scattering particles to the surface of neutral DOPC vesicles is evidenced from Figures 52 a, b. It has been seen that in some cases (Fig. 52c) it could be possible that a gold particle has entered a vesicle.

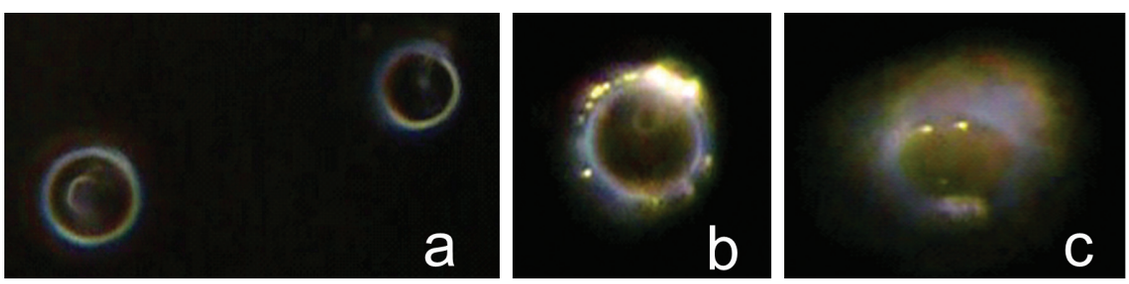

Figure 52. *Dark-field microscopy image of a DOPC giant unilamellar vesicle freshly prepared before incubation (a) and after incubation with Au NPs: b. Au NPs on the vesicle's surface, c. Au NPs inside the vesicle.*

In another experiment negatively charged vesicles with the membrane from the lipid DOPS (1,2-Dioleoyl-sn-Glycero-3-{Phospho-L-Serine} sodium salt) were used. As is seen from fig. 7 the Au/mPEG-SH NPs (bright scattering spots in the top part of the image) are not binding to the vesicles (seen as circles in the bottom part of the image). Thus, the amphiphilic Au/mPEG-SH NPs did not react with the membrane from DOPS. Presumably, it could be explained by the presence of citrate on the surface of nanoparticles, not fully replaced during the ligand exchange, resulting in electrostatic repulsion with negatively charged membrane.

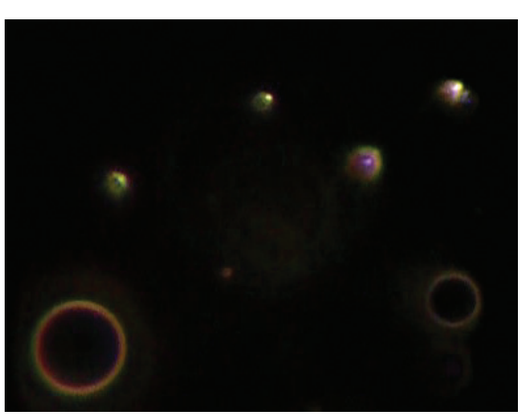

Figure 53. *DFM images of a DOPS GUVs (spherical formations) incubated with Au/mPEG-SH (bright spots above the GUVs).*

Conclusions to the chapters 4.3.-4.4.

A facile aqueous synthesis of the amphiphilic gold NPs stabilized by thiolated methoxypolyethylene glycols of different molar masses has been demonstrated. The approach of one-pot amphiphilic Au NPs synthesis allows obtaining stable high concentrated gold colloids. The Au/mPEG-SH nanocrystals are compatible with media of different polarity. They maintain characteristic plasmon band in various solvents. Variation of synthetic parameters enables control of NPs' sizes. The synthetic method developed could be applicable for synthesis of other noble metal particles like palladium, platinum, and silver.

It has been shown that the amphiphilic Au NPs could be used for a vesicles tagging through the binding of individual nanoparticles to the lipid membrane. Further investigations of bio-applicability of these NPs are foreseen.

4.5. Amphiphilic Iron Oxide nanocrystals

Iron oxide (Fe_3O_4) nanocrystals are important size-dependent magnetic material. They can be synthesized directly in water by coprecipitation of Fe^{3+} and Fe^{2+} containing salts or alternatively by thermal decomposition of iron acetylacetonate, iron carbonyl or iron carboxylates. Coprecipitation methods are not very effective because NCs obtained mainly have low crystallinity and high polydispersity, they also tend to agglomeration in solution due to insufficient coverage by stabilizers.[168-170] With this respect, thermodecomposition method is more preferable, since it provides monodisperse NCs soluble in most organic solvents like chloroform, hexane, toluene, etc. [107, 171] They are, however, are not compatible with aqueous media. In this part of the work the applicability of PEG derivatives for the fabrication of water compatible and/or amphiphilic magnetite NPs has been investigated.

The synthesis of magnetic NCs was carried out in an oxygen-free environment which not only protects iron oxide particles from the oxidation but also reduces the size of the particles as compared with those grown in the presence of oxygen.[137] In order to optimize the synthesis of amphiphilic magnetic nanocrystals a series of experiments has been performed employing different approaches as described below.

In the first step, organically soluble iron oxide NPs capped by oleic acid were synthesized (synthesis 1, Experimental Part) using the method of Park et al.[103] TEM images of as synthesized highly crystalline and shaped NCs are shown in Fig. 54. Ligand exchanges with mPEG-SH aiming at a preparation of the stable amphiphilic magnetic NPs were performed after the synthesis. It was found that thiolated mPEG derivative was not effective for phase transfer of magnetite NPs. NPs treated by mPEG-SH can be solved in

toluene, however the further transfer from toluene to water has not been observed as it was realized for the amphiphilic CdTe and Au nanocrystals (see above). The inefficient stabilization of iron-oxide-based NPs by thiolated mPEG may be explained in terms of binding energies (Fe-S $\Delta H_{f\ 298}$ =339 kJ/mol, Fe-O $\Delta H_{f\ 298}$ =409 kJ/mol).[172] At the same time, according to literature data [173, 174] carboxyl group is able for strong binding to Fe_3O_4 NPs with one or two oxygen atoms interacting with the metal on the surface.

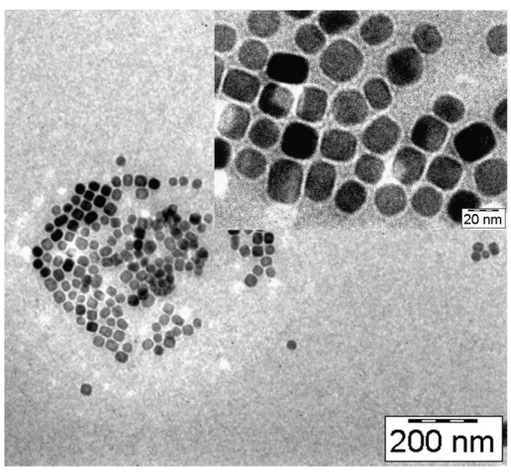

Figure 54. *TEM overview of the magnetite nanoparticles synthesized according to Park et al.[103]*

Therefore, in the second step (Synthesis 2, Experimental Part) we attempted to synthesize amphiphilic magnetite NPs directly in the presence of mPEG functionalized with carboxylic group. The synthesis of monodisperse magnetite nanoparticles with an average size range of 10-15 nm was performed through the thermal decomosition of $Fe(acac)_3$, based on the approach developed by Sun et al. [104, 106]. In this case oleic acid originally used as one of the stabilizers was replaced by mPEG350-COOH (Figure 55).

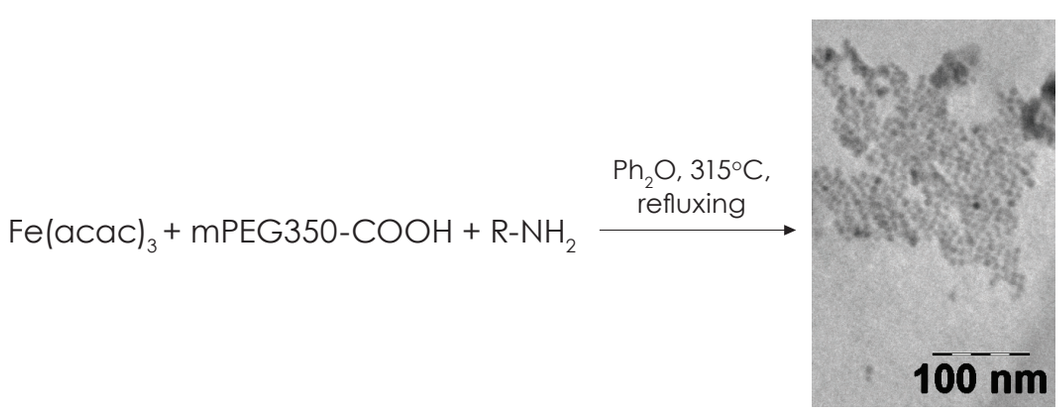

Figure 55. *Reaction conditions and TEM image of magnetic NPs from the synthesis 2. $R\text{-}NH_2$ = oleylamine ($CH_3(CH_2)_7\text{-}CH{=}CH\text{-}(CH_2)_8\text{-}NH_2$).*

As illustrated in Figure 55, decomposition of $Fe(acac)_3$ in the presence of surfactants (oleylamine and mPEG-COOH) at high temperature in diphenyl ether leads to monodisperse Fe_3O_4 nanoparticles, which can be easily isolated from reaction by-products and the solvent. Unfortunately, also in this case the final magnetite nanoparticles were dispersable only in nonpolar solvents. This implied that further search for more hydrophilic and simultaneously efficient stabilization was necessary.

Therefore in the next step diphenyl ether used as a solvent was replaced by mPEG-OH and long chained oleylamine was replaced by shorter dodecylamine. Two various mPEG-COOH with different polymer chain length, namely mPEG350-COOH and mPEG750-COOH, were used as amphiphilic stabilizers (synthesis 3 a, b). TEM images of the mPEG750-COOH stabilized NPs are depicted in Figure 56. The nanoparticles possess high crystallinity and their average size is of 8-10 nm.

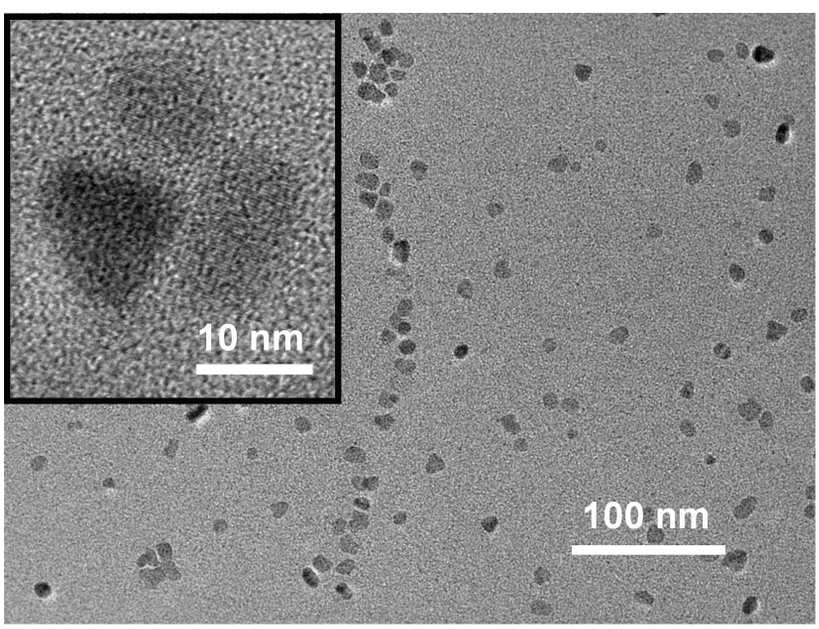

Figure 56. *TEM images of magnetite NPs synthesized with mPEG-COOH750.*

As is seen from Table 2, using mPEG-OH as a media and mPEG-COOH (independent on the chain length) in combination with dodecylamine as a stabilizer we achieved versatile solubility of the obtained particles, i.e. after being precipitated and washed they can be solved in various polar (including water) and nonpolar solvents. Unfortunately, they are still not able for spontaneous transfer through the interface from nonpolar (e.g. toluene) to polar (water) solvents.

Solvent	Hex	THF	Acetone	MeOH	$CHCl_3$	toluene	DMF	DMSO	H_2O
Solubility	-	+	+	+	+	+	+	+	+

Table 2. *Solubility of the as-prepared Fe_3O_4/mPEG350COOH and Fe_3O_4/mPEG750COOH NCs in different solvents.*

In the next step we further simplified synthetic system consisting of iron acetylacetonate dissolved only in mPEG-OH (Synthesis 4, Experimental Part). As is seen from TEM images presented in Figure 57, 5-10 nm particles are formed by thermal decomposition. Similar to the case described above, these NPs also exhibit versatile solubility, but not able for spontaneous phase transfer. It may be also noted, that these magnetite NPs have formed on ring-like structures on the substrates. Similar structures were observed from self-assemblies of hexadecylamine-stabilized magnetic $CoPt_3$ NPs [175]. The reason for this ring formation is in two important effects: contact line pinning and the relative importance of evaporation at the edge of the droplet.

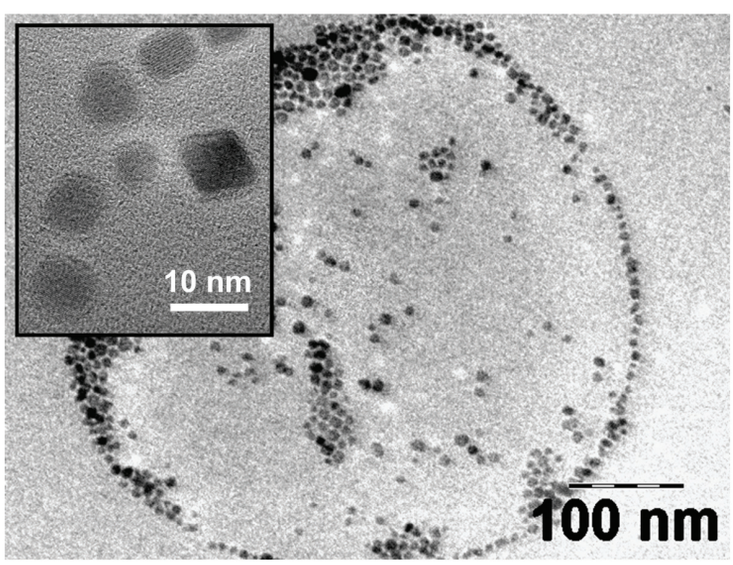

Figure 57. *TEM images of magnetic NPs from the synthesis 4 (only mPEG350 as solvent and stabilizer).*

As a final step in the optimization of the magnetite synthesis iron acetylacetonate dissolved in mPEG-OH was decomposed in presence of mPEG750-SH as stabilizer. Figure 58 shows the TEM images of thus synthesized magnetite nanoparticles. The formed NPs are crystalline (as it seen from HRTEM image), but not so well-shaped as those shown in figure 54.

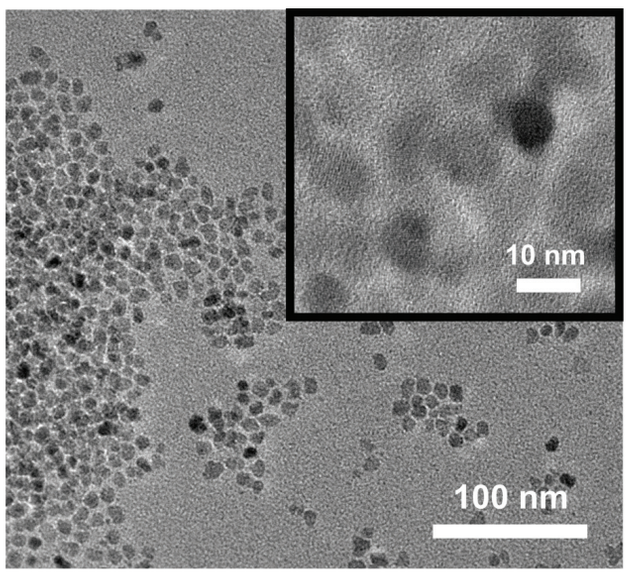

Figure 58. *TEM images of magnetic NPs from the synthesis 5.*

The crystal structure of the mPEG-COOH750-capped amphiphilic Fe_3O_4 NPs was examined by powder X-ray diffraction (Figure 59). The position and relative intensity of all diffraction peaks at 30.2, 35.6, 43.2, 53.7, 57.23 and 62.74 can be assigned to (220), (311), (400), (422) and (511), respectively, which match well with those of magnetite (JCPDS card 19-0629).

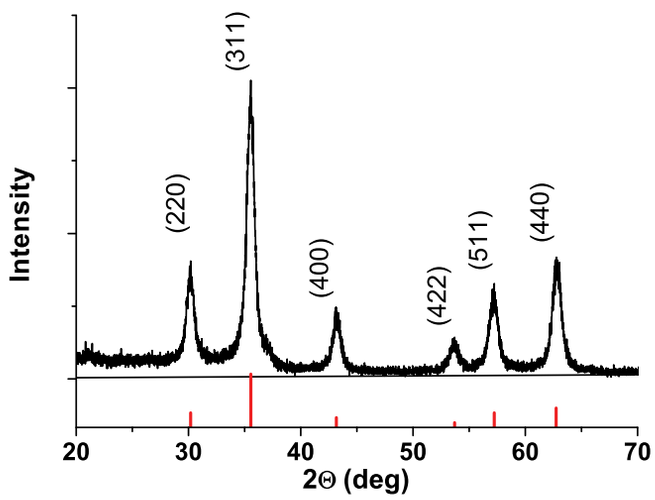

Figure 59. *XRD pattern of amphiphilic Fe_3O_4 NCs prepared by thermolysis in mPEG-OH (synthesis 5). Red - standard reflexes of bulk Fe_3O_4.*

Thus obtained magnetite nanoparticles have shown their ability for spontaneous phase transfer in the two layer (toluene-water) solvents system (Fig. 60). The NPs can be readily dispersed in various solvents (including H_2O) without additional surface modification. Magnetic properties of the Fe_3O_4 NPs were evaluated by the magnet attraction effect (Figure 60, right). Their attraction to the magnet confirms, that the NPs have achieved a minimal magnetic domain size, which is reported to be in the range of 4-18 nm for Fe_3O_4 at room temperature.[176]

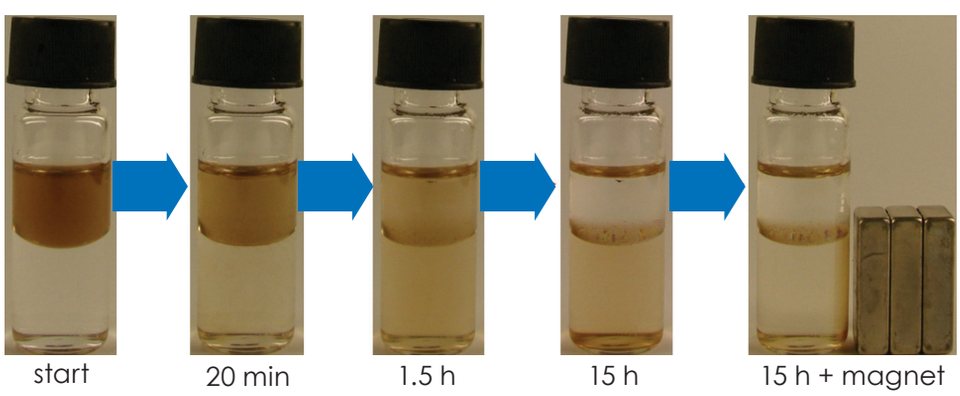

Figure 60. *Spontaneous phase transfer of mPEG-COOH750-capped amphiphilic Fe_3O_4 NPs (from synthesis 5) from toluene (upper phase) to water (bottom phase); right image demonstrates also magnetic attraction of the NPs transferred in water.*

Conclusions to the chapter 4.5.

A straightforward one-pot method for obtaining amphiphilic iron oxide NPs covalently covered by monocarboxyl-terminated polyethylene glycol is reported. The nanocrystals synthesized can be completely transferred from toluene into water without any loss. In the one pot synthesis developed, mPEG derivatives were used as a solvent and as a surfactant. The whole process is simple, inexpensive and beneficial for large-scale production (due to wide availability of the precursors). It also eliminates the multi-step solution (buffer) exchange and purification.

SUMMARY

This dissertation was focused on the preparation of different polyethyleneglycole-based stabilizers as well as on the development of novel synthetic approaches for obtaining colloidal semiconductor, metal and metal oxide nanocrystals. It has been proved that the proper design and the tuning of the ligand structure (thiolation or carboxylation) of polyethyleneglycol impart amphiphilic properties to the nanocrystals.

The synthesis of semiconductor CdTe nanocrystals was possible in different solvents (water, polar and nonpolar organics) resulting in QDs emitting at 540-640 nm with photoluminescence quantum yield reaching 30%. The ability of amphiphilic nanoparticles to spontaneous phase-transfer between solvents of different polarity makes them promising tagging object for bio-applications. For example, the permeation of amphiphilic luminescent CdTe nanocrystals through the lipid bi-layers of giant unilamellar vesicles achieved in the present work confirms the applicability of these nanocrystals for labeling and tracking whole cells and/or intracellular processes.

A facile, one-pot, one-phase (aqueous) approach to the synthesis of amphiphilic Au nanoparticles is developed. This approach allows obtaining stable high concentrated gold colloids compatible with media of different polarity. The synthetic method developed has a general nature and, thus, it could be applied also for synthesis of other noble metal nanoparticles, which may be a topic of further research in this field. The amphiphilic Au nanoparticles show an ability to tag vesicles through the selective binding to the lipid membrane.

Amphiphilic magnetite NPs were also obtained by one-pot synthesis. In this case efficient stabilization and amphiphilic properties were achieved by application of specially designed polyethyleneglycole stabilizer, possessing functional carboxylic group. Magnetite nanoparticles synthesized can be completely transferred from the organic solvents into water without any losses. The magnetic properties of the nanoparticles retain in various solvents. Using a simple compound as stabilizer as well as a reaction media makes the synthesis of this important type of magnetic nanoparticles very attractive and promising for upscaling.

REFERENCES

1. Ozin, G. A.; Arsenault, A. C., Nanochemistry. A chemical approach to nanomaterials. 2005.

2. Gerion, D.; Pinaud, F.; Williams, S. C.; Parak, W. J.; Zanchet, D.; Weiss, S.; Alivisatos, A. P., Synthesis and Properties of Biocompatible Water-Soluble Silica-Coated CdSe/ZnS Semiconductor Quantum Dots. J. Phys. Chem. B 2001, 105 (37), 8861-8871.

3. Pellegrino, T.; Manna, L.; Kudera, S.; Liedl, T.; Koktysh, D.; Rogach, A. L.; Keller, S.; Rädler, J.; Natile, G.; Parak, W. J., Hydrophobic nanocrystals coated with an amphiphilic polymer shell: A general route to water soluble nanocrystals. Nano Lett. 2004, 4 (4), 703-707.

4. Melancon M.P.; Lu W.; Yang Z.; Zhang R.; Cheng Z.; Elliot A.M.; Stafford J.; Olson T.; Zhang J.Z.; Chun, L., Therapeutics, Targets, and Development: *In vitro* and *in vivo* targeting of hollow gold nanoshells directed at epidermal growth factor receptor for photothermal ablation therapy. Mol. Cancer Ther. 2008, 7, 1730-1739.

5. Gao, X.; Cui, Y.; Levenson, R. M.; Chung, L. W. K.; Nie, S., *In vivo* cancer targeting and imaging with semiconductor quantum dots. Nat. Biotech. 2004, 22 (8), 969-976.

6. Bruns, O. T.; Ittrich, H.; Peldschus, K.; Kaul, M. G.; Tromsdorf, U. I.; Lauterwasser, J.; Nikolic, M. S.; Mollwitz, B.; Merkel, M.; Bigall, N. C.; Sapra, S.; Reimer, R.; Hohenberg, H.; Weller, H.; Eychmüller, A.; Adam, G.; Beisiegel, U.; Heeren, J., Real-time magnetic resonance imaging and quantification of lipoprotein metabolism *in vivo* using nanocrystals. Nat. Nano 2009, 4 (3), 193-201.

7. Gaponik N.; Talapin D.V.; Rogach A.L.; Eychmüller A.; Weller H., Efficient Phase Transfer of Luminescent Thiol-Capped Nanocrystals: From Water to Nonpolar Organic Solvents. Nano Lett. 2002, 2 (8), 803-806.

8. Jiang, H.; Jia, J., Complete reversible phase transfer of luminescent CdTe nanocrystals mediated by hexadecylamine. J. Mater. Chem. 2008, 18 (3), 344-349.

9. Wuister, S. F.; Swart, I.; van Driel, F.; Hickey, S. G.; Donega, C. d. M., Highly Luminescent Water-Soluble CdTe Quantum Dots. Nano Lett. 2003, 3 (4), 503-507.

10. Aldana, J.; Wang, Y. A.; Peng, X., Photochemical Instability of CdSe Nanocrystals Coated by Hydrophilic Thiols. J. Am. Chem. Soc. 2001, 123 (36), 8844-8850.

REFERENCES

11. Yu, W. W.; Falkner, J. C.; Shih, B. S.; Colvin, V. L., Preparation and characterization of monodisperse PbSe semiconductor nanocrystals in a noncoordinating solvent. Chem. Mater. 2004, 16 (17), 3318-3322.

12. Gittins, D. I.; Caruso, F., Spontaneous phase transfer of nanoparticulate metals from organic to aqueous media. Angew. Chem. Int. Ed. 2001, 40 (16), 3001-3004.

13. Gittins, D. I.; Caruso, F., Biological and physical applications of water-based metal nanoparticles synthesised in organic solution. ChemPhysChem 2002, 3 (1), 110-113.

14. Tromsdorf, U. I.; Bruns, O. T.; Salmen, S. C.; Beisiegel, U.; Weller, H., A Highly Effective, Nontoxic T1 MR Contrast Agent Based on Ultrasmall PEGylated Iron Oxide Nanoparticles. Nano Lett. 2009, 9, 4434-4440.

15. Muir, B. W.; Moffat, B. A.; Harbour, P.; Coia, G.; Zhen, G.; Waddington, L.; Scoble, J.; Krah, D.; Thang, S. H.; Chong, Y. K.; Mulvaney, P.; Hartley, P., Combinatorial Discovery of Novel Amphiphilic Polymers for the Phase Transfer of Magnetic Nanoparticles. J. Phys. Chem. C 2009, 113 (38), 16615-16624.

16. Sperling, R. A.; Parak, W. J., Surface modification, functionalization and bioconjugation of colloidal inorganic nanoparticles. Phil. Trans. Math. Phys. Eng. Sci. 2010, 368 (1915), 1333-1383.

17. Uyeda, H. T.; Medintz, I. L.; Jaiswal, J. K.; Simon, S. M.; Mattoussi, H., Synthesis of compact multidentate ligands to prepare stable hydrophilic quantum dot fluorophores. J. Am. Chem. Soc. 2005, 127 (11), 3870-3878.

18. Dubois, F.; Mahler, B.; Dubertret, B.; Doris, E.; Mioskowski, C., A Versatile Strategy for Quantum Dot Ligand Exchange. J. Am. Chem. Soc. 2006, 129 (3), 482-483.

19. Selvan, S. T.; Tan, T. T.; Ying, J. Y., Robust, non-cytotoxic, silica-coated CdSe quantum dots with efficient photoluminescence. Adv. Mater. 2005, 17 (13), 1620-1625.

20. Gómez, D. E.; Pastoriza-Santos, I.; Mulvaney, P., Tunable whispering gallery mode emission from quantum-dot-doped microspheres. Small 2005, 1 (2), 238-241.

21. Kovalenko, M. V.; Scheele, M.; Talapin, D. V., Colloidal Nanocrystals with Molecular Metal Chalcogenide Surface Ligands. Science 2009, 324 (5933), 1417-1420.

REFERENCES

22. Petruska, M. A.; Bartko, A. P.; Klimov, V. I., An Amphiphilic Approach to Nanocrystal Quantum Dot-Titania Nanocomposites. J. Am. Chem. Soc. 2004, 126 (3), 714-715.

23. Fan, H. Y.; Leve, E. W.; Scullin, C.; Gabaldon, J.; Tallant, D.; Bunge, S.; Boyle, T.; Wilson, M. C.; Brinker, C. J., Surfactant-assisted synthesis of water-soluble and biocompatible semiconductor quantum dot micelles. Nano Lett. 2005, 5 (4), 645-648.

24. Dubertret, B.; Skourides, P.; Norris, D. J.; Noireaux, V.; Brivanlou, A. H.; Libchaber, A., *In Vivo* Imaging of Quantum Dots Encapsulated in Phospholipid Micelles. Science 2002, 298 (5599), 1759-1762.

25. Bentzen, E. L.; Tomlinson, I. D.; Mason, J.; Gresch, P.; Warnement, M. R.; Wright, D.; Sanders-Bush, E.; Blakely, R.; Rosenthal, S. J., Surface Modification To Reduce Nonspecific Binding of Quantum Dots in Live Cell Assays. Bioconj. Chem. 2005, 16 (6), 1488-1494.

26. Chen, Y.; Thakar, R.; Snee, P. T., Imparting Nanoparticle Function with Size-Controlled Amphiphilic Polymers. J. Am. Chem. Soc. 2008, 130 (12), 3744-3745.

27. Anderson, R. E.; Chan, W. C. W., Systematic Investigation of Preparing Biocompatible, Single, and Small ZnS-Capped CdSe Quantum Dots with Amphiphilic Polymers. ACS Nano 2008, 2 (7), 1341-1352.

28. Wu, X.; Liu, H.; Liu, J.; Haley, K. N.; Treadway, J. A.; Larson, J. P.; Ge, N.; Peale, F.; Bruchez, M. P., Immunofluorescent labeling of cancer marker Her2 and other cellular targets with semiconductor quantum dots. Nat. Biotechnol. 2003, 21 (1), 41-46.

29. Chang, E.; Thekkek, N.; Yu, W.; Colvin, V.; Drezek, R., Evaluation of Quantum Dot Cytotoxicity Based on Intracellular Uptake. Small 2006, 2 (12), 1412-1417.

30. Derfus, A. M.; Chan, W. C. W.; Bhatia, S. N., Intracellular Delivery of Quantum Dots for Live Cell Labeling and Organelle Tracking. Adv. Mater. 2004, 16 (12), 961-966.

31. Kirchner, C.; Liedl, T.; Kudera, S.; Pellegrino, T.; Javier, A. M.; Gaub, H. E.; Stolzle, S.; Fertig, N.; Parak, W. J., Cytotoxicity of colloidal CdSe and CdSe/ZnS nanoparticles. Nano Lett. 2005, 5 (2), 331-338.

32. Chan, W. C. W.; Maxwell, D. J.; Gao, X.; Bailey, R. E.; Han, M.; Nie, S., Luminescent quantum dots for multiplexed biological detection and imaging. Curr. Opin. Biotechnol. 2002, 13 (1), 40-46.

REFERENCES

33. Nikolic, M. S.; Krack, M.; Aleksandrovic, V.; Kornowski, A.; Förster, S.; Weller, H., Tailor-made ligands for biocompatible nanoparticles. Angew. Chem. Int. Ed. 2006, 45 (39), 6577-6580.

34. Nagasaki, Y.; Ishii, T.; Sunaga, Y.; Watanabe, Y.; Otsuka, H.; Kataoka, K., Novel Molecular Recognition via Fluorescent Resonance Energy Transfer Using a Biotin-PEG/Polyamine Stabilized CdS Quantum Dot. Langmuir 2004, 20 (15), 6396-6400.

35. Rogach, A. L., Semiconductor Nanocrystal Quantum Dots: Synthesis, Assembly, Spectroscopy and Applications. Springer: Wien, New York: 2008; p 73-100.

36. Talapin, D. V.; Lee, J.-S.; Kovalenko, M. V.; Shevchenko, E. V., Prospects of Colloidal Nanocrystals for Electronic and Optoelectronic Applications. Chem. Rev. 2010, 110 (1), 389-458.

37. Schmid, G., Nanoparticles: From Theory to Application, 2nd, Completely Revised and Updated Edition. WILEY-VCH Verlag GmbH & Co. KGaA, Weinheim: 2010; p 533.

38. Goesmann, H.; Feldmann, C., Nanoparticulate Functional Materials. Angew. Chem. Int. Ed. 2010, 49, 1362-1395.

39. Bruchez Jr, M.; Moronne, M.; Gin, P.; Weiss, S.; Alivisatos, A. P., Semiconductor nanocrystals as fluorescent biological labels. Science 1998, 281 (5385), 2013-2016.

40. Michalet, X.; Pinaud, F. F.; Bentolila, L. A.; Tsay, J. M.; Doose, S.; Li, J. J.; Sundaresan, G.; Wu, A. M.; Gambhir, S. S.; Weiss, S., Quantum dots for live cells, *in vivo* imaging, and diagnostics. Science 2005, 307 (5709), 538-544.

41. Sharma, P.; Brown, S.; Walter, G.; Santra, S.; Moudgil, B., Nanoparticles for bioimaging. Adv. Colloid Interface Sci. 2006, 123-126, 471-485.

42. Hines, M. A.; Guyot-Sionnest, P., Synthesis and characterization of strongly luminescing ZnS- Capped CdSe nanocrystals. J. Phys. Chem. 1996, 100 (2), 468-471.

43. Talapin, D. V.; Mekis, I.; Gotzinger, S.; Kornowski, A.; Benson, O.; Weller, H., CdSe/CdS/ZnS and CdSe/ZnSe/ZnS core-shell-shell nanocrystals. J. Phys. Chem. B 2004, 108 (49), 18826-18831.

44. Jaiswal, J. K.; Goldman, E. R.; Mattoussi, H.; Simon, S. M., Use of quantum dots for live cell imaging. Nat. Meth. 2004, 1 (1), 73-78.

REFERENCES

45. Henglein, A., Photodegradation and fluorescence of colloidal cadmium sulfide in aqueous solution. Ber. Bunsenges. Phys. Chem. 1982, 86, 301-305.

46. Fojtik, A.; Weller, H.; Henglein, A., Photochemistry of semiconductor colloids. Size quantification effects in Q-cadmium arsenide. Chem. Phys. Lett. 1985, 120 (6), 552-554.

47. Henglein, A., Small-Particle Research - Physicochemical Properties of Extremely Small Colloidal Metal and Semiconductor Particles. Chem. Rev. 1989, 89 (8), 1861-1873.

48. Spanhel, L.; Haase, M.; Weller, H.; Henglein, A., Photochemistry of colloidal semiconductors. 20. Surface modification and stability of strong luminescing CdS particles. J. Am. Chem. Soc. 1987, 109 (19), 5649-5655.

49. Rajh, T.; Micic, O. I.; Nozik, A. J., Synthesis and characterization of surface-modified colloidal cadmium telluride quantum dots. J. Phys. Chem. 1993, 97 (46), 11999-12003.

50. Rogach, A. L.; Katsikas, L.; Kornowski, A.; Su, D.; Eychmüller, A.; Weller, H., Synthesis and characterization of thiol-stabilized CdTe nanocrystals. Ber. Bunsenges. Phys. Chem. 1996, 100 (11), 1772-1778.

51. Rogach, A. L.; Franzl, T.; Klar, T. A.; Feldmann, J.; Gaponik, N.; Lesnyak, V.; Shavel, A.; Eychmüller, A.; Rakovich, Y. P.; Donegan, J. F., Aqueous synthesis of thiol-capped CdTe nanocrystals: State-of-the-art. J. Phys. Chem. C 2007, 111 (40), 14628-14637.

52. Gaponik, N.; Rogach, A. L., Thiol-capped CdTe nanocrystals: progress and perspectives of the related research fields. Phys. Chem. Chem. Phys. 2010, 12 (31), 8685-8693.

53. Wang, Y.; Tang, Z. Y.; Correa-Duarte, M. A.; Pastoriza-Santos, I.; Giersig, M.; Kotov, N. A.; Liz-Marzan, L. M., Mechanism of strong luminescence photoactivation of citrate-stabilized water-soluble nanoparticles with CdSe cores. J. Phys. Chem. B 2004, 108 (40), 15461-15469.

54. Gaponik, N.; Talapin, D. V.; Rogach, A. L.; Hoppe, K.; Shevchenko, E. V.; Kornowski, A.; Eychmüller, A.; Weller, H., Thiol-capping of CdTe nanocrystals: An alternative to organometallic synthetic routes. J. Phys. Chem. B 2002, 106 (29), 7177-7185.

55. Zhang, H.; Cui, Z.; Wang, Y.; Zhang, K.; Ji, X.; Lu, C.; Yang, B.; Gao, M., From water-soluble CdTe nanocrystals to fluorescent nanocrystal-polymer transparent composites using polymerizable surfactants. Adv. Mater. 2003, 15 (10), 777-780.

REFERENCES

56. Koktysh, D. S.; Gaponik, N.; Reufer, M.; Crewett, J.; Scherf, U.; Eychmüller, A.; Lupton, J. M.; Rogach, A. L.; Feldmann, J., Near-infrared electroluminescence from HgTe nanocrystals. ChemPhysChem 2004, 5 (9), 1435-1438.

57. Gaponik, N., Assemblies of thiol-capped nanocrystals as building blocks for use in nanotechnology. J. Mater. Chem. 2010, 20 (25), 5174-5181.

58. Murray, C. B.; Norris, D. J.; Bawendi, M. G., Synthesis and characterization of nearly monodisperse CdE (E = sulfur, selenium, tellurium) semiconductor nanocrystallites. J. Am. Chem. Soc. 1993, 115 (19), 8706-8715.

59. de Mello Donega, C. D.; Liljeroth, P.; Vanmaekelbergh, D., Physicochemical evaluation of the hot-injection method, a synthesis route for monodisperse nanocrystals. Small 2005, 1 (12), 1152-1162.

60. Gaponik, N.; Hickey, S. G.; Dorfs, D.; Rogach, A. L.; Eychmüller, A., Progress in the Light Emission of Colloidal Semiconductor Nanocrystals. Small 2010, 6, 1364-1378.

61. Chan, W. C. W.; Nie, S., Quantum dot bioconjugates for ultrasensitive nonisotopic detection. Science 1998, 281 (5385), 2016-2018.

62. Mattoussi, H.; Mauro, J. M.; Goldman, E. R.; Anderson, G. P.; Sundar, V. C.; Mikulec, F. V.; Bawendi, M. G., Self-assembly of CdSe-ZnS quantum dot bioconjugates using an engineered recombinant protein. J. Am. Chem. Soc. 2000, 122 (49), 12142-12150.

63. Gill, R.; Zayats, M.; Willner, I., Semiconductor quantum dots for bioanalysis. Angew. Chem. Int. Ed. 2008, 47 (40), 7602-7625.

64. Akerman, M. E.; Chan, W. C. W.; Laakkonen, P.; Bhatia, S. N.; Ruoslahti, E., Nanocrystal targeting *in vivo*. Proc. Natl. Acad. Sci. U.S.A. 2002, 99 (20), 12617-12621.

65. Travert-Branger, N.; Dubois, F.; Carion, O.; Carrot, G.; Mahler, B.; Dubertret, B.; Doris, E.; Mioskowski, C., Oligomeric PEG-phospholipids for solubilization and stabilization of fluorescent nanocrystals in water. Langmuir 2008, 24 (7), 3016-3019.

66. Yu, W. W.; Chang, E.; Falkner, J. C.; Zhang, J.; Al-Somali, A. M.; Sayes, C. M.; Johns, J.; Drezek, R.; Colvin, V. L., Forming biocompatible and nonaggregated nanocrystals in water using amphiphilic polymers. J. Am. Chem. Soc. 2007, 129 (10), 2871-2879.

REFERENCES

67. Wang, C.-H.; Hsu, Y.-S.; Peng, C.-A., Quantum dots encapsulated with amphiphilic alginate as bioprobe for fast screening anti-dengue virus agents. Biosens. Bioelectron. 2008, 24 (4), 1012-1019.

68. Nida, D. L.; Nitin, N.; Yu, W. W.; Colvin, V. L.; Richards-Kortum, R., Photostability of quantum dots with amphiphilic polymer-based passivation strategies. Nanotechnol. 2008, 19 (3), 035701.

69. Liu, W.; Howarth, M.; Greytak, A. B.; Zheng, Y.; Nocera, D. G.; Ting, A. Y.; Bawendi, M. G., Compact biocompatible quantum dots functionalized for cellular imaging. J. Am. Chem. Soc. 2008, 130 (4), 1274-1284.

70. Chen, Y.-H.; Wang, C.-H.; Chang, C.-W.; Peng, C. A., In situ formation of viruses tagged with quantum dots. Integr. Biol. 2010, 2 (5-6), 258-264.

71. Sperling, R. A.; Rivera Gil, P.; Zhang, F.; Zanella, M.; Parak, W. J., Biological applications of gold nanoparticles. Chem. Soc. Rev. 2008, 37 (9), 1896-1908.

72. Wilson, R., The use of gold nanoparticles in diagnostics and detection. Chem. Soc. Rev. 2008, 37 (9), 2028-2045.

73. Mirkin, C. A.; Letsinger, R. L.; Mucic, R. C.; Storhoff, J., A DNA-Based Method for Rationally Assembling Nanoparticles into Macroscopic Materials. Nature 1996, 382, 607-609.

74. Rosi, N. L.; Mirkin, C. A., Nanostructures in Biodiagnostics. Chem. Rev. 2005, 105 (4), 1547-1562.

75. Liu, R.; Liew, R.; Zhou, J.; Xing, B., A Simple and Specific Assay for Real-Time Colorimetric Visualization of β-Lactamase Activity by Using Gold Nanoparticles. Angew. Chem. Int. Ed. 2007, 46 (46), 8799-8803.

76. Fleischmann, M.; Hendra, P. J.; McQuillan, A. J., Raman spectra of pyridine adsorbed at a silver electrode. Chem. Phys. Lett. 1974, 26 (2), 163-166.

77. Jeanmaire, D. L.; Van Duyne, R. P., Surface raman spectroelectrochemistry: Part I. Heterocyclic, aromatic, and aliphatic amines adsorbed on the anodized silver electrode. J. Electroanal. Chem. Interfacial Electrochem. 1977, 84 (1), 1-20.

78. Elghanian, R.; Storhoff, J. J.; Mucic, R. C.; Letsinger, R. L.; Mirkin, C. A., Selective Colorimetric Detection of Polynucleotides Based on the Distance-Dependent Optical Properties of Gold Nanoparticles. Science 1997, 277 (5329), 1078-1081.

REFERENCES

79. Faraday, M., The Bakerian Lecture: Experimental Relations of Gold (and Other Metals) to Light. Philos. Trans. R. Soc. London 1857, 147, 145-181.

80. Shan, J.; Nuopponen, M.; Jiang, H.; Viitala, T.; Kauppinen, E.; Kontturi, K.; Tenhu, H., Amphiphilic Gold Nanoparticles Grafted with Poly(N-isopropylacrylamide) and Polystyrene. Macromol. 2005, 38 (7), 2918-2926.

81. Nuopponen, M.; Tenhu, H., Gold Nanoparticles Protected with pH and Temperature-Sensitive Diblock Copolymers. Langmuir 2007, 23 (10), 5352-5357.

82. Edwards, E. W.; Chanana, M.; Wang, D.; Möhwald, H., Stimuli-responsive reversible transport of nanoparticles across water/oil interfaces. Angew. Chem. Int. Ed. 2008, 47 (2), 320-323.

83. Brust, M.; Walker, M.; Bethell, D.; Schiffrin, D. J.; Whyman, R., Synthesis of Thiol-derivatised Gold Nanoparticles in a Two-phase Liquid-Liquid System. J. Chem. Soc., Chem. Commun. 1994, (7), 801-802.

84. Templeton, A. C.; Wuelfing, W. P.; Murray, R. W., Monolayer-protected cluster molecules. Acc. Chem. Res. 2000, 33 (1), 27-36.

85. Zanchet, D.; Micheel, C. M.; Parak, W. J.; Gerion, D.; Alivisatos, A. P., Electrophoretic Isolation of Discrete Au Nanocrystal/DNA Conjugates. Nano Lett. 2001, 1 (1), 32-35.

86. Wuelfing, W. P.; Gross, S. M.; Miles, D. T.; Murray, R. W., Nanometer Gold Clusters Protected by Surface-Bound Monolayers of Thiolated Poly(ethylene glycol) Polymer Electrolyte. J. Am. Chem. Soc. 1998, 120 (48), 12696-12697.

87. Luo, S.; Xu, J.; Zhang, Y.; Liu, S.; Wu, C., Double Hydrophilic Block Copolymer Monolayer Protected Hybrid Gold Nanoparticles and Their Shell Cross-Linking. J. Phys. Chem. B 2005, 109 (47), 22159-22166.

88. Yuan, J.-J.; Schmid, A.; Armes, S. P.; Lewis, A. L., Facile Synthesis of Highly Biocompatible Poly(2-(methacryloyloxy)ethyl phosphorylcholine)-Coated Gold Nanoparticles in Aqueous Solution. Langmuir 2006, 22 (26), 11022-11027.

89. Kickelbick, G., Concepts for the incorporation of inorganic building blocks into organic polymers on a nanoscale. Prog. Polym. Sci. 2003, 28 (1), 83-114.

90. Hoffman, A. S., Intelligent polymers in medicine and biotechnology. Macromol. Symp. 1995, 98, 645-664.

REFERENCES

91. Nath, N.; Chilkoti, A., Creating "Smart" Surfaces Using Stimuli Responsive Polymers. Adv. Mater. 2002, 14, 1243-1247.

92. Laaksonen, P.; Kivioja, J.; Paananen, A.; Kainlauri, M.; Kontturi, K.; Ahopelto, J.; Linder, M. B., Selective Nanopatterning Using Citrate-Stabilized Au Nanoparticles and Cystein-Modified Amphiphilic Protein. Langmuir 2009, 25 (9), 5185-5192.

93. Imura, Y.; Morita, C.; Endo, H.; Kondo, T.; Kawai, T., Reversible phase transfer and fractionation of Au nanoparticles by pH change. Chem. Commun. 2010, 46 (48), 9206-9208.

94. Shimmin, R. G.; Schoch, A. B.; Braun, P. V., Polymer size and concentration effects on the size of gold nanoparticles capped by polymeric thiols. Langmuir 2004, 20 (13), 5613-5620.

95. Zubarev, E. R.; Xu, J.; Sayyad, A.; Gibson, J. D., Amphiphilic Gold Nanoparticles with V-Shaped Arms. J. Am. Chem. Soc. 2006, 128 (15), 4958-4959.

96. Foos, E. E.; Snow, A. W.; Twigg, M. E.; Ancona, M. G., Thiol-terminated Di-, Tri-, and tetraethylene oxide functionalized gold nanoparticles: A water-soluble, charge-neutral cluster. Chem. Mater. 2002, 14 (5), 2401-2408.

97. Zheng, M.; Davidson, F.; Huang, X., Ethylene glycol monolayer protected nanoparticles for eliminating nonspecific binding with biological molecules. J. Am. Chem. Soc. 2003, 125 (26), 7790-7791.

98. Sun, C.; Du, K.; Fang, C.; Bhattarai, N.; Veiseh, O.; Kievit, F.; Stephen, Z.; Lee, D.; Ellenbogen, R. G.; Ratner, B.; Zhang, M., PEG-Mediated Synthesis of Highly Dispersive Multifunctional Superparamagnetic Nanoparticles: Their Physicochemical Properties and Function *In Vivo*. ACS Nano 2010, 4 (4), 2402-2410.

99. Šafařík, I.; Šafaříková, M., Magnetic Nanoparticles and Biosciences. Monatshefte für Chemie / Chemical Monthly 2002, 133 (6), 737-759.

100. Suslick, K. S.; Choe, S.-B.; Cichowlas, A. A.; Grinstaff, M. W., Sonochemical synthesis of amorphous iron. Nature 1991, 353 (6343), 414-416.

101. Suslick, K. S.; Fang, M.; Hyeon, T., Sonochemical Synthesis of Iron Colloids. J. Am. Chem. Soc. 1996, 118 (47), 11960-11961.

102. Pascal, C.; Pascal, J. L.; Favier, F.; Elidrissi Moubtassim, M. L.; Payen, C., Electrochemical Synthesis for the Control of γ-Fe_2O_3 Nanoparticle Size. Morphology, Microstructure, and Magnetic Behavior. Chem. Mater. 1998, 11 (1), 141-147.

REFERENCES

103. Park, J.; An, K.; Hwang, Y.; Park, J. E. G.; Noh, H. J.; Kim, J. Y.; Park, J. H.; Hwang, N. M.; Hyeon, T., Ultra-large-scale syntheses of monodisperse nanocrystals. Nat. Mater. 2004, 3 (12), 891-895.

104. Sun, S.; Zeng, H.; Robinson, D. B.; Raoux, S.; Rice, P. M.; Wang, S. X.; Li, G., Monodisperse MFe2O4 (M = Fe, Co, Mn) Nanoparticles. J. Am. Chem. Soc. 2004, 126 (1), 273-279.

105. Xun, W.; Jing, Z.; Qing, P.; Yadong, L., A general strategy for nanocrystal synthesis. Nature 2005, 437, 121-124.

106. Sun, S.; Zeng, H., Size-Controlled Synthesis of Magnetite Nanoparticles. J. Am. Chem. Soc. 2002, 124 (28), 8204-8205.

107. Woo, K.; Hong, J.; Choi, S.; Lee, H.-W.; Ahn, J.-P.; Kim, C. S.; Lee, S. W., Easy Synthesis and Magnetic Properties of Iron Oxide Nanoparticles. Chem. Mater. 2004, 16 (14), 2814-2818.

108. Tourinho, F. A.; Franck, R.; Massart, R., Aqueous ferrofluids based on manganese and cobalt ferrites. J. Mater. Sci. 1990, 25 (7), 3249-3254.

109. Fauconnier, N.; Bée, A.; Roger, J.; Pons, J. N., Synthesis of aqueous magnetic liquids by surface complexation of maghemite nanoparticles. J. Mol. Liq. 1999, 83 (1-3), 233-242.

110. Li, J.; Dai, D.; Zhao, B.; Lin, Y.; Liu, C., Properties of Ferrofluid Nanoparticles Prepared by Coprecipitation and Acid Treatment. J. Nanopart. Res. 2002, 4 (3), 261-264.

111. Butterworth, M. D.; Bell, S. A.; Armes, S. P.; Simpson, A. W., Synthesis and Characterization of Polypyrrole-Magnetite-Silica Particles. J. Colloid. Interface Sci. 1996, 183 (1), 91-99.

112. Deng, J.; Ding, X.; Zhang, W.; Peng, Y.; Wang, J.; Long, X.; Li, P.; Chan, A. S. C., Magnetic and conducting Fe_3O_4-cross-linked polyaniline nanoparticles with core-shell structure. Polymer 2002, 43 (8), 2179-2184.

113. Tartaj, P.; Morales, M. P.; González-Carreno, T.; Veintemillas-Verdaguer, S.; Serna, C. J., Advances in magnetic nañoparticles for biotechnology applications. J. Magn. Magn. Mater. 2005, 290-291 (Part 1), 28-34.

114. Yuk, J. S.; Rose, J.; Alocilja, E. C., Characterization of polyaniline-coated magnetic nanoparticles for application in a disposable membrane strip biosensor. Eur. Phys. J. Appl. Phys. 2010, 50 (1), 11401.

115. Vestal, C. R.; Zhang, Z. J., Atom Transfer Radical Polymerization Synthesis and Magnetic Characterization of MnFe2O4/Polystyrene Core/Shell Nanoparticles. J. Am. Chem. Soc. 2002, 124 (48), 14312-14313.

116. Park, J.-I.; Cheon, J., Synthesis of solid solution and core-shell type cobalt-platinum magnetic nanoparticles via transmetalation reactions. J. Am. Chem. Soc. 2001, 123 (24), 5743-5746.

117. Ma, D.; Guan, J.; Dénommée, S.; Enright, G.; Veres, T.; Simard, B., Multifunctional Nano-Architecture for Biomedical Applications. Chem. Mater. 2006, 18 (7), 1920-1927.

118. Pardoe, H.; Chua-anusorn, W.; St. Pierre, T. G.; Dobson, J., Structural and magnetic properties of nanoscale iron oxide particles synthesized in the presence of dextran or polyvinyl alcohol. J. Magn. Magn. Mater. 2001, 225 (1-2), 41-46.

119. Nishio, Y.; Yamada, A.; Ezaki, K.; Miyashita, Y.; Furukawa, H.; Horie, K., Preparation and magnetometric characterization of iron oxide-containing alginate/poly(vinyl alcohol) networks. Polymer 2004, 45 (21), 7129-7136.

120. Hee Kim, E.; Sook Lee, H.; Kook Kwak, B.; Kim, B.-K., Synthesis of ferrofluid with magnetic nanoparticles by sonochemical method for MRI contrast agent. J. Magn. Magn. Mater. 2005, 289, 328-330.

121. Lutz, J.-F.; Stiller, S.; Hoth, A.; Kaufner, L.; Pison, U.; Cartier, R., One-Pot Synthesis of PEGylated Ultrasmall Iron-Oxide Nanoparticles and Their *in Vivo* Evaluation as Magnetic Resonance Imaging Contrast Agents. Biomacromol. 2006, 7 (11), 3132-3138.

122. Peng, S.; Wang, C.; Xie, J.; Sun, S., Synthesis and stabilization of monodisperse Fe nanoparticles. J. Am. Chem. Soc. 2006, 128 (33), 10676-10677.

123. Robinson, D. B.; Persson, H. H. J.; Zeng, H.; Li, G.; Pourmand, N.; Sun, S.; Wang, S. X., DNA-Functionalized MFe2O4 (M = Fe, Co, or Mn) Nanoparticles and Their Hybridization to DNA-Functionalized Surfaces. Langmuir 2005, 21 (7), 3096-3103.

124. Yu, W. W.; Chang, E.; Sayes, C. M.; Drezek, R.; Colvin, V. L., Aqueous dispersion of monodisperse magnetic iron oxide nanocrystals through phase transfer. Nanotechnol. 2006, 17 (17), 4483-4487.

125. Kim, B. S.; Qiu, J. M.; Wang, J. P.; Taton, T. A., Magnetomicelles: Composite nanostructures from magnetic nanoparticles and cross-linked amphiphilic block copolymers. Nano Lett. 2005, 5 (10), 1987-1991.

126. Chen, Y.; Ji, T.; Rosenzweig, Z., Synthesis of Glyconanospheres Containing Luminescent CdSe-ZnS Quantum Dots. Nano Lett. 2003, 3 (5), 581-584.

REFERENCES

127. Jun, Y. W.; Lee, J. H.; Cheon, J., Chemical Design of Nanoparticle Probes for High-Performance Magnetic Resonance Imaging. Angew. Chem. Int. Ed. 2008, 47, 5122-5135.

128. Portney, N.; Ozkan, M., Nano-oncology: drug delivery, imaging, and sensing. Anal. Bioanal.Chem. 2006, 384 (3), 620-630.

129. Goodman, C. M.; McCusker, C. D.; Yilmaz, T.; Rotello, V. M., Toxicity of Gold Nanoparticles Functionalized with Cationic and Anionic Side Chains. Bioconj. Chem. 2004, 15 (4), 897-900.

130. Ryman-Rasmussen, J. P.; Riviere, J. E.; Monteiro-Riviere, N. A., Surface Coatings Determine Cytotoxicity and Irritation Potential of Quantum Dot Nanoparticles in Epidermal Keratinocytes. J. Invest. Dermatol. 2006, 127 (1), 143-153.

131. Duan, H.; Nie, S., Cell-Penetrating Quantum Dots Based on Multivalent and Endosome-Disrupting Surface Coatings. J. Am. Chem. Soc. 2007, 129 (11), 3333-3338.

132. Lovric, J.; Cho, S. J.; Winnik, F. M.; Maysinger, D., Unmodified Cadmium Telluride Quantum Dots Induce Reactive Oxygen Species Formation Leading to Multiple Organelle Damage and Cell Death. Chemistry & Biology 2005, 12 (11), 1227-1234.

133. Forestier, J., L'aurotherapie dans les rheumatisms chroniques. Bull. Soc. Med. Hop. Paris 1929, 53, 323-327.

134. Nativo, P.; Prior, I. A.; Brust, M., Uptake and Intracellular Fate of Surface-Modified Gold Nanoparticles. ACS Nano 2008, 2 (8), 1639-1644.

135. Lewinski, N.; Colvin, V.; Drezek, R., Cytotoxicity of Nanoparticles. Small 2008, 4, 26-49.

136. Niidome, T.; Yamagata, M.; Okamoto, Y.; Akiyama, Y.; Takahashi, H.; Kawano, T.; Katayama, Y.; Niidome, Y., PEG-modified gold nanorods with a stealth character for *in vivo* applications. J. Controlled Release 2006, 114 (3), 343-347.

137. Gupta, A. K.; Wells, S., Surface-modified superparamagnetic nanoparticles for drug delivery: preparation, characterization, and cytotoxicity studies. IEEE Trans. Nanobiosci. 2004, 3 (1), 66-73.

138. Wan, S.; Huang, J.; Guo, M.; Zhang, H.; Cao, Y.; Yan, H.; Liu, K., Biocompatible superparamagnetic iron oxide nanoparticle dispersions stabilized with poly(ethylene glycol)-oligo(aspartic acid) hybrids. J. Biomed. Mater. Res. A 2007, 80A, 946-954.

REFERENCES

139. Hu, F.; Neoh, K. G.; Cen, L.; Kang, E.-T., Cellular Response to Magnetic Nanoparticles "PEGylated" via Surface-Initiated Atom Transfer Radical Polymerization. Biomacromol. 2006, 7 (3), 809-816.

140. Chun, C.-H.; Wang, Y.-C.; Huang, H.-Y.; Wu, L.-C.; Yang, C.-S., Ultrafine PEG-coated poly(lactic- co -glycolic acid) nanoparticles formulated by hydrophobic surfactant-assisted one-pot synthesis for biomedical applications. Nanotechnology 2011, 22 (18), 185601.

141. Kievit, F. M.; Veiseh, O.; Bhattarai, N.; Fang, C.; Gunn, J. W.; Lee, D.; Ellenbogen, R. G.; Olson, J. M.; Zhang, M., PEI-PEG-Chitosan-Copolymer-Coated Iron Oxide Nanoparticles for Safe Gene Delivery: Synthesis, Complexation, and Transfection. Adv. Funct. Mater. 2009, 19, 2244-2251.

142. Fang, C.; Zhang, M., Multifunctional magnetic nanoparticles for medical imaging applications. J. Mater. Chem. 2009, 19 (35), 6258-6266.

143. Qiao, R.; Yang, C.; Gao, M., Superparamagnetic iron oxide nanoparticles: from preparations to *in vivo* MRI applications. J. Mater. Chem. 2009, 19 (35), 6274-6293.

144. Du, Y. J.; Brash, J. L., Synthesis and characterization of thiol-terminated poly(ethylene oxide) for chemisorption to gold surface. J. Appl. Polym. Sci. 2003, 90, 594-607.

145. Essahli, M.; Ganachaud, F.; In, M.; Boutevin, B., Phosphonic acid functionalized polyethylene glycol and derivatives. J. Appl. Polym. Sci. 2008, 108, 483-490.

146. Barrera, C.; Herrera, A. P.; Rinaldi, C., Colloidal dispersions of monodisperse magnetite nanoparticles modified with poly(ethylene glycol). J. Colloid. Interfac. Sci. 2009, 329 (1), 107-113.

147. García-Sáez, A. J.; Carrer, D. C.; Schwille, P., Fluorescence Correlation Spectroscopy for the Study of Membrane Dynamics and Organization in Giant Unilamellar Vesicles. Methods. Mol. Biol. 2010, 606, 493-508.

148. Brown, K. R.; Walter, D. G.; Natan, M. J., Seeding of colloidal Au nanoparticle solutions. 2. Improved control of particle size and shape. Chem. Mater. 2000, 12 (2), 306-313.

149. Ziegler, C.; Eychmüller, A., Seeded Growth Synthesis of Uniform Gold Nanoparticles with Diameters of 15-300 nm. J. Phys. Chem. C 2011, accepted.

150. Lu, X.; Niu, M.; Qiao, R.; Gao, M., Superdispersible PVP-Coated Fe3O4 Nanocrystals Prepared by a "One-Pot" Reaction. J. Phys. Chem. B 2008, 112 (46), 14390-14394.

151. Grabolle, M.; Spieles, M.; Lesnyak, V.; Gaponik, N.; Eychmüller, A.; Resch-Genger, U., Determination of the Fluorescence Quantum Yield of Quantum Dots: Suitable Procedures and Achievable Uncertainties. Anal. Chem. 2009, 81 (15), 6285-6294.

152. Kim, K.; Kim, T. H.; Choi, J. H.; Lee, J. Y.; Hah, S. S.; Yoo, H. O.; Hwang, S. S.; Ryu, K. N.; Kim, H. J.; Kim, J., Synthesis of a pH-Sensitive PEO-Based Block Copolymer and its Application for the Stabilization of Iron Oxide Nanoparticles. Macromol. Chem. Phys. 2010, 211, 1127-1136.

153. Reichardt, C., Solvents and Solvent Effects in Organic Chemistry. WILEY-VCH Verlag GmbH & Co. KGaA: Weinheim, 2003; p 2063-2066.

154. Gaponenko, S. V.; Bogomolov, V. N.; Petrov, E. P.; Kapitonov, A. M.; Yarotsky, D. A.; Kalosha, I. I.; Eychmüller, A. A.; Rogach, A. L.; McGilp, J.; Woggon, U.; Gindele, F., Spontaneous emission of dye molecules, semiconductor nanocrystals, and rare-earth ions in opal-based photonic crystals. J. Lightwave Technol. 1999, 17 (11), 2128-2137.

155. Eychmüller, A., Structure and photophysics of semiconductor nanocrystals. J. Phys. Chem. B 2000, 104 (28), 6514-6528.

156. Kapitonov, A. M.; Stupak, A. P.; Gaponenko, S. V.; Petrov, E. P.; Rogach, A. L.; Eychmüller, A., Luminescence Properties of Thiol-Stabilized CdTe Nanocrystals. J. Phys. Chem. B 1999, 103 (46), 10109-10113.

157. Arizpe-Chávez, H.; Espinoza-Beltrán, F. J.; Ramírez-Bon, R.; Zelaya-Angel, O.; González-Hernández, J., Cubic to hexagonal phase transition in CdTe polycrystalline thin films by oxygen incorporation. Solid State Commun. 1997, 101 (1), 39-43.

158. Borchert, H.; Talapin, D. V.; Gaponik, N.; McGinley, C.; Adam, S.; Lobo, A.; Möller, T.; Weller, H., Relations between the photoluminescence efficiency of CdTe nanocrystals and their surface properties revealed by synchrotron XPS. J. Phys. Chem. B 2003, 107 (36), 9662-9668.

159. Bao, H.; Gong, Y.; Li, Z.; Gao, M., Enhancement effect of illumination on the photoluminescence of water-soluble CdTe nanocrystals: Toward highly fluorescent CdTe/CdS core-shell structure. Chem. Mater. 2004, 16 (20), 3853-3859.

160. Reeves, J. P.; Dowben, R. M., Formation and properties of thin-walled phospholipid vesicles. J. Cell. Physiol. 1969, 73 (1), 49-60.

REFERENCES

161. Angelova, M. I.; Dimitrov, D. S., Liposome electroformation. Faraday Discuss. Chem. Soc. 1986, 81, 303-311.

162. Angelova, M.; Soléau, S.; Méléard, P.; Faucon, F.; Bothorel, P., Preparation of giant vesicles by external AC electric fields. Kinetics and applications. Progr. Coll. Polym. Sci. 1992, 89, 127-131.

163. Méléard, P.; Bagatolli, L. A.; Pott, T., Giant Unilamellar Vesicle Electroformation: From Lipid Mixtures to Native Membranes Under Physiological Conditions. Methods Enzymol. 2009, 465, 161-176.

164. Alvarez, M. M.; Khoury, J. T.; Schaaff, T. G.; Shafigullin, M. N.; Vezmar, I.; Whetten, R. L., Optical Absorption Spectra of Nanocrystal Gold Molecules. J. Phys. Chem. B 1997, 101 (19), 3706-3712.

165. Mulvaney, P., Surface plasmon spectroscopy of nanosized metal particles. Langmuir 1996, 12 (3), 788-800.

166. Heath, J. R.; Knobler, C. M.; Leff, D. V., Pressure/Temperature Phase Diagrams and Superlattices of Organically Functionalized Metal Nanocrystal Monolayers: The Influence of Particle Size, Size Distribution, and Surface Passivant. J. Phys. Chem. B 1997, 101 (2), 189-197.

167. Shimizu, T.; Teranishi, T.; Hasegawa, S.; Miyake, M., Size evolution of alkanethiol-protected gold nanoparticles by heat treatment in the solid state. J. Phys. Chem. B 2003, 107 (12), 2719-2724.

168. Butterworth, M. D.; Illum, L.; Davis, S. S., Preparation of ultrafine silica- and PEG-coated magnetite particles. Colloids Surf., A 2001, 179 (1), 93-102.

169. Forge, D.; Roch, A.; Laurent, S.; Tellez, H.; Gossuin, Y.; Renaux, F.; Vander Elst, L.; Muller, R. N., Optimization of the Synthesis of Superparamagnetic Contrast Agents by the Design of Experiments Method. J. Phys. Chem. C 2008, 112 (49), 19178-19185.

170. Guin, D.; Manorama, S. V., Room temperature synthesis of monodispersed iron oxide nanoparticles. Mater. Lett. 2008, 62 (17-18), 3139-3142.

171. Park, J.; Lee, E.; Hwang, N. M.; Kang, M.; Sung, C. K.; Hwang, Y.; Park, J. G.; Noh, H. J.; Kim, J. Y.; Park, J. H.; Hyeon, T., One-nanometer-scale size-controlled synthesis of monodisperse magnetic iron oxide nanoparticles. Angew. Chem. Int. Ed. 2005, 44 (19), 2872-2877.

172. Dean, J. A., Lange's Handbook of Chemistry. 15th ed.; McGraw-Hill, Inc.: New York: 1999; pp 4.41-44.43.

173. Liu, Q.; Xu, Z., Self-Assembled Monolayer Coatings on Nanosized Magnetic Particles Using 16-Mercaptohexadecanoic Acid. Langmuir 1995, 11 (12), 4617-4622.

174. Hu, F.; MacRenaris, K. W.; A. Waters, E.; Schultz-Sikma, E. A.; Eckermann, A. L.; Meade, T. J., Highly dispersible, superparamagnetic magnetite nanoflowers for magnetic resonance imaging. Chem. Commun. 2010, 46 (1), 73-75.

175. Govor, L. V.; Bauer, G. H.; Reiter, G.; Shevchenko, E.; Weller, H.; Parisi, J., Self-Assembly of $CoPt_3$ Nanoparticle Rings Based on Phase-Separated Hexadecylamine Droplet Structure. Langmuir 2003, 19 (23), 9573-9576.

176. Laurent, S.; Forge, D.; Port, M.; Roch, A.; Robic, C.; Vander Elst, L.; Muller, R. N., Magnetic Iron Oxide Nanoparticles: Synthesis, Stabilization, Vectorization, Physicochemical Characterizations, and Biological Applications. Chem. Rev. 2008, 108 (6), 2064-2110.

CURRICULUM VITAE

Aliaksei Dubavik

Chair of Physical Chemistry and Electrochemistry
TU Dresden
Bergstrasse, 66b
01062 Dresden
GERMANY

Tel: +49(0)35146336117
Fax: +49(0)35146337164
e-mail: a.dubavik@chemie.tu-dresden.de
http://www.chm.tu-dresden.de/pc2

Academic degree: Master of Science
Date and place of birth: 23 April, 1982, Kremenchug (Ukraine)
Citizenship: Belarus
Marital status: Married

Research interests

Nanochemistry (synthesis and characterization of colloidal quantum dot nanoparticles, noble metal and magnetic nanocrystals);
Polymer Chemistry (synthesis and modification of polymers)

Education

2008-2011 - Ph.D. student, TU Dresden (Physical Chemistry, group of Prof. Dr. A. Eychmüller)
2004-2005 - Master study, Belarusian State University (Master of Science degree)
1999-2004 - study, Belarusian State University, Chemistry Department. (Diploma in Chemistry)

Research and Professional experience

1999-2005 - Junior Research Scientist, Physico-Chemical Research Institute, BSU (Minsk)
2005-2007 - Chemist, pharmaceutical company (Moscow)
Since 2008 - Research Scientist, Physical Chemistry, TU Dresden

Memberships

Deutsche Bunsen Gesellschaft (German Bunsen Society)

Teaching Experience

2008-2010 - TU Dresden: Tutor in Basic course of Physical Chemistry (2nd year students). Tutor in practical teaching in course of Special Physical Chemistry for advanced students.

Conference Contributions -contributed talks

- Novel Amphiphilic Nanocrystals for Bioapplications
  Deutsche Bunsen-Gesellschaft, 13-15 May 2010 (University Bielefeld, Germany)
- Amphiphilic Colloidal Nanocrystals in Nanobiotechnology
  Nano 2009 Perspectives in Nanoscience and Nanotechnology, 28-30 September (Donostia-San Sebastian, Spain)

Conference Contributions - contributed posters

- Functionalization of Colloidal Nanocrystals by Amphiphilic Stabilizers
  International Conference NaNaX4, 11-15 April 2010 (Munich/Tutzing, Germany)
- Amphiphilic Nanocrystals for Bioapplications
  International Conference on Functional Nanocoatings, 28-31 March 2010 (TU Dresden, Germany)
- Synthesis and Characterization of Amphiphilic Nanocrystals
  Deutsche Bunsen-Gesellschaft, 21-23 May 2009 (University Köln, Germany)

Participation in the Projects

2008-2009 DFG-Project "Hydrophobic/hydrophilic Switchable Nanoparticles for Biolabeling"

2008-2010 DFG SPP "Bio-nano responses" NANOFATE Project (Interactions of hydrophobic and hydrophilic semiconductor quantum dots with cell model systems for liver and adipose tissue)

2010 EU FP7 projects INNOVASOL and the NoE Nanophotonics4Energy

CURRICULUM VITAE

Publications in Scientific journals

Accepted/Published

Dubavik A., Lesnyak V., Gaponik N., Eychmüller A. Amphiphilic Gold Nanoparticles. Chem. Comm. 2011, submitted

Lesnyak V., Wolf A., Dubavik A., Voitekhovich S., Gaponik N., Eychmüller A. 3D Assembly of Semiconductor and Metal Nanocrystals: Hybrid CdTe/Au Structures with Controlled Content. J. Am. Chem. Soc. 2011, submitted

Vrublevsky, I.; Chernyakova, K.; Ispas, A.; Bund, A.; Gaponik, N.; Dubavik, A. Photoluminescence properties of heat-treated porous alumina films formed in oxalic acid. J. Lumin. 2011, 131 (5), 938-942

Thiessen W., Dubavik A., Lesnyak V., Gaponik N., Eychmüller A., Wolff T. Amphiphilic and magnetic behavior of Fe_3O_4 nanocrystals. Phys. Chem. Chem. Phys. 2010, 12, 2063

Lesnyak V., Dubavik A., Plotnikov A., Gaponik N., Eychmüller A. One-step aqueous synthesis of blue-emitting glutathione-capped $ZnSe_{1-x}Te_x$ alloyed nanocrystals. Chem. Comm. 2010, 46, 886

Dubavik A., Lesnyak V., Thiessen W., Gaponik N., Wolff T., Eychmüller A. Synthesis of amphiphilic CdTe nanocrystals. J. Phys. Chem. C 2009, 113, 4748

Kostjuk S.V.; Dubovik A.; Vasilenko I.V.; Frolov A.N.; Kaputsky F.N. Kinetic and mechanistic study of the quasiliving cationic polymerization of styrene with the 2-phenyl-2-propanol/$AlCl_3$xOBu$_2$ initiating system. Eur. Polym. J. 2007, 43 (3), 968-979

Kostjuk S.V., Dubovik A., Vasilenko I.V.; Mardykin V.P.; Gaponik L.V., Kaputsky F.N., Antipin L.M. Novel initiating system based on $AlCl_3$ etherate for quasiliving cationic polymerization of styrene. Polym. Bull. 2004, 52 (3-4) 227-234

Languages

belarusian - native speaker;
russian - native speaker;
english - fluent (2002 - participant of student working program in the USA);
german, french - basic.

References

Prof. Dr. Alexander Eychmüller
Dr. Nikolai Gaponik
Dr. Vladimir Lesnyak
Dr. Sergej Kostjuk

Erklärung über Anfertigung der Dissertation

Hiermit versichere ich, dass ich die vorliegende Arbeit ohne unzulässige Hilfe Dritter und ohne Benutzung anderer als der angegebenen Hilfsmittel angefertigt habe; die aus fremden Quellen direkt oder indirekt übernommenen Gedanken sind als solche kenntlich gemacht. Die Arbeit wurde bisher weder im Inland noch im Ausland in gleicher oder ähnlicher Form einer anderen Prüfungsbehörde vorgelegt.

Diese Dissertation wurde in Zeitraum Januar 2008 bis März 2011 an der Technischen Universität Dresden unter der wissenschaftlichen Betreuung von Prof. Dr. rer. nat. habil. Alexander Eychmüller angefertigt.

Es existieren keine früheren Promotionsverfahren.

Ich erkenne hiermit die Promotionsordnung der Fakultät Mathematik und Naturwissenschaften an der Technischen Universität Dresden vom 20 März 2000 an.

Dresden, 25.03.2011

Aliaksei Dubavik